Aus der Professur für Hydrologie

der Agrar- und Umweltwissenschaftlichen Fakultät

Improving the determination of soil hydraulic properties of peat soils at different scales

Dissertation

zur Erlangung des akademischen Grades

Doktor der Ingenieurwissenschaften (Dr.-Ing.)

an der Agrar- und Umweltwissenschaftlichen Fakultät

der Universität Rostock

vorgelegt von

MSc. Ullrich Mathias Dettmann

Rostock, 2016

urn:nbn:de:gbv:28-diss2017-0094-8

Gutachter:

Prof. Dr. Konrad Miegel (Universität Rostock)

Prof. Dr. Andy Baird (University of Leeds)

Dr. Michel Bechtold (Thünen Institut für Agrarklimaschutz, Braunschweig)

Eingereicht am: 15. Dezember 2015

Verteidigt am: 13. Mai 2016

Contents

List of Figures

List of Tables

List of symbols and abbreviations

Symbols

$A_{surface}$	(cm or m)	Integral of the surface storage
$A_{zl,soil}$	(cm or m)	Integral of the soil moisture profile above *zl*
$A_{zu,soil}$	(cm or m)	Integral of the soil moisture profile above *zu*
α	(cm^{-1})	Van Genuchten-Mualem shape parameter
α_2	(cm^{-1})	Bimodal van Genuchten-Mualem shape parameter
b	(-)	Parameter vector in objective function
b_d	(g cm^{-3})	Bulk density
CI_{95}	(%)	95% confidence intervals
ΔA_{soil}	(cm or m)	Difference of the integrals of two soil moisture profiles
$\Delta A_{surface}$	(cm or m)	Difference of the heights of two open water surfaces
$\Delta\mu$	(cm)	Optimized offset to the measured mean surface elevation of the microrelief
Δz	(cm or m)	Water level difference (*zu* - *zl*) or distance between the upper and lower tensiometer at evaporation experiments
Δz_{obs}	(m)	Observed water level changes
Δz_{sim}	(m)	Simulated water level changes
ε	(%)	Porosity
F_s	(-)	Cumulative frequency distribution
$F_s(z)$	(-)	Cumulative frequency distribution of the surface elevations
h	(cm)	Pressure head
h_i	(cm)	Pressure head at time step *i*
$\overline{h_i}$	(cm)	Mean pressure head between two time steps
Δh_i	(cm)	Mean difference between tensiometer readings at time step *i*
i	(-)	Time step
j	(-)	Measurement set in objective function
K_s	(cm d^{-1}or cm h^{-1})	Saturated hydraulic conductivity
$K_{(h)}$	(cm d^{-1}or cm h^{-1})	Hydraulic conductivity function
K_i	(cm d^{-1}or cm h^{-1})	Hydraulic conductivity corresponding to $\overline{h_i}$

$K_{(\theta)}$	(cm d^{-1}or cm h^{-1})	Hydraulic conductivity function
m	(-)	Different set of measurements or van Genuchten-Mualem shape parameter
N	(-)	Numbers of observations
n	(-)	Van Genuchten-Mualem shape parameter
n_j	(-)	Number of measurement of the jth measurement set
n_2	(-)	Bimodal van Genuchten-Mualem shape parameter
P	(mm)	Precipitation
$p_j^*(ti)$	(-)	Observation at t_i for the jth measurement set
$p_j(t_i,b)$	(-)	Prediction at t_i for the jth measurement set
Φ	(-)	Objective function value
$\hat{R}$	(-)	Gelman and Rubin (1992) convergence criteria
S_e	(-)	Effective saturation
S_y	(-)	Specific yield
$S_{y,flat}$	(-)	Specific yield for flat soil surface
$S_{y,soil}$	(-)	Soil specific yield
$S_{y,surface}$	(-)	Surface specific yield
$S_{y,uneven}$	(-)	Specific yield for uneven soil surface
t_i	(-)	Time at time step i
Δt_i	(s or h)	Time increment
θ	(cm^3 cm^{-3})	Volumetric water content
$\theta(z)$	(cm^3 cm^{-3})	Volumetric water content at pressure head $h = z$
θ_i	(cm^3 cm^{-3})	Mean volumetric water content at time step i
$\Delta\theta_i$	(cm^3 cm^{-3})	Mean volumetric water content change at time step i
θ_r	(cm^3 cm^{-3})	Residual volumetric water content
θ_s	(cm^3 cm^{-3})	Saturated volumetric water content
σ	(cm or m)	Standard deviation
τ	(-)	Van Genuchten-Mualem shape parameter
μ	(cm)	Mean surface elevation of the microrelief
v_j	(-)	Weighting factor in the objective function for each measurement set
ω	(-)	Weighting factor for bimodal van Genuchten-Mualem
$\mathbf{x}$	(-)	Parameter vector
zl	(cm or m)	Lower water level

zu	(cm or m)	Upper water level
$z_{elev,min}$	(cm)	Lowest elevation of the soil surface
$z_{elev,max}$	(cm)	Highest elevation of the soil surface
z_m	(cm)	Distance from the bottom of the samples to the middle of the two tensiometer at evaporation experiments
$\mathbf{zu}_{obs}$	(m)	Vector with observations for DREAM optimization
$\mathbf{zu}_{sim}$	(m)	Vector with simulated *zu* for DREAM optimization

Abbreviations

1D	One-dimensional
DREAM	DifferRential Evolution Adaptive Metropolis
GHG	Greenhouse gases
MSO	Multi-step outflow experiment
pdf	Posterior density function
SOC	soil organic carbon
TDR	Time domain reflectometry
VG	Van Genuchten model
vGM	Van Genuchten-Mualem model
WRC	Water retention characteristic

Field sites

AK	Anklam
GM	Großes Moor
SF	Schechenfilz
SW	Spreewald
ZA	Zarnekow

Abstract

Biogeochemical processes in peat soils are primarily controlled by the soil moisture. To understand and accurately model soil moisture and hydrological dynamics in peatlands in general, knowledge about soil hydraulic properties is crucial. Up to now, most studies determined peat soil hydraulic properties in the laboratory on relatively small soil samples under steady state conditions. However, hydraulic properties determined under steady state conditions might not accurately simulate water flow under transient conditions. Due to the high content of soil organic matter, strong heterogeneity, and shrinkage and swelling of peat, accompanied by changing bulk densities, it is often questioned whether both the Richards' equation and standard hydraulic functions (e.g. the van-Genuchten-Mualem model) developed for mineral soils are suitable for describing peat soil moisture dynamics. Despite the significance for an accurate description of transient flow processes in the unsaturated zone, there are only a very few studies that actually test the applicability of those standard hydraulic functions. Furthermore, due to spatial variability and scale dependency, hydraulic properties obtained in the laboratory may not be representative for field conditions. Soil samples are often too small to sample a representative elementary volume, which adequately accounts for the soil heterogeneity and thus field scale processes. Further, samples in the laboratory may behave different than under field conditions, e.g. exhibit different shrinkage characteristics once cut from the coherent soil body and root system. Hence, for various applications, *in situ* measurements should be preferred because they obtain data in the natural environment. Unfortunately, there are several difficulties for the determination of the soil hydraulic properties at the field scale, especially for the determination of the soil water retention characteristics, which commonly require accurate *in situ* measurements of the water content. However, accurate *in situ* measurements of the water content are difficult to obtain in peat soils with high contents of soil organic matter.

The aim of this thesis is to improve the characterization of unsaturated hydraulic properties of peat soils and the understanding of hydrological processes in peatlands in general. This is done with two major topics at different scales (laboratory and field).

In the first major part, the applicability of the commonly applied Richards' equation and van Genuchten-Mualem based models was evaluated with transient laboratory evaporation experiments for a broad range of different peat types and other organic soils. In numerical simulations using HYDRUS-1D, the experimental data was used for an inverse estimation of

the soil hydraulic properties. The results demonstrate that peat soil moisture dynamics can be accurately modeled with the Richards' equation and with van Genuchten-Mualem based models if adequate model set-ups are chosen. For very wet conditions, macropores must be taken into account. This can be done by a simple macropore approach, using a bimodal van Genuchten-Mualem based model with only one additional fitting parameter, i.e. the macropore fraction. At dry conditions the van Genuchten-Mualem 'tortuosity' parameter τ can deviate very much from the default value of 0.5 often used for mineral soils. Optimizing τ did strongly reduce the model error at dry conditions when high pressure head gradients occurred. Both findings as well as the derived hydraulic parameters can improve practical applications like large scale simulations or pedotransfer function development.

In the second major part of this thesis, soil water retention characteristics were determined for a *Sphagnum* bog by a new developed *in situ* method. The method is applicable to shallow groundwater systems and builds on two assumptions: (1) in shallow groundwater systems with medium- to highly conductive soils the soil moisture profile is always close to hydrostatic equilibrium and (2) over short time periods, lateral fluxes into and out of the system are negligible. Given these assumptions hold true, the height of a water level rise due to a precipitation event mainly depends on the soil water retention characteristics, the precipitation amount, the initial water table depth and, if present, the microrelief. This dependency was used to determine soil water retention characteristics by Bayesian inversion.

As many near-natural peatlands, the *Sphagnum* bog investigated in the second major part of this thesis is characterized by a distinctive microrelief. For this case, the soil moisture profiles do not only depend on the soil water retention characteristics but also on the microrelief. To consider the microrelief effects on the soil moisture profiles and consequentially on the water level rises, a new conceptual one-dimensional expression was derived in a separate study. Thereby, the soil moisture profiles were calculated as a spatial average and reduced horizontally, as the soil volume covers only parts of the total volume. Combining the changed soil moisture profiles with the surface storage (fraction of the inundated areas) and dividing it by the water level change, results into a variable that is known as specific yield. Specific yield is often used for the analysis and the modeling of water level fluctuations.

Using the derived equation *in situ* soil water retention characteristics for the *Sphagnum* bog could be constrained to a plausible range for the low suction range. Results indicate that the approach is a promising tool to characterize field variability of soil water retention characteristics with commonly available data.

Overall, this thesis improves the characterization of unsaturated hydraulic properties for different types of peat and other organic soils at the laboratory and the field scale. Furthermore, results improve the understanding of the hydrological processes in peatlands in general. With the first major topic suggestions for a general improvement of the unsaturated hydrological modeling in peatlands could be made. The second major topic was separated into two studies. First, a novel one-dimensional expression for calculating specific yield for shallow groundwater systems with microrelief has been derived. The equation improves the general understanding of water level fluctuations of shallow groundwater systems with microrelief and can improve several applications, e.g. evapotranspiration estimates following the pioneering work of White (1932) or spatially distributed hydrological models. Furthermore, it is the basis for the development of a novel *in situ* method for determining soil water retention characteristics in shallow groundwater systems, which was successfully tested for a *Sphagnum* bog.

Zusammenfassung

Die biogeochemischen Prozesse in Torfböden hängen im Wesentlichen von der Bodenfeuchte ab. Um die Bodenfeuchte und die generellen hydrologischen Dynamiken in Mooren zu verstehen und zu modellieren, sind Kenntnisse über die hydraulischen Eigenschaften entscheidend. Bisher wurden in den meisten Studien die hydraulischen Eigenschaften von Torfen hauptsächlich im Labor an kleinen Bodenproben unter stationären Bedingungen bestimmt. Allerdings ist unsicher, ob stationär bestimmte hydraulische Eigenschaften den Wasserfluss unter instationären Bedingungen genau beschreiben können. Auf Grund des hohen Anteils an organischem Material, starker Heterogenität, Schrumpfung und Quellung, einhergehend mit sich ändernden Lagerungsdichten, ist fragwürdig, ob die Richards‘ Gleichung und Parametrisierungen der hydraulischen Eigenschaften (z.B. das van Genuchten-Mualem Model), welche für mineralische Böden entwickelt wurden, geeignet sind die Bodenfeuchtedynamik in Torfböden zu beschreiben. Trotz der Wichtigkeit einer genauen Beschreibung der instationären Flüsse in der ungesättigten Zone gibt es nur sehr wenige Studien, welche die Anwendbarkeit der oben genannten hydraulischen Standardfunktionen testen. Darüber hinaus müssen, auf Grund der räumlichen Variabilität und Skalenabhängigkeit, hydraulische Eigenschaften, welche im Labor bestimmt wurden, nicht zwangsläufig repräsentativ für Feldbedingungen sein. Bodenproben sind oft zu klein um ein repräsentatives Volumen aufzunehmen, welches adäquat die Bodenheterogenität und damit die Prozesse unter Feldbedingungen darstellt. Darüber hinaus können Bodenproben im Labor ein anderes Verhalten aufweisen als der Boden unter Feldbedingungen, z.B. durch ein unterschiedliches Schrumpfungsverhalten nachdem der Boden aus der zusammenhängenden Bodenmatrix und dem Wurzelsystem entnommen wurde. Daher sollten für viele Anwendungen *in situ* Messungen bevorzugt werden, da sie die hydraulischen Eigenschaften in der natürlichen Umgebung bestimmen. Unglücklicherweise gibt es verschiedene Schwierigkeiten für die Bestimmung von hydraulischen Eigenschaften unter Feldbedingungen. Dies betrifft insbesondere die Bestimmung der Retentionseigenschaften, für welche genaue *in situ* Messungen des Wassergehaltes nötig sind. Für Böden mit hohem Anteil an organischem Material sind diese allerdings schwer durchführbar.

Das Ziel dieser Arbeit ist es, die Bestimmung der ungesättigten hydraulischen Eigenschaften von Torfen sowie das generelle Verständnis über hydrologische Prozesse in Mooren zu verbessern. Dies erfolgte mit zwei inhaltlichen Schwerpunktthemen auf unterschiedlichen Skalen (Labor und Feld).

Im ersten Teil dieser Arbeit wurde die Anwendbarkeit der üblicherweise verwendeten Richards‘ Gleichung und die von van Genuchten-Mualem basierten Modellen für verschiedene Torfarten und andere organische Böden im Labor, mit Hilfe von instationären Verdunstungsversuchen, untersucht. In numerischen Simulationen mit HYDRUS-1D wurden hydraulische Eigenschaften mit den experimentellen Daten und inverser Parameteroptimierung bestimmt. Die Ergebnisse zeigen, dass die Bodenfeuchtedynamik in Torfen mit der Richards‘ Gleichung und van Genuchten-Mualem basierten Modellen gut beschrieben werden kann, wenn geeignete Modeleinstellungen vorgenommen werden. Unter nassen Bedingungen müssen Makroporen berücksichtigt werden. Dies kann mit einem vergleichsweise einfachen bimodalen van Genuchten-Mualem basiertem Model mit einem zusätzlichen Optimierungsparameter, dem Makroporenanteil, verwirklicht werden. Unter trockenen Bedingungen kann der van Genuchten-Mualem ‘Tortuositäts’ Parameter τ stark von dem oft für mineralische Böden verwendeten Wert 0.5 abweichen. Die Optimierung des Parameters τ reduzierte den Modelfehler unter trockene Bedingungen daher erheblich, wenn große vertikale Gradienten innerhalb der Bodensäule vorlagen. Beide Ergebnisse und die bestimmten hydraulischen Eigenschaften können praktische Anwendungen wie z.B. groß-skalige Modellierungen oder die Entwicklung von Pedotransferfunktionen verbessern.

Im zweiten Hauptteil dieser Arbeit wurden Wasserretentionseigenschaften, für ein *Sphagnum* Hochmoor, mit einer neu entwickelten *in situ* Methode bestimmt. Die Methode ist für Standorte mit oberflächennahen Grundwasserständen anwendbar und beruht auf zwei Annahmen: (1) in oberflächennahen Grundwassersystemen, mit mittleren bis hohen hydraulischen Leitfähigkeiten, ist das Bodenfeuchteprofil annähernd unter hydrostatischem Gleichgewicht und (2) für kurze Zeiträume sind laterale Flüsse aus dem System heraus vernachlässigbar. Unter den getroffenen Annahmen hängt der Anstieg des Wasserstands durch ein Niederschlagsereignis somit hauptsächlich von den Wasserretentionseigenschaften, der Niederschlagsmenge, dem initialen Wasserstand und, falls vorhanden, dem Mikrorelief ab. Diese Abhängigkeit wurde verwendet um Wasserretentionseigenschaften mit bayesscher Inversion zu bestimmen.

Wie in vielen naturnahen Mooren, ist das *Sphagnum* Hochmoor, welches im zweiten Hauptteil der Arbeit untersucht wurde, durch ein ausgeprägtes Mikrorelief gekennzeichnet. In diesem Fall hängen die Bodenfeuchteprofile nicht nur von den Wasserretentionseigenschaften, sondern auch von dem Mikrorelief ab. Um den Effekt des Mikroreliefs auf die Bodenfeuchteprofile und daraus folgend auf die Anstiege des

Wasserstands zu berücksichtigen, wurde eine neue konzeptionelle, eindimensionale Gleichung in einer separaten Studie hergeleitet. Dabei wurden die Bodenfeuchteprofile als räumlicher Durchschnitt interpretiert und horizontal reduziert, da das Bodenvolumen in diesem Fall nur einen Teil des Gesamtvolumens umfasst. Durch die Kombination der geänderten Bodenfeuchteprofile mit dem Oberflächenspeicher (Anteil der überschwemmten Flächen) und durch Division mit der Wasserstandsänderung erhält man den Speicherkoeffizienten eines Bodens. Der Speicherkoeffizient wird häufig für die Analyse und die Modellierung von Wasserstandsänderungen verwendet.

Mit Hilfe der hergeleiteten Gleichung konnten Wasserretentionseigenschaften für das *Sphagnum* Hochmoor, für niedrige Unterdrücke, zu plausiblen Werten eingegrenzt werden. Die Ergebnisse deuten darauf hin, dass der Ansatz eine vielversprechende Methode ist, um die Feldvariabilität der Wasserretentionseigenschaften mit häufig verfügbaren Daten zu beschreiben.

Insgesamt verbessert diese Arbeit die Charakterisierung von ungesättigten hydraulischen Eigenschaften für verschiedene Torfarten und andere organische Böden unter Labor- und Feldbedingungen, sowie das allgemeine Verständnis über die hydrologischen Prozesse in Mooren. Im ersten Hauptthema konnten Empfehlungen für ein generelles Verbessern der ungesättigten hydrologischen Modellierung gemacht werden. Das zweite Hauptthema wurde in zwei separate Studien aufgeteilt. Als erstes wurde eine neue eindimensionale Gleichung für die Berechnung des Speicherkoeffizienten für Grundwassernahe Standorte mit Mikrorelief hergeleitet. Die Gleichung verbessert das allgemeine Verständnis über Wasserstands Schwankungen von grundwassernahen Standorten mit Mikrorelief, wodurch verschiedene Anwendungen profitieren können, z.B. die Berechnung der Evapotranspiration, basierend auf der wegweisenden Arbeit von White (1932) oder flächendifferenzierte hydrologische Modelle. Darüber hinaus ist sie die Grundlage für die Entwicklung einer neuen *in situ* Methode für die Bestimmung von Wasserretentionseigenschaften von Böden mit oberflächennahen Grundwassersystemen, welche erfolgreich für ein *Sphagnum* Hochmoor getestet wurde.

Acknowledgements

First of all, I would like to thank Prof. Dr. Konrad Miegel who generously supervised this work at the University Rostock.

I wish to thank Prof. Dr. Andy Baird for accepting to examine this thesis and the review for section 3 of this thesis that included several helpful comments and suggestions.

Special thanks goes out to Dr. Michel Bechtold who supervised this work at the Thünen Institute. He supported my work with his excellent ideas and comments. His enthusiastic nature about scientific issues not only inspired me, but also helped me with various challenges during this work. He is the best supervisor whom I imagine. Thanks Michel.

The entire ‘Moorteam’ would not work without Dr. Bärbel Tiemeyer. From beginning to the end she supported me in way that goes far beyond the helpfulness of most people. She always took the time to answer questions and gave excellent, constructive and, if necessary, critical comments. She taught me lots of things about scientific work. Thanks Bärbel.

I also wish to thank Dr. Enrico Frahm. He gave me the opportunity to work on this interesting topic and always supported me in everything. Without his enthusiastic field and laboratory work many parts of this thesis would not have been possible. Respect for dealing with UP. It’s always nice to have competent and funny soccer talks. Let’s Go Hansa. Thanks Enrico.

I would like to express my thanks to Dr. Annette Freibauer. It is impressive to see her way to be the boss. Always strives to reduce Greenhouse gas emissions from peatlands into the atmosphere, she already managed to create a great working atmosphere. Thanks Annette.

Great thanks goes out to the entire ‘Moorteam’. It is a great pleasure to work with nice people who bring fun and interesting conversations into your daily life. Thanks Annelie, Annette, Arndt, Bärbel, Johanna, Katharina, Merten, Michel, Steffan and Thomas.

During this work there have been hundreds of technical problems which could never be solved without the competent work of various technicians. Particular noteworthy is the enormous support of Dirk Lempio, Maik ‘Gyver’ Hunzinger and Mark Jantz.

I also want to thank Andreas Laggner for being a dictionary about every electronic device ever build on this planet. Thanks Andy.

Christian, be ready for the ‘Große Hafenrundfahrt’ and remember R.F. Grima. The challenge goes on!

Personally, I would like to thank my parents for everything and making me what I am today.

Finally, I would like to thank my family for bringing so much fun and happiness into my live. Thanks Anne and Felina.

1 Introduction

1.1 Motivation

Peatlands are water-dependent ecosystems with specific hydrological conditions. In the upper peat layer fluctuating shallow water levels lead to frequently varying conditions controlling the physical, chemical and biological processes (Bragazza et al., 2006; Dimitrov et al., 2010; Holden et al., 2004; Lafleur et al., 2005). The peat soil hydraulic properties crucially influence these site specific water level fluctuations as well as time-variable fluxes like evapotranspiration, groundwater recharge, surface runoff and interflow.

Peatlands have an substantial influence on the hydrological cycle in terms of water quantity and quality (Bullock and Acreman, 2003). Furthermore, the hydrology of peatlands influences carbon sequestration and release processes, nutrient availability and biodiversity (Grover and Baldock, 2013; Holden, 2005; Joosten et al., 2012; Waddington et al., 2015). Worldwide peatlands are drained for economical uses with consequences for the catchment hydrology, physical and chemical properties of peat, water chemistry and biodiversity. In order to predict the influences of the hydrological disturbances or modifications in the course of restoration projects, understanding of the hydrological processes in peatlands is crucial.

Therefore, the understanding of water flow processes in the unsaturated zone is of major importance. Water flow in the unsaturated zone is commonly modeled with the Richards' equation (Richards, 1931). Therefore an accurate knowledge about the soil hydraulic properties, namely the soil water retention characteristic (*WRC*) and the unsaturated hydraulic conductivity function (*K(h)* or *K(θ)*, in the following referred as *K(h)*) is needed.

The soil hydraulic properties of peat soils are unique and dependent on the original plant substrate (Baden and Eggelsmann, 1963). Undecomposed peat soils are characterized by a high saturated hydraulic conductivity (K_s) (Morris et al., 2015), high saturated water contents (up to 98%) (Paavilainen and Päivänen, 1995) and abrupt dewatering capacities with decreasing pressure heads (increased suction) (Bartels and Kuntze, 1968; Letts et al., 2000; Price et al., 2008). Proceeding decomposition of the organic particles results in smaller pores and higher bulk densities (Boelter, 1969; Moore et al., 2015) and thus in decreased K_s values (Morris et al., 2015). Therefore, the dewatering capacity of decomposed peat soils is decreased although they still have high moisture contents compared to mineral soils. Under changing moisture regimes, peat soils are characterized by distinctive shrinkage and swelling

which leads to changing pore space geometries and therefore to temporally variable hydraulic properties (Hendriks, 2004; Price and Schlotzhauer, 1999).

Commonly hydraulic properties are determined in laboratory experiments imposing steady state (e.g. hanging water column, pressure plate apparatus) (Reynolds et al., 2002b) or transient conditions (e.g. evaporation experiments, multi-step outflow experiments) (Gardner and Miklich, 1962; Hopmans et al., 2002; van Dam et al., 1994; Wind, 1968). An alternative approach is the hydraulic characterization under field conditions with infiltration, borehole and well permeameter methods or by simultaneous measurements of the water content (θ) and pressure head (Durner and Lipsius, 2005; Reynolds et al., 2002a). Once measured, hydraulic properties can be parameterized by hydraulic functions describing the measured data by a continuous function over the whole moisture range. One of the most commonly applied function is the model of van Genuchten–Mualem (*vGM*) (van Genuchten, 1980; Mualem, 1976). The parameters of the hydraulic functions can be determined with inverse parameter optimization. Thereby the Richards' equation is solved numerically and the parameters are optimized by minimizing the deviations between measured and predicted state or flux variables (Kool et al., 1987). For mineral soils transient laboratory experiments are frequently combined with inverse parameter optimization to investigate the model performance of the Richards' equation and the influence and sensitivity of certain *vGM* parameters on model results (Romano and Santini, 1999; Šimůnek et al., 1998).

Various studies determined peat soil hydraulic properties in the laboratory (Bartels and Kuntze, 1973; Boelter, 1969; Grover and Baldock, 2013; Ilnicki, 1982; Letts et al., 2000) and plenty of them parameterized the soil hydraulic properties with the *vGM* model (Kechavarzi et al., 2010; Olszta and Kowalski, 1996; Price et al., 2008; Price and Whittington, 2010; Thompson and Waddington, 2013; Weiss et al., 1998). Most studies derived the soil hydraulic properties under static equilibrium conditions. Only very few studies determined hydraulic properties of peat soils with dynamic transient experiments combined with inverse parameter optimization (Gnatowski et al., 2010; Schwärzel et al., 2006). However, soil hydraulic properties which are determined under static equilibrium conditions might not be applicable to simulate water flow under transient conditions as hydraulic properties might depend on the dynamics of the water flow (Durner and Flühler, 2005). Furthermore, the applicability of the Richards' equation on peat soils is questionable, as the fundamental assumption that the soil matrix has a static pore space geometry is not fulfilled, due to the distinctive shrinkage and swelling characteristics of peat soils under changing moisture regimes (Clothier and Scotter,

2002; Price and Schlotzhauer, 1999). Hence, an aim of this thesis is to evaluate how accurate the dynamic and nonlinear water flow in the unsaturated zone can be modeled with the Richards' equation.

Furthermore, to my knowledge, no study has focused on the influence and sensitivity of different *vGM* parameters on the model performance of hydrological models in peatlands so far. This is crucially important for a better description of vertical moisture distribution profiles and water level fluctuations in peatlands and therefore a part of this thesis.

In peatlands macropore flow is an important process, leading to rapid infiltration and drainage in the upper peat layer and therefore to rapid changes in near-surface water contents (Dimitrov et al., 2010). Empirical dual/multi-porosity models with effective parameters and assuming a single domain represent the simplest concept to account for macropore flow. Durner (1994) combined two *vGM* models weighted by the factor ω to a 'bimodal' function representing the entire pore system. Thus, the shape of the *WRC* and *K(h)*, influenced by the macropores, can be depicted more accurately than treating the soil as a unimodal pore system. However, to my knowledge no study tried to describe macropore flow in peat soils by this comparatively easy approach, although results are often similar to more complex concepts (Köhne et al., 2009). Hence, this thesis evaluates the applicability of the multimodal *vGM* based model of Durner (1994) (for the *WRC*) and Priesack and Durner (2006) (for *K(h)*) to describe macropore flow in peat soils.

Many peatlands are characterized by a distinctive microrelief that influences groundwater level dynamics at shallow water levels when partial inundation occurs and as well at low water levels due to the heterogeneously distributed soil volume. Water level dynamics are often analyzed and modeled with the variable specific yield (S_y). For homogeneous zones of deeper groundwater systems, this value is constant. In contrast, for shallow groundwater systems with homogeneous soils, it changes with depth, depending on the distance to the soil surface (Duke, 1972; Crosbie et al., 2005; Cheng et al., 2014; Wang and Pozdniakov, 2014). A conceptual one-dimensional (1D) expression for calculating S_y as spatial average including any microrelief effect, applicable for different soil hydraulic functions and soil surface elevation frequency distributions, would improve the detailed physical and quantitative understanding of water level fluctuations and estimations about the ability of the system to store or release water. Hence, the development of a 1D expression for calculating S_y as spatial average including any microrelief effect is another focus of this work. Furthermore, it is the

fundamental basis for the third study of this thesis which has the aim to develop a new method for the *in situ* determination of *WRC* for shallow groundwater systems.

This is done because hydraulic properties obtained in the laboratory often differ with *in situ* determined hydraulic properties and *in situ* determined hydraulic properties might be more representative for field conditions. Unfortunately, for shallow groundwater systems, knowledge about soil hydraulic properties at the field scale is scarce, especially for the determination of the *WRC*. Thus, the development of a new *in situ* method for the determination of *WRC* in shallow groundwater systems, with commonly available data, is an aim of this thesis as mentioned above.

1.2 Hydrological and ecological functions of peatlands

Peatlands are widely known for their important hydrological, ecological, and carbon storage functions. Although they cover only about 3 % of the land surface worldwide (Maltby and Proctor, 1996), they store about 10 % of the available freshwater resources (Holden, 2005) and about 15 – 30 % of the world's soil carbon (Limpens et al., 2008).

General peatlands can be distinguished between ombrotrophic bogs (primarily dependent on precipitation) and minerotrophic fens (primarily dependent on groundwater input) (Du Rietz, 1949; Du Rietz, 1954; Wheeler and Proctor, 2000). Water levels near the surface are needed for peat soils to develop from dead plant material under anoxic conditions. Hence, peatlands are dependent on shallow water levels and peat soils consist of partially decomposed plant residuals (Holden, 2005; Winde, 2011). The hydrological functioning of peatlands is often described by a two-layer system, distinguishing between an upper active layer ('acrotelm') and a more decomposed lower layer ('catotelm') (Ingram, 1978; Ingram, 1983; Ivanov, 1981; Morris et al., 2011). Usually, the hydraulic conductivity is high in the 'acrotelm' and low in the 'catotelm'. Fluctuating water levels are within the 'acrotelm' while the 'catotelm' is permanently saturated (Holden and Burt, 2003a; Holden, 2005; Price et al., 2003). The fluctuating shallow water level depth dynamics within the 'acrotelm' as response to boundary fluxes are primarily controlled by the soil hydraulic properties in and above the range of the water level fluctuations. Furthermore, the hydraulic properties strongly control the time-variable boundary fluxes like evapotranspiration, groundwater recharge, surface runoff and interflow, and consequently the whole water balance.

Peatlands support a wide range of important ecosystem services and substantially influence the hydrological cycle (Bullock and Acreman, 2003). Peat soils can contain up to 98% water

per volume (Paavilainen and Päivänen, 1995) and thus store or release large amounts of water. Hence, peatlands are often reported for their ability to either attenuate or accentuate floods (Blackwell et al., 2002; Daigneault et al., 2012; Holden and Burt, 2003a; Holden et al., 2004; Ogawa and Male, 1986). Furthermore, they play an important role in terms of water supply and purification (Daigneault et al., 2012).

Peatlands are of special importance because of their role in the global carbon cycle (Limpens et al., 2008). Approximately 455 x 10^{15} g carbon is stored in peat soils (Gorham, 1991), twice as much as the total biomass of all forests (Joosten et al., 2013). By the accumulation and conservation of dead plant material, peatlands act as a natural sink of greenhouse gases (GHG) (Byrne et al., 2004; Worrall et al., 2010) and as a sink of nutrients, e.g. nitrate and phosphate (Kellogg and Bridgham, 2003; Silvan et al., 2005). From the Holocene to now, peatlands have contributed to global cooling (Frolking and Roulet, 2007; Limpens et al., 2008). Furthermore, peatlands can regulate the local climate, they are habitats for unique plants and birds and they have an important meaning as recreation areas and as cultural heritage (Joosten et al., 2012).

However, worldwide natural peatlands are drained for economical uses like agriculture, forestry or peat harvesting (Maltby, 1991), e.g. in Germany about 95% are drained (Joosten and Couwenberg, 2012). Peatlands react very sensitive to changes in their specific hydrological conditions, with consequences for the catchment hydrology, physical and chemical peat properties, water chemistry and biodiversity. By drainage, anoxic conditions turn to oxic conditions. Thus, the microbiological activity is increased, leading to peat degradation, subsidence and reduced accumulation of plants. As a result, soil organic carbon (*SOC*) contents in peat soils decrease and peatlands turn from a sink into a source of GHGs, mostly CO_2 and N_2O (Maljanen et al., 2010). Furthermore, the enhanced mineralization causes the release of nutrients, especially nitrate, phosphate and dissolved organic carbon (Holden et al., 2004; Kellogg and Bridgham, 2003; Silvan et al., 2005). Thus, peatlands became a source of pollution.

The biogeochemical processes during peat degradation are primarily governed by the availability of oxygen, which is a function of soil moisture, which is in turn controlled by the soil hydraulic properties and the time-variable boundary conditions (Kechavarzi et al., 2010).

1.3 The importance of hydrological models for peatlands

Whether peatlands are drained or not, the understanding of the hydrology of peatlands is from particular importance, as it is the most important condition influencing peatland ecology, functions and processes (Rydin and Jeglum, 2013). Hydrological models can improve the understanding or prediction of hydrological conditions by a physical or statistical representation of a hydrological system and its processes on different scales (Karamouz et al., 2012).

Thus, water resource management strategies, like the estimation of groundwater recharges and discharges for a sustainable drinking water extraction, the estimation of groundwater flow directions and velocities, or the calculation of drain distances for drainage and wetting purposes can be supported (Fraser et al., 2001; Gilvear et al., 1997; Melesse and Abtew, 2015; Querner et al., 2010; Robinson, 2008; Taniguchi et al., 2008) . For flood control, hydrological models can improve the estimate of the free water storage capacity and water release behavior before and after heavy rainfall periods for the prediction accuracy of forecasting models (De Roo et al., 2003). Further, hydrological models can support water level monitoring, interpretation and modification in the course of restoration projects, which are of crucial importance for nature conservation. Modeling studies may be helpful for the understanding and quantification of solutes and nutrients release and transport in streamflows or groundwater (Hoag and Price, 1997; Kadlec and Hammer, 1988; Van Beek et al., 2007). With respect to global warming, hydrological models of peatlands can improve the understanding and quantification of GHG emission dynamics and the influences of climate change on water budgets. Rewetting helps to mitigate the negative effects caused by the drainage of peatlands. Therefore, numerical simulations of the water flow in the saturated and unsaturated zone are needed to develop optimal rewetting strategies.

As mentioned in section 1.2, both the hydrological and the biogeochemical processes in peatlands are strongly dependent on the changing hydrodynamic conditions in the unsaturated zone, which are commonly modeled with the Richards' equation. For the application of the Richards' equation, the hydraulic properties, i.e. the *WRC* and *K(h)* need to be known. Hence, to understand and accurately model soil moisture dynamics and peatland hydrological functioning in general, knowledge about soil hydraulic properties is crucial.

1.4 Soil hydraulic properties

1.4.1 Physical and hydraulic properties of peat soils

Flow processes in peatlands vary widely depending on the physical and hydraulic properties of the peat soil. Those are unique and dependent on the composition of the vegetation, plant origin, degree of decomposition, water supply and chemical water quality. By definition, peat soils have high *SOC* contents (Ad-hoc-AG Boden, 2005). Further, peat soils are characterized by porosities (ε) up to 98% (Paavilainen and Päivänen, 1995). Dependent on the soil moisture, peat soils shrink and swell accompanied by changing pore space geometries. This leads to temporal variable hydraulic properties (Hendriks, 2004; Price and Schlotzhauer, 1999). Dependent on the original plant substrate, peat soils are characterized by a high spatial variability of the physical and hydraulic properties (Baden and Eggelsmann, 1963). Within fields and regions the variability can be further enhanced by peat decomposition due to drainage causing decreasing ε and *SOC* (Beckwith et al., 2003; Holden and Burt, 2003a).

Near the surface, pristine peatlands are typically characterized by high hydraulic conductivities, due to large pore sizes of the living and lightly decomposed plant material (Boelter, 1969; Letts et al., 2000). Thereby macropore flow is an important process leading to rapid changes in near-surface water contents (Dimitrov et al., 2010). In the lower peat layers the peat material is more dense, compressed and decomposed. Thus, pore sizes are decreased and less interconnected and consequentially the peat has a lower saturated hydraulic conductivity (K_s) (Boelter, 1969; Grover and Baldock, 2013; Morris et al., 2015). The *WRC* of pristine peat soils are characterized by an abrupt dewatering capacity with decreasing pressure heads (higher suctions) (Bartels and Kuntze, 1968; Letts et al., 2000; Price et al., 2008).

Due to artificial drainage, the physical and hydraulic properties of peat soils change. By decomposition, the size of organic particles decreases, which in turn results in smaller pores (Boelter, 1969). This leads to lower saturated water contents, decreasing hydraulic conductivities (Morris et al., 2015) and a less steep dewatering behavior with decreasing pressure heads (Grover and Baldock, 2013).

1.4.2 Determination of soil hydraulic properties

Hydraulic properties such as the *WRC* and the *K(h)* can be determined by various methods at different scales. Generally, **laboratory** and **field** methods and **direct** and **indirect** determination can be distinguished (Durner and Lipsius, 2005). Direct methods obtain hydraulic properties by direct measurements in the laboratory or field. Indirect methods

estimate hydraulic properties by more easily measured data using regression, neural network algorithms or close-form equations (Durner and Lipsius, 2005). A briefly introduction is given in the following.

For measurements of *K(h)* it should be mentioned that for both laboratory and field applications measurements tend to be highly variable in space and time, therefore spatial and/or temporal replications are required (Reynolds et al., 2002a).

Laboratory methods

In the laboratory, hydraulic properties are measured on small soil samples. Standard methods for the *WRC* are the hanging water column and the pressure plate apparatus. For both methods the samples are placed on a porous plate and dewatered progressively with different pressure heads, until hydraulic equilibrium is reached in the sample. The hanging water column and the pressure plate apparatus are often combined. Due to the dissolution of gases from the water, the hanging water column apparatus is limited to pressure heads of approximately 0 to -850 cm (Dane and Hopmans, 2002). For lower pressure heads the pressure plate apparatus can be used. For both methods θ is determined gravimetrically by drying the samples in an oven at the end of the experiment. *WRC* derived by hanging water columns and the pressure plate apparatus are given as 'point'-like measurements for the pressure heads, which are imposed for dewatering. Waiting for hydraulic equilibria can be time consuming.

An alternative approach for the determination of the soil matrix potential is the chilled-mirror dew point method (Schelle et al., 2013). Thereby the point at which condensation appears is detected by a photoelectric cell with simultaneous measurements of the temperature. The relative humidity is calculated from these two values and then used in the Kelvin equation (Campbell et al., 2007) to calculate the total potential of the soil water (Schelle et al., 2013). For the WP4C Potentiameter® accuracies are described in the operator's manual with 1% for matrix potentials from approximately $5 \cdot 10^4$ to $3 \cdot 10^6$ cm and with ~500 cm for matrix potentials from $0 - 5 \cdot 10^4$ cm (Decagon Devices, 2014). Following this, the accuracy is increasing with increasing matrix potentials.

In the laboratory, hydraulic conductivities are commonly measured at particular saturations. Thereby an constant head or constant flux boundary condition is applied to the top or bottom of the sample, imposing steady state conditions (Durner and Lipsius, 2005; Reynolds et al., 2002b). Calculations are based on Darcy's law (Darcy, 1856). Constant head or flux experiments are widely used for the determination of K_s. To measure the unsaturated

hydraulic conductivity, negative pressure heads can be applied at the lower boundary. Thereby "unit gradient" conditions within the soil column must be adjusted by the flux into the top boundary. However, "unit gradient" conditions are hard to adjust.

Therefore, dynamic transient laboratory experiments such as evaporation (Gardner and Miklich, 1962; Schindler, 1980; Wendroth et al., 1993; Wind, 1968) or multi-step outflow (MSO) experiments (van Dam et al., 1994; Hopmans et al., 2002) are becoming increasingly popular. For both methods, the *WRC* and *K(h)* relationships can be obtained simultaneously from one soil sample. Therefore, pressure heads and the fluxes out of the soil column need to be measured.

In evaporation experiments, the soil sample is placed on a weighting scale. Mean pressure heads are measured for each time step (h_i) with at least two tensiometers. The mean water content (θ_i) for each time step is calculated by the weight loss during the experiment and by gravimetrical determination of the total θ at the end of the experiment. Following this, the *WRC* can easily be obtained directly from the measurement data. The hydraulic conductivity (K_i) corresponding to h_i between two time steps can be derived by inverting Darcy's law (Peters and Durner, 2008). Evaporation experiments terminate when gases dissolute from the water at pressure heads of approximately -800 cm. Therefore hydraulic properties can be obtained for a pressure head range from approximately 0 – -800 cm. However, at pressure heads close to zero when the pressure conditions are close to hydrostatic equilibrium conditions, K_i cannot be determined exactly by evaporation experiments due to the high hydraulic conductivity (Wendroth et al., 1993; Šimůnek et al., 1998). The correct measurement of low gradients is limited by the accuracy of the tensiometers. Furthermore, evaporation experiments rely on linearization assumptions about the vertical distributions of θ and the pressure heads. With decreasing pressure heads they are only approximately fulfilled and nonlinearity increases. Peters and Durner (2008) therefore introduced an integral approach eliminating linearization errors.

In MSO experiments, the soil sample is placed on a porous plate and then dewatered stepwise with decreasing pressure heads (increasing suctions) (Schelle et al., 2010). In contrast to most other common methods, hydraulic properties can be determined for watering and dewatering conditions. However, similar to the hanging water column and pressure plate apparatus, MSO experiments require hydraulic equilibria within the soil column and consequently this can be time consuming. Furthermore, the hydraulic properties are only obtained for the imposed suctions and not over the whole pressure head range as in evaporation experiments.

Both, evaporation and multistep-outflow experiments can determine the hydraulic properties directly. An advantage of the direct determination is the possibility to account for decreasing soil volumes caused by shrinkage in the calculation of the volumetric water content.

Field Methods

There are several field methods available for determining the hydraulic properties of a soil *in situ*. Field methods can be divided into infiltration and borehole or well permeameter methods. Most field methods obtain hydraulic conductivities. It should be mentioned that at field conditions, saturation usually cannot be achieved due to air entrapment in the porous medium. Thus, typically the field saturated hydraulic conductivity is measured (Reynolds et al., 2002a). For simplification the field saturated hydraulic conductivity is referred to as K_s in the following.

There are numerous infiltration based methods for obtaining hydraulic conductivities. Very popular and widely used are ring infiltrometer methods with ponded constant head conditions, adjusting a quasi-stationary flux which is controlled by K_s (Durner and Lipsius, 2005). To guarantee downward flow and avoid lateral fluxes during infiltration, the usage of double ring infiltrometer is advisable. Ring infiltrometer methods can be combined with time domain reflectometry (TDR) measurements to measure *K(h)* for pressure heads down to -60 cm (Parkin et al., 1995). An alternative measurement technique is given by tension disc infiltrometer, which are widely used for the determination of *K(h)* close to saturation and the effect of macropores and preferential flow paths on infiltration (Baird, 1997; Reynolds et al., 2002a). Thus, water infiltration is provided by a reservoir tower and pressure heads, either positive or negative, are imposed with a bubble tower above the surface with a moveable air-entry tower tube (Durner and Lipsius, 2005). With tension disc infiltrometer, near-saturated hydraulic conductivities for pressure heads of approximately > -25 cm can be measured (Bodhinayake et al., 2004).

Borehole and well permeameter methods are based on removing or adding water in an auger-hole or a piezometer. By monitoring the subsequent temporal water level rise or decline, K_s can be calculated. Borehole methods such as bail tests (Hvorslev, 1951) are used for shallow groundwater depths. For greater groundwater depths, a piezometer can be used. Borehole and well permeameter methods integrate K_s values over the soil horizons, at which the water level is raised or declined.

Measuring of the *WRC in situ* is difficult, but possible by simultaneous monitoring of pressure heads and θ. This can be combined with infiltration methods for determining both the *WRC* and *K(h)*.

Pedotransfer functions

Pedotransfer functions obtain hydraulic properties indirectly from soil properties, which are easier to measure. Thereby, statistical models estimate the hydraulic properties by soil properties like soil texture, ε, bulk density or *SOC* content (Schaap, 2005). To my knowledge, in contrast to mineral soils, pedotransfer functions are not available for peat soils and therefore will not be discussed any further in this thesis.

Hydraulic functions

Hydraulic functions describe measured data by a continuous function over the whole moisture range. Several functions have been developed in the last decades (Brooks and Corey, 1964; Campbell, 1974; van Genuchten, 1980; Ippisch et al., 2006; Kosugi, 1996; Peters, 2013), whereby the van Genuchten-Mualem model (*vGM*) (van Genuchten, 1980; Mualem, 1976) has become one of the most commonly applied hydraulic functions. Mualem (1976) derived *K(h)* from the pore-size distribution of a soil. Through the interpretation of the *WRC* as a statistical measure of its equivalent pore size distribution, *K(h)* and the *WCR* can be described with the same parameters. In the case of the *vGM* model two additional parameters, K_s and τ, are needed for *K(h)*. Clearly, K_s defines the saturation point at *K(h)*. The parameter τ accounts for the tortuosity structure of the connected pores.

The close-form equation of van Genuchten is commonly used to infer *K(h)* by the *WRC* of a soil, which are comparably easy to measure. Therefore K_s needs to be measured separately. The pore-connectivity parameter τ can only be determined by conductivity measurements at different θ. Based on data from 45 mineral soils (clays, loams and sands), Mualem (1976) proposed an average value of 0.5 for the parameter τ. However, this value can differ with different kinds of soils (Schuh and Cline, 1990; Yates et al., 1992). For peat soils this is more likely, as τ is related to the organic matter content (Wösten et al., 1995).

The *vGM* model can only account for a unimodal pore size distribution, neglecting macropores. A simple concept to account for macropores are bi-/multimodal hydraulic functions which combine two or more *vGM* models weighted by the factor ω (Durner, 1994; Priesack and Durner, 2006).

Inverse parameter optimization

Inverse parameter optimization of transient flow processes is widely used for the estimation of hydraulic properties. Thereby, the model parameters which give the best fit to the measured data are estimated by minimizing the deviation between measured and predicted state or flux variables (Kool et al., 1987; Vrugt and Dane, 2005). The advantage of the inverse approach is that the most suitable parameter values or ranges are determined simultaneously and thus consistently for both the *WRC* and *K(h)* without linearization assumptions.

1.4.3 Scale dependency and method selection

In the preceding sections various methods for the determination of soil hydraulic properties have been described. However, obtaining representative soil hydraulic properties, including their field variability and scale dependency, remains an ongoing research challenge in soil science (Jury et al., 2011). Optimally, hydraulic properties should be obtained for a representative elementary volume of the soil heterogeneity that is characteristic for the specific porous medium and condition. However, it is virtually impossible to define a representative elementary volume as enlarging the volume will lead to the inclusion of new structural elements of larger size (Durner and Flühler, 2005). Thus, obtaining hydraulic properties is always a matter of scale and choice of an appropriate method, which in turn always depends on the scale of interest, as all methods present specific advantages.

Both laboratory and field methods provide several advantages and disadvantages. In the laboratory, the experimental conditions can be thoroughly controlled and experiments can be conducted on several replications. Furthermore, hydraulic properties can be determined separately for every soil layer and over a wide moisture range. However, sample sizes are commonly very small and determined hydraulic properties may not be representative for field conditions (Basile et al., 2003). Additionally, soil samples may behave differently in the laboratory compared to the soil under field conditions, as it is the case for clay and peat that present different shrinkage characteristics once cut from the coherent soil body and root system (Mitchell, 1991; Mitchell and Van Genuchten, 1992).

In contrast to laboratory methods, field methods obtain hydraulic properties in their natural environment as spatial average, including the influence of local-scale heterogeneity, preferential pathways and the interactions between different soil layers (Durner and Lipsius, 2005; Reynolds et al., 2002a; Wollschläger et al., 2009). This provides a major advantage for large scale applications. However, there are several difficulties of common *in situ* methods.

Hydraulic conductivities obtained from borehole/well permeameter based methods are substantially influenced by the lateral fluxes of the soil layer with the highest K_s value. Thus, if K_s values of the single soil layers are needed, laboratory measurements should be preferred. In shallow groundwater systems, which comprise many peatlands, infiltration methods are problematic due to the influence of the shallow water level that lowers infiltration. The *in situ* determination of the *WRC* is limited to simultaneous monitoring of pressure heads and θ as 'point'-like measurements. This requires accurate measurement equipment. Measurements of θ often require soil specific calibrations, especially for soils with high *SOC* contents and distinctive shrinkage and swelling characteristics (Nagare et al., 2011; Pepin et al., 1992; Shibchurn et al., 2005). Thus, unfortunately knowledge about *WRC* at the field scale is scarce.

Therefore it is common practice to determine hydraulic properties in laboratory and scale them to larger soil volumes. If upscaled hydraulic properties are representative for larger scales depends on the soil type and heterogeneity as well as the envisaged accuracy of the specific issue. If field data is available, the accuracy of estimated hydraulic parameters should be evaluated by forward predictions.

Inverse parameter optimization provides a promising approach for the determination of soil hydraulic properties in laboratory and at field sites, as it accounts for the highly dynamic and nonlinear water flow in the unsaturated zone with a physical process based representation of the system. In the laboratory, boundary conditions can be accurately measured and therefore obtained hydraulic properties might be less uncertain for the specific sample than for field applications for which the required measurement inputs (e.g. precipitation, evaporation, surface- and groundwater in- and outputs) besides the observed state variables are often difficult to measure and uncertain.

Besides the major challenges of determining soil hydraulic properties like scale dependency and field variability, there are several difficulties, such as hysteresis, water repellency, compressibility, shrinkage and swelling. Those might be enhanced by the physical soil properties of peat soils and are discussed in section 5.2.

1.5 Aims and objectives

The hydrology of peatlands is the most important condition influencing peatland ecology, functions and processes (Rydin and Jeglum, 2013). Understanding peatland hydrology is strongly related to the understanding of unsaturated zone processes. In this context, the central theme of this thesis is to improve the characterization of unsaturated hydraulic properties of peat soils and the understanding of hydrological processes in peatlands in general. Accordingly, standard hydraulic functions were evaluated and peat soil hydraulic properties were determined at different scales, as soil hydraulic properties strongly depend on the scale of interest.

Considering that, first, laboratory evaporation experiments for different peat and other organic soils were conducted. The transient experiments had the following objectives:

- investigate the applicability of the Richards' equation for peat and other organic soils
- investigate the applicability of uni- and bimodal *vGM* based models to describe the hydraulic gradients and water fluxes for different peat and other organic soils and give recommendations how model parameter configuration should be set for an accurate modeling of the hydrological conditions of peatlands
- investigate the applicability of a simplified bimodal *vGM* based model to account for macropore flow in peat and other organic soils
- determine hydraulic properties for a broad range of different peat and other organic soils

Second, for an accurate understanding of water level fluctuations, knowledge about S_y is crucial. In uneven landscapes S_y is influenced by the microrelief. Thus, a conceptual 1D expression to calculate S_y for shallow groundwater systems with microrelief was derived with the following objectives:

- derive the mathematical basis for the development of a new *in situ* method for the determination of *WRC* in terms of the third part (section 4) of the thesis
- improve the physical and quantitative understanding of shallow water level fluctuations which are dependent on the *WRC*, the boundary fluxes in and out of the system and, if present, the microrelief
- improve the possibility to estimate the ability of shallow groundwater systems either to store or to release water and therefore contribute to a better estimation of boundary fluxes in and out of the system, in particular evapotranspiration and groundwater

recharge

Third, based on the derived 1D expression a new *in situ* method for the determination of the *WRC* was developed. The particular objectives were:

- provide a simple approach for the *in situ* determination of *WRC* for shallow groundwater systems with commonly available data
- determine the *WRC* of a *Sphagnum* peat *in situ* as spatial average (approximately several meters) around a dip well
- characterize the field variability of the *WRC* within a *Sphagnum* bog

1.6 Thesis Outline

The main results of this thesis and their discussion are given in section 2 to 4 and are based on three manuscripts that have been published or which are currently under review in international peer-reviewed journals. Fundamentals about peatland hydrology and soil hydraulic properties, given in the preceding introduction, are partly repeated in each of the following chapters.

Chapter 2: Dettmann, U., Bechtold, M., Frahm, E., & Tiemeyer, B. (2014): On the applicability of unimodal and bimodal van Genuchten–Mualem based models to peat and other organic soils under evaporation conditions. Journal of Hydrology, 515, 103-115.

Chapter 3: Dettmann, U., & Bechtold, M. (2015): One dimensional expression to calculate specific yield for shallow groundwater systems with microrelief. Hydrological Processes, in press.

Chapter 4: Dettmann, U., & Bechtold, M. (2015): Simple approach for the *in situ* determination of soil water retention characteristics in shallow groundwater systems. Submitted to Water Resources Research. Under review.

2 On the applicability of unimodal and bimodal van Genuchten-Mualem based models to peat and other organic soils under evaporation conditions

Abstract

Soil moisture is one of the key parameters controlling biogeochemical processes in peat and other organic soils. To understand and accurately model soil moisture dynamics and peatland hydrological functioning in general, knowledge about soil hydraulic properties is crucial. As peat differs in several aspects from mineral soils, the applicability of standard hydraulic functions (e.g. van Genuchten–Mualem model) developed for mineral soils to peat soil moisture dynamics might be questionable. In this study, the hydraulic properties of five types of peat and other organic soils from different German peatlands have been investigated by laboratory evaporation experiments. Soil hydraulic parameters of the commonly-applied van Genuchten–Mualem model and the bimodal model by Durner (1994) were inversely estimated using HYDRUS-1D and global optimization. The objective function included measured pressure heads and cumulative evaporation. The performance of eight model set-ups differing in the degree of complexity and the choice of fitting parameters were evaluated. Depending on the model set-up, botanical origin and degree of peat decomposition, the quality of the model results differed strongly. We show that fitted 'tortuosity' parameters τ of the van Genuchten–Mualem model can deviate very much from the default value of 0.5 that is frequently applied to mineral soils. Results indicate a rather small decrease of the hydraulic conductivity with increasing suction compared to mineral soils. Optimizing τ did therefore strongly reduce the model error at dry conditions when high pressure head gradients occurred. As strongly negative pressure heads in the investigated peatlands rarely occur, we also reduced the range of pressure heads in the inversion to a 'wet range' from 0 to -200 cm. For the 'wet range' model performance was highly dependent on the inclusion of macropores. Here, fitting only the macropore fraction of the bimodal model as immediately drainable additional pore space seems to be a practical approach to account for the macropore effect, as the fitting of the full bimodal model led to only marginal further improvement of model performance. This keeps the number of parameters low and thus provides a model that is more easily managed in pedotransfer function development and practical applications like large scale simulations. Our findings point out first options to improve the performance of the frequently-used simple single-domain models when they are applied to organic soils. We

suggest further performance evaluation of these models during wetting periods when they are known to fail to describe preferential and non-equilibrium flow phenomena.

Keywords: Peat, Hydrus, hydraulic properties, van Genuchten-Mualem, unsaturated zone, macropore flow

2.1 Introduction

Physical, chemical and biological processes in peatlands are strongly controlled by the specific hydrological conditions of these environments (Dimitrov et al., 2010; Holden et al., 2004; Lafleur et al., 2005), which are in particular the fluctuating high water levels leading to frequently varying conditions in the upper part of the peat. Water levels close to the ground surface throughout the whole year are needed for peat soils to develop from dead plant material under anoxic conditions. Once the hydrological conditions are disturbed, peatland ecosystems react very sensitively, with consequences for the catchment hydrology, peat physical and chemical properties, water chemistry and biodiversity. Land use requiring drainage leads to aerobic conditions in the soil and thus peat degradation (Holden et al., 2004). Generally, natural peatlands store carbon and act as sinks for atmospheric carbon dioxide (Bragazza et al., 2006; Limpens et al., 2008; Minkkinen, 1999). Due to increased microbiological activity, drained peat soils become hotspots of anthropogenic emissions of the greenhouse gases (GHG) CO_2 and N_2O (Maljanen et al., 2010), and the carbon stock decreases. Furthermore, the enhanced mineralization causes the release of nutrients, especially nitrate, and dissolved organic carbon (Holden et al., 2004). Not only Histosols (WRB, 2008), but also other organic soils with a lower soil organic carbon (*SOC*) content meeting the definition of organic soils according to IPCC (2006), are important sources of GHGs (Leiber-Sauheitl et al., 2013). These organic soils have rarely been studied so far. For simplification, we will refer in the following to both peat soils and 'low *SOC*' organic soils as organic soils.

The biogeochemical processes during peat degradation are mainly controlled by the availability of oxygen, which is in turn controlled by the soil moisture (Rodriguez-Iturbe et al., 2001). Hence, the hydrological and biogeochemical processes in a peatland are strongly dependent on the changing hydrodynamic conditions in the unsaturated zone (Kechavarzi et al., 2010). The hydraulic soil properties strongly control the time-variable state variables and fluxes in peatlands like water table depth, evapotranspiration, groundwater recharge, surface runoff and interflow, and thus the whole water balance. As about 95% of the peatlands in Germany are drained for agriculture, forestry or peat mining (Joosten and Couwenberg,

2012), it is important to study the unsaturated flow and transport processes of degraded peats to improve the understanding of the amount and dynamics of GHG emissions and nutrient release. Rewetting helps to mitigate the negative effects caused by the drainage of peatlands. Therefore, numerical simulations of the water flow in the saturated and unsaturated zone are needed to develop optimal rewetting strategies. Commonly, water flow in the unsaturated zone is modeled with Richards' equation. For its application, the hydraulic properties, i.e., the water retention and unsaturated hydraulic conductivity function need to be known.

Hydraulic properties are commonly determined by laboratory measurements on small core samples. Standard methods are the hanging water column and pressure plate apparatus for the water retention curve (WRC) and the constant or falling head experiments for the hydraulic conductivity function ($K_{(\theta)}$). As measuring $K_{(\theta)}$ is difficult, empirical relationships were developed to derive this function from the water retention characteristics and saturated hydraulic conductivity (K_s). Mualem (1976) derived the unsaturated hydraulic conductivity from the pore-size distribution of a soil. Through the interpretation of the WRC as a statistical measure of its equivalent pore size distribution, $K_{(\theta)}$ can be inferred from measured data of the WRC and K_s (van Genuchten, 1980). In his model for $K_{(\theta)}$, Mualem (1976) used the parameters that describe the WRC and two additional parameters K_s and τ. τ is related to the tortuosity structure of the connected pores. Over the last decades, the van Genuchten-Mualem (*vGM*) model has become one of the most commonly applied models to describe hydraulic properties. However, estimating $K_{(\theta)}$ requires K_s and τ. The parameter τ can only be determined by conductivity measurements at different water contents. Based on data from 45 mineral soils (clays, loams and sands), Mualem (1976) proposed an average value of 0.5 for the pore-connectivity parameter τ. Another issue of the *vGM* model is that it can only account for a unimodal pore size distribution, neglecting macropores. Based on van Genuchten and Nielsen (1985) and Luckner et al. (1989), Schaap and Leij (2000) pointed out that K_s measurements are sensitive to macropore flow.

Macropore flow is an important process in heterogeneous soils in which larger pores are present. Induced by the larger pores the hydraulic conductivity strongly increases at pressure heads near saturation. When water moves along connected macropore pathways, bypassing the porous soil matrix during wetting conditions, preferential flow and non-equilibrium flow occurs (Šimůnek et al., 2003). Different macropore approaches were developed to improve macropore flow modeling in the unsaturated zone (e.g. dual/multi-porosity models, dual/multi-permeability models) (Jarvis, 2007; Köhne et al., 2009; Šimůnek et al., 2003).

Empirical dual/multi-porosity models with effective parameters and assuming a single domain represent the simplest concept. Durner (1994) combined two *vGM* models weighted by the factor ω to a 'bimodal' model representing the entire pore system. Therefore, the shape of the WRC and unsaturated hydraulic conductivity function, influenced by the macropores, can be depicted more accurately than treating the soil as a unimodal pore system. Although the dual/multi-porosity models can account for the increasing hydraulic conductivity near saturation, they are not able to describe the basic physics of the preferential flow process because Richards' equation based single-domain models will produce uniform wetting fronts assuming instantaneous equilibrium (Šimůnek et al., 2003). Nevertheless, Köhne et al. (2009) pointed out, that equilibrium single-domain models often yield results similar to two domain approaches, unless dynamic shrinkage cracks are present. Besides this simple single-domain dual/multi-porosity approach, numerous more complex concepts have been developed over the last decades that are able to describe the non-equilibrium flow process. E.g. Hendriks et al. (1999) introduced a complex macropore geometry model, which is implemented in the SWAP model (Kroes et al., 2008).

The frequently demonstrated importance of accounting for macropore flow is well recognized and hydrological model software for small and large scale applications like, e.g., Hydrus, SWAP, SIMGRO, Feflow, Hydrogeosphere and Parflow provide options to apply both the common unimodal hydraulic functions like the *vGM* model and bi- or multi-modal approaches (e.g., in Hydrogeosphere, see Brunner and Simmons, 2012). However, our impression is that the unimodal *vGM* model is still most frequently applied (e.g., Bolger et al., 2011; Ferguson and Maxwell, 2010; Li et al., 2008), e.g., due to computational efficiency reasons or the lack of data on macroporosity. When model calibration worked well in these studies, this showed either that the macroporosity effect was negligible at the specific setting and for the specific objective or that the structural model error could be compensated by other model parameters.

The importance of macroporosity on flow and transport may be even more important for peatland environments (Dimitrov et al., 2010; Holden, 2009). Compared to mineral soils, the hydraulic properties of peat soils differ in several aspects. By definition, they have a high amount of *SOC* (Ad-hoc-AG Boden, 2005). Typically they have high porosities (ε) and distinctive shrinkage and swelling characteristics (Hendriks, 2004). Dependent on the original plant substrate, peat soils are characterized by a high spatial variability of the hydraulic properties (Baden and Eggelsmann, 1963). Within fields and regions the variability can be

further enhanced by peat degradation due to drainage causing decreasing ε and *SOC* (Beckwith et al., 2003; Holden and Burt, 2003b). For mineral soils, many studies focused on the model performance of the Richards' equation and the influence and sensitivity of certain *vGM* parameters on model results (Romano and Santini, 1999; Šimůnek et al., 1998). However, studies about organic soils are rare. As organic soils differ in several aspects from mineral soils, the applicability for describing organic soil moisture dynamics with standard flow equations and the influence of different *vGM* parameters on the model performance should be investigated. Dynamic transient laboratory experiments such as evaporation or multi-step outflow (MSO) experiments are good methods to investigate the accuracy of models. First introduced by Gardner and Miklich (1962), several evaporation methods have been developed (Plagge et al., 1990; Schindler, 1980; Wendroth et al., 1993; Wind, 1968). With simultaneous measurements of evaporation and pressure heads at different depths, both the WRC and $K_{(\theta)}$ can be directly determined for the same sample. However, this method relies on linearization assumptions about the vertical distributions of water contents and pressure heads, which are only approximately fulfilled. The alternative approach is given by the inverse parameter estimation, in which the parameters of hydraulic functions are optimized by minimizing the deviations between measured and predicted state and flux variables, resulting in optimal parameter sets (Kool et al., 1987). The advantage of the inverse approach is that the most suitable parameter values or ranges are determined simultaneously and thus consistently for both the water retention and hydraulic conductivity function without linearization assumptions. Residuals can be used to quantify model errors.

Very few studies applied inverse parameter optimization to dynamical flow experiments with organic soils. Schwärzel et al. (2006) investigated fen peats in Germany with evaporation experiments and Gnatowski et al. (2010) fen peats from Poland with MSO experiments. Both laboratory experiments were simulated with the Richards' equation and the *vGM* model. Schwärzel et al. (2006) compared directly derived and inversely optimized hydraulic properties and generally found a good agreement for dry conditions (pressure heads < -100 cm). They explained the deviations between 0 and -100 cm by the very small pressure head gradients at the beginning of the experiment which cause relative high uncertainties in the directly estimated hydraulic conductivity near saturation (see also Šimůnek et al., 1998). Furthermore, they tested the accuracy of the estimated hydraulic functions by forward predictions using data from an additional lysimeter. Hydraulic properties derived from transient field and laboratory experiments described the dynamic of the drying process well. In their MSO experiments, Gnatowski et al. (2010) found a good agreement between

measured and simulated outflow. However, the cumulative outflow was the only observation. Hence no predictions about the accuracy of the modeled pressure heads could be made. Neither study has tested the influence of the different *vGM* parameters and the applicability of the *vGM* model in detail. Moreover, only a small part of the broad variety of organic soils was analyzed and the studies neglected macropores. As the soil moisture in peatlands is often near saturation, macropore flow is an important pathway in the upper peat layers, causing rapid changes in near-surface water contents with a minor effect on the matrix potential (Dimitrov et al., 2010; Holden, 2009). To our knowledge, no studies tried to describe macropore flow with a bimodal model for organic soils. Dimitrov et al. (2010) modeled the peat subsurface hydrology by coupling the Hagen-Poiseuille equation for gravitational macropore flow and the Richards' equation for matrix flow. They found better water content predictions with this coupled approach as compared to the Richards' equation alone.

In this study, we investigate the applicability of the *vGM* and the bimodal model to describe the hydraulic gradients and water fluxes for five different organic soils during evaporation experiments. Because our experiments are limited to evaporation conditions, the general problems of single-domain models in modeling preferential macropore flow during infiltration are not investigated in our study. In contrast to previous studies, here we systematically compare the performance of different models (unimodal and bimodal) with different parameter set-ups (fixing or optimizing certain *vGM* parameters). This is done for a relatively large sample volume compared to common evaporation experiments and thus provides more effective parameters that are needed for large scale hydrologic models. We analyze the impact of fitting K_s and τ which are often fixed to measured or default values. The objective of this systematic analysis is to provide a reference that allows the estimation of model performance that is achieved in practical applications depending on the data availability. Finally, we derive suggestions on which model and parameter configuration to choose when modeling the hydrology of peatlands with *vGM* and bimodal models.

2.2 Material and methods

2.2.1 Site descriptions

Evaporation experiments were performed for organic soils from five different study sites spread over Germany (Tab. 2.1). Detailed information about the determination of the parameters in Tab. 2.1 is given in section 2.2.3. The investigated organic soils cover a broad range of different soil properties with bulk densities (b_d) from 0.06 to 0.60 (g cm^{-3}), porosities

(ε) from 63% to 93%, *SOC* from 18% to 46% and saturated hydraulic conductivities (K_s) from 41 to 612 cm d^{-1}.

The Schechenfilz (SF) is one of the last near-natural bog complexes in Germany. Thus, the *Sphagnum* peat from this site is the only pristine and weakly decomposed (H = 2 on the von Post scale) soil in the study. The von Post scale of decomposition classifies the degree of peat humification based on the proportion of visible plant remains and soil water color (von Post and Granlund, 1926). As the peat was locked under permanently water saturated conditions, it has the highest *SOC* content of all samples. Due to the high amount of macropores in the *Sphagnum* moss K_s is high (612 cm d^{-1}).

As most peatlands in Germany are drained for agriculture or forestry, all other samples are from sites which are currently drained or had been drained in the past. Typically for organic topsoils in Germany, these peat samples are strongly decomposed (H = 10). The two study sites Anklam (AK) and Zarnekow (ZA) are both located in the valley of the river Peene. Both peatlands have riverine fen characteristics and evolved as an association of 'percolation mire', 'terrestrialisation mire' and 'flood mire' (Succow, 2012). The different soil properties result from different land use and drainage histories. AK was rewetted 30 years ago, and the vegetation cover is characterized by a succession to sedges, reeds and willows. Accordingly, the upper part of the soil is interspersed with undecomposed leaves and small branches causing a high K_s value of 610 cm d^{-1} and a high amount of macropores. In contrast, Zarnekow is still drained and used as extensive grassland. The progressive degradation and compaction of the peat can be seen in the K_s value which is an order of magnitude lower than that of AK.

The Spreewald (SW) is an alder forest with an extensive system of drainage channels where organic soils developed from paludification processes (initial accumulation of organic matter over mineral soils) and temporary flooding. The samples were taken in an area where a 30 cm thick organic sediment horizon was formed during a limnic period.

As a result of drainage, peat cutting and deep ploughing, the soil from Großes Moor (GM) is the most degraded peat in this study. After peat cutting, only a shallow (around 30 cm) peat layer had remained and was mixed with the underlying sand. The resulting material shows the highest b_d, the lowest ε and the lowest *SOC* of all investigated soils in this study and thus is most similar to mineral soils.

Tab. 2.1: Soil properties (5 –25 cm) of the study sites: Bulk density (b_d), porosity (ε), soil organic carbon content (SOC) and saturated hydraulic conductivity (K_s).

Site	Location	Peatland type	Peat substrate	Land use/ Vegetation	von Post	b_d (g cm^{-3})	ε (%)	SOC (%)	K_s (cm d^{-1})
Schechenfilz (SF)	47° 48' N 11° 19' E	Bog	Sphagnum peat (fibric)	Natural	2	0.06	93	46	612[a] (n = 4) (range: 19 – 1334)
Anklam (AK)	53° 51' N 13° 40' E	Fen	Sedges, reeds, fossil woods (sapric)	Reed, sedges, willows	10	0.16	85	41	610[a] (n = 5) (range: 53 – 2746)
Zarnekow (ZA)	53° 52' N 12° 52' E	Fen	Sedges, reeds (sapric)	Extensive grassland	10	0.36	76	28	41[a] (n = 5) (range: 5 – 322)
Spreewald (SW)	51° 53' N 14° 2' E	Fen	Amorphous organic sediment (sapric)	Alder forest	-	0.35	80	20	-
Großes Moor (GM)	52° 34' N 10° 39' E	Bog	Amorphous peat (sapric)	Extensive grassland	10	0.60	63	18	53[a] (n = 6) (range: 7 – 70)

[a]**Median**

2.2.2 **Evaporation experiments**

For each study site, two replicates of evaporation experiments were conducted with undisturbed samples (diameter: 30 cm, height: 20 cm). For the study site SW, only one replicate could be analyzed due to wrong pressure head readings caused by loose tensiometers.

The soil cores were taken vertically near the surface by manually hammering PVC rings that were sharpened at the bottom edge into the peat and excavating the whole sample. The samples represented the near-surface layer of the organic soils (5 - 25 cm). At the grassland and the forest sites, the turf and the litter were removed before sampling. After collection, the samples were sealed with a plastic bag and stored at 4 °C. For the evaporation experiments the samples were sealed at the bottom and placed on a scale (Signum 1, Sartorius, Göttingen, Germany; measuring accuracy 0.1 g). Three tensiometers (T8, UMS GmbH, Munich, Germany; measuring accuracy 5 hPa) with cups of 6 cm length and 2.5 cm diameter were inserted vertically at 5.5 cm, 9.5 cm and 15.5 cm depth. The samples were saturated slowly from the bottom until saturation. After saturation, the evaporation experiments started at pressure head conditions of 0 cm at the top of the sample. The experiments were conducted at room temperature which was given by the conditions in our lab and ranged from 17 to 23 °C for most of the times but sporadically also reached 34 °C due to weak lab ventilation in summer. To speed up the experiments, the soil surface was ventilated by a fan. To avoid measurement errors of the scale, the fan stopped for the weight measurements every 10 min. As organic soils have distinctive shrinkage characteristics, vertical and horizontal subsidence of the sample was measured by placing a grid on the columns. The experiments were

terminated when the tensiometer cups of the upper tensiometer reached the air entry value at pressure heads of around -800 cm.

2.2.3 Basic soil properties

After the end of the experiment, samples were dried at 80°C for 7 days. Standard mass balance calculations based on the weight at the beginning and end of the experiment, the soil mass and the soil volume yielded b_d and the water content at the beginning and end of the experiment. Here, we assumed the whole porosity to be interconnected and that full saturation was achieved at the beginning of the experiment. The *vGM* parameter θ_s (see section 2.2.5.1) and given ε values in Tab. 2.1 thus equal the water content at the beginning of the experiment. In practice, full saturation is difficult to achieve at atmospheric conditions, and entrapped air occurs. Thus real θ_s and ε values are probably higher. *SOC* was measured on a LECO TrueMac CN (LECO Corporation, St. Joseph, Michigan, USA) after sieving and grinding the samples.

For all soils except SW, separate K_s measurements on 250 cm³ samples were done in the laboratory by constant head experiments. To limit edge effects during sampling, a large block of the fibrous peat from the SF was cut and frozen. After pre-drilling, the steel rings for the constant head experiments were inserted into the frozen peat at a depth of 10 cm. Samples from the other sites were conventionally taken from a small pit in the field.

2.2.4 Direct determination of soil hydraulic properties

For evaporation experiments, the hydraulic properties can be derived directly or by inverse modeling (Section 2.2.5) using predefined analytical expressions like the *vGM* Model (van Genuchten, 1980; Mualem, 1976).

In the direct determination, the WRC and *K(θ)* result from the pressure head and total water content data at different time steps by algebraic calculations (Plagge et al., 1990; Wendroth et al., 1993; Wind, 1968). In 1980, Schindler, introduced a simplified evaporation method with tensiometer readings at only two depths. The retention function is derived by the mean water content (θ_i) and the mean pressure heads (h_i) for each time step. As described in detail in Peters and Durner (2008), the water flux through the sample between two time steps (t_{i-1} and t_i) is assumed to be equal to $q_i = z_m \cdot \Delta\theta_i / \Delta t_i$ at the middle of the two tensiometer depths with $\Delta\theta_i$ as mean water content change, Δt_i as time increment and z_m as distance from the bottom of the samples to the middle of the two tensiometer. The hydraulic conductivity (K_i)

corresponding to the mean pressure head between two time steps ($\overline{h_i}$) is derived by inverting Darcy's law:

$$K_i(\overline{h_i}) = -\frac{q_i}{\Delta h_i / \Delta z + 1} \quad 2.1$$

Δh_i is the mean difference between the tensiometer readings and Δz the distance between the upper and lower tensiometer.

At pressure heads close to zero, when the pressure conditions are close to hydrostatic equilibrium conditions, K_i cannot be determined exactly by this method due to the high hydraulic conductivity (Wendroth et al., 1993; Šimůnek et al., 1998). The correct measurement of low gradients is limited by the accuracy of the tensiometers. Furthermore, the direct estimation of the hydraulic properties is based on the assumption that the water contents and pressure heads are decreasing linearly over the sample. This assumption can only be fulfilled approximately and the nonlinearity increases with lower pressure heads in the column (Peters and Durner, 2008).

An advantage of the direct determination of the hydraulic properties is the possibility to account for shrinkage in the derivation of the hydraulic properties by using the decreasing soil volumes from the shrinkage measurements to calculate the volumetric moisture content.

2.2.5 Inverse determination of soil hydraulic properties

2.2.5.1 Soil hydraulic functions

Two soil hydraulic functions were used in this paper to describe the soil hydraulic properties by inverse parameter optimization. The first one was the commonly-applied van Genuchten-Mualem function (van Genuchten, 1980; Mualem, 1976):

$$\theta(h) = \theta_r + \frac{(\theta_s - \theta_r)}{(1 + (\alpha h)^n)^m} \quad 2.2$$

$$S_e(h) = \frac{\theta(h) - \theta_r}{\theta_s - \theta_r} = \frac{1}{(1 + (\alpha h)^n)^m} \quad 2.3$$

$$K(\theta) = K_s S_e^{\tau} [1 - (1 - S_e^{1/m})^m]^2 \quad 2.4$$

where h (cm) is pressure head, θ, θ_r and θ_s (cm^3 cm^{-3}) are the current, residual and saturated water contents. α (cm^{-1}), n (-), m (-) are empirical parameters where m is calculated by $m = 1- 1/n$. S_e is the effective saturation of the sample.

As a second approach, a bimodal model (Durner, 1994) was used for a more accurate description of the hydraulic properties, especially at high water contents. Following Durner (1994), the porous medium can be divided into i overlapping *vGM* functions weighted by factor ω_i.

$$S_e = \sum_{i=1}^{k} \omega_i \left(\frac{1}{1+(\alpha_i h)^{n_i}} \right)^{m_i} \qquad 2.5$$

with the sum of ω_1 to ω_k being equal to 1. Further analysis is restricted to the bimodal model with $k = 2$. By combining the bimodal retention functions with Mualem's (1976) pore-size distribution model, the bimodal unsaturated hydraulic conductivity can be described with the following equation (Priesack and Durner, 2006).

$$K(S_e) = K_s \left(\sum_{i=1}^{k} \omega_i S_{e_i}\right)^{\tau} \left(\frac{\sum_{i=1}^{k} \omega_i \alpha_i [1-(1-S_{e_i}^{1/m_i})^{m_i}]}{\sum_{i=1}^{k} \omega_i \alpha_i} \right)^2 \qquad 2.6$$

During inverse modeling, the secondary pore system leads to higher fitted saturated hydraulic conductivities. The unimodal *vGM* function depicts the saturated hydraulic conductivity by fitting the function predominantly to the data of the soil matrix, and thus the shape of the hydraulic properties in the macropore range cannot be described (Durner, 1994).

2.2.5.2 Modeling scheme

The numerical forward modeling was conducted using the finite-element code HYDRUS-1D (Šimůnek et al., 2013) which numerically solves the Richards' equation (Richards, 1931). According to the location of the tensiometers, observation nodes were placed at 5.5 cm, 9.5 cm and 15.5 cm depth. The soil profile (20 cm) was discretized into 100 elements with an element refinement towards the top. Simulations were started at full saturation ($h = 0$ cm at top). The top boundary condition was set to atmospheric with the evaporative water loss during the experiment (cm h^{-1}) as potential evaporation rate. The bottom boundary was set to no flow. All simulations were terminated when the measured upper tensiometer readings reached the minimum pressure head of -800 cm.

Global inverse parameter optimization was performed with the 'Shuffled complex evolution' (SCE-UA) algorithm of Duan et al. (1992). The differences between measured and simulated pressure heads and evaporation rates were minimized by using an objective function (Φ) defined in Šimůnek et al. (1998):

$$\Phi(\mathbf{b},\mathbf{p}) = \sum_{j=1}^{m} v_j \sum_{i=1}^{n_j} \left[p_j^*(t_i) - p_j(t_i,\mathbf{b}) \right]^2 \qquad 2.7$$

where m describes the two different sets of measurements, i.e., pressure heads and evaporation rates, n_j is the number of measurements of the jth measurement set, $p_j^*(t_i)$ and $p_j(t_i,b)$ are the observations and predictions at time (t_i) for the jth measurement set, **b** is the parameter vector, and v_j is a weighting factor.

The contributions of the two measurement sets to the objective function were normalized by measured data variances σ_j^2 and n_j:

$$v_j = \frac{1}{\eta_j \sigma_j^2} \qquad 2.8$$

2.2.5.3 Model set-ups and parameter limits

As hydraulic experiments with organic soils are rare, we applied different model set-ups to analyze how the parameters influence the model performance of both the *vGM* and the bimodal model.

All model set-ups were run for pressure heads at the upper tensiometer from approximately 5.5 cm at the beginning to approximately -800 cm at the end of the experiment. For simplicity this range is referred to as **full range**. According to logged tensiometer readings at the sampled field sites over the last two years that showed a value of -150 cm at 10 cm depth as the lowest pressure head, a wet pressure head range has been defined from 5 to -200 cm at the upper tensiometer, and the experimental data from drier conditions were not considered during inverse parameter estimation. This set of model runs focused on the derivation of appropriate hydraulic properties for the wet field conditions and is referred to in the following as **wet range**.

Tab. 2.2 gives an overview on the realized model set-ups. All set-ups were performed for the wet and the full pressure head range. θ_s was set to a fixed value for all model set-ups according to the saturated water content at the beginning of the experiment. θ_r, α and n were optimized in all experiments. Further, we compared the performance of models with K_s fixed

to the median of the directly measured values with ones in which K_s is optimized. We stress that the directly measured K_s values were determined at separate smaller samples. They are thus not 'directly' measured in a strict sense, as they were not determined for the large samples. As K_s measurements are generally highly variable, measured values at the small samples showed rather large variation. The applied directly measured K_s values are the medians of the measurements (Tab. 2.1). All parameter limits are listed in Tab. 2.3.

Durner (1994) pointed out that the failure of conductivity estimation methods can mostly be attributed to incorrect values of τ. Mualem's (1976) proposed value of 0.5 was often applied as default in subsequent studies. As no organic soils were included in his original data set, the applicability to organic soils is questionable. Hence, in this study differences in model accuracy were determined by running models with optimized τ and with τ of 0.5.

For the bimodal model, ω was fitted in all cases. One model set-up included the fitting of all three additional parameters. To lower the model complexity of the bimodal model, also set-ups with fixed α_2 and n_2 values were conducted with $\alpha_2 = 1$ and $n_2 = 10$. These values were set very high to represent only the very large macropores.

Tab. 2.2: Overview of model set-ups (fit: parameter was fitted, measured: parameter was fixed to separately determined value).

Model	θ_r (cm^3 cm^{-3})	α (cm^{-1})	n (-)	K_s (cm d^{-1})	τ (-)	ω (-)	α_2 (cm^{-1})	n_2 (-)
3p	fit	fit	fit	measured	0.5	-	-	-
4p	fit	fit	fit	fit	0.5	-	-	-
4p_t	fit	fit	fit	measured	fit	-	-	-
5p	fit	fit	fit	fit	fit	-	-	-
4p_d	fit	fit	fit	measured	0.5	fit	1	10
5p_d	fit	fit	fit	fit	0.5	fit	1	10
6p_d	fit	fit	fit	fit	fit	fit	1	10
8p_d	fit	fit	fit	fit	fit	fit	fit	fit

Tab. 2.3: Overview of parameter limits.

Parameter	θ_r (cm^3 cm^{-3})	α (cm^{-1})	n (-)	K_s (cm d^{-1})	τ (-)	ω (-)	α_2 (cm^{-1})	n_2 (-)
Limit	0 – 0.5	0.002 – 0.5	1.01 – 2.5	0.12 – 120000	-10 – 30	0 – 0.4	0.02 – 1	1.5 - 10

2.3 Results and discussion

2.3.1 Impact of model set-ups on model performance

All model set-ups from Tab. 2.2 were applied to all soils. Fig. 2.1 shows the objective function value Φ for all model set-ups for the **full** (Fig. 2.1a) and **wet range** (Fig. 2.1b). Despite the normalization of Φ with the data variances (equation 2.8), lower Φ were observed for the wet range. The better fits can be explained by the hydraulic gradients that occurred for the wet range, which are closer to hydrostatic equilibrium than for the full range, a situation that is more easily reproduced by the model as pressure heads at hydrostatic equilibrium can be described by the retention function solely. Hence the fits are less dependent to the fit of the hydraulic conductivity function. Therefore, any structural model errors, arising by the simultaneous description of retention and unsaturated hydraulic conductivity function are less affecting model performance than for the full range where gradients in the columns are higher.

Large variances of Φ for a specific model set-up indicate that the performance of this set-up strongly depends on the soil type. It is apparent that the fitting of some parameters lead to a high improvement of the model performance. This is further analyzed in detail with cross-plots (Fig. 2.2, Fig. 2.3, Fig. 2.6) in which one parameter is changed individually from 'fixed' to 'fitted', while keeping the rest of the model set-up the same. With these plots, the influence of single parameter for different soils can be illustrated. In these cases, fitting one additional parameter always leads to an equal or lower Φ due to an additional degree of freedom. However, if the model set-up changes in the sense that the model structure is changing (e.g. a sensitive parameter is fixed and additional parameters are fitted), more parameters do not obligatorily lead to a better model performance (e.g. for the full range 5p_d performs worse than 4p_t, see Fig. 2.1a). A complete list of all optimized parameters and Φ of all model set-ups is given in an on-line supplementary table.

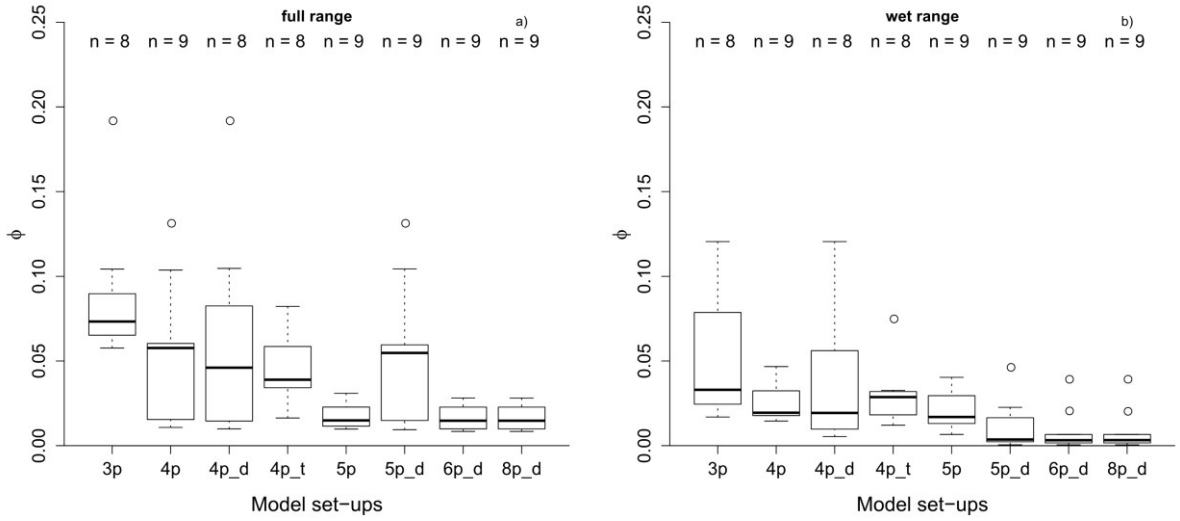

Fig. 2.1: Objective function value (Φ) of different model set-ups for all sites for full range (a) and wet range (b). For description of the used model set-ups see Tab. 2.2.

2.3.2 **Impact of fitting τ**

Schwärzel et al. (2006) found only minor improvements when varying τ and consequently used $\tau = 0.5$ as suggested by Mualem (1976). In contrast, in our study we found a high sensitivity of the model performance on τ. The highest sensitivity was observed for the samples with high gradients in the column. High gradients have been observed for SF and SW, less distinctive gradients for ZA and low gradients for AK and GM. Fig. 2.2 compares Φ of the model set-ups with τ fixed to 0.5 and Φ of the model set-ups in which τ was optimized. Fig. 2.2 indicates that the fitting of τ strongly reduces Φ value in most cases, especially for the pressure head range from 0 - -800 cm referred to as full range (Fig. 2.2a).

For the **full range** (Fig. 2.2a), the most pronounced improvements of Φ can be observed for the *Sphagnum* peat (SF), the amorphous organic sediment (SW) and the degraded peat of Zarnekow (ZA). For the degraded peat of Anklam, $\Delta\Phi$ is almost one order of magnitude smaller. Only low pressure head gradients were measured for the AK samples even at dry conditions, indicating a relatively high hydraulic conductivity even at dry conditions. This turns τ into a weakly sensitive parameter for fitting the experimental data. For the amorphous peat of GM, even at low pressure heads, gradients in the columns were still relatively low. The fitted τ values ranged between 0.25 and 3.06 and are relatively close to the default value for mineral soils (0.5) that was applied to the reference model set-ups. Hence, for GM, τ has a low sensitivity on the model performance, also shown by almost the same Φ comparing the model set-ups.

For the other soils the optimized τ values are negative (-1.5 to -4.4), except for the 4p_t model from AK ($\tau > 2$). Negative τ values lead to a less steep decrease of the unsaturated hydraulic conductivity function with decreasing pressure heads. Thus, high evaporation rates can be sustained at lower pressure heads. The results coincide with those of several authors which observed a rather small decrease of the hydraulic conductivity function with increasing suction (corresponding to negative τ values) for organic soils. Price and Whittington (2010) fitted simultaneous water retention data and unsaturated hydraulic conductivity data to *vGM* parameter using the RETC code of van Genuchten et al. (1991). They found negative τ values ranging from -1.81 to -4.38 for a *Sphagnum* peat. A data set of evaporation experiments on organic soils collected by Schindler and Müller (2010) also showed rather small decrease of the hydraulic conductivity with increasing suctions. To our knowledge, this data has not been analyzed further. A more detailed comparison with this data is therefore difficult to conduct. The mostly negative τ values resulting from our optimizations and the studies above indicate a less steep decrease of the unsaturated hydraulic conductivity than would be predicted with the default value of $\tau = 0.5$. There might be two reasons for this. First, the influence of τ on the model performance may be related to the measured shrinkage in the experiments. The samples with the highest shrinkage (SF and SW, shrinkage ~ 15 – 20 %) showed the strongest improvement of Φ when optimizing τ. For the soils with less shrinkage (e.g. GM, shrinkage ~5%), the reduction of Φ was less distinctive. Rezanezhad et al. (2009) pointed out that the main factors controlling hydraulic conductivity are the tortuosity, porosity and the hydraulic radius of the pores. Bearing in mind that τ is related to the description of the tortuosity with decreasing water contents, our results indicate that τ is able to partly account for the impact of the shrinkage on the unsaturated hydraulic conductivity. Beside the aspect of shrinkage, the very negative τ values that are needed to reproduce the less steep decrease of the unsaturated hydraulic conductivity also may hint to a structural deficit of the *vGM* model, representing the soil as a capillary bundle, neglecting film and corner flow (Peters, 2013). Accounting for these flow contributions may probably also help to describe the less steep decreasing conductivity function. Gnatowski et al. (2009) found τ values for herbaceous peat (reed and sedge, H_4 to H_7) generally greater than 0 and for moss peat (fibrous structure) samples τ values from -5 to 5. As Gnatowski et al. (2009) performed MSO experiments with cumulative outflow as the only observation in the objective function, the results are not so comparable.

For the **wet range** (Fig. 2.2b), the improvement gained by fitting τ is much smaller compared to the full range (Fig. 2.2a), except for the *Sphagnum* peat and the '3p vs. 4p_t' comparisons. Comparing the '3p and 4p_t' model set-ups shows a strong reduction of Φ also for the wet

range, except for one sample of GM (Fig. 2.2a and b) and one sample of AK (Fig. 2.2b). Parameter τ is a shape parameter in the unsaturated hydraulic conductivity function, and thus it can partly compensate for errors introduced by the fixed measured K_s values in these cases. However, for all other comparisons and soils, even if the range of the optimized τ values is quite large, the default value of $\tau = 0.5$ can be used to model the investigated peat soils for the wet range with an acceptable accuracy. Results indicate that τ is a less sensitive parameter in the wet range.

The analysis of the influence of fitting τ on the model performance showed that when considering the full pressure head range τ represents a crucial parameter for modeling flow in peat soils. Fitted values of τ strongly differed from the default value of 0.5 commonly used for mineral soils. However, from field tensiometer data at the sample sites, we know that these quite low pressure heads do not occur at field conditions in depths of 10 cm or deeper in our investigated soils. They may occur in the upper centimeters (0 – 10 cm depth) very rarely during the year. Depending on the intended model application and the objective of a peatland hydrological study (e.g., analysis and modeling of peatland water level fluctuations), it might be more important to produce an accurate model for the smaller pressure head range (0 to -200 cm). If lower pressure heads occur during dry periods, the model application should be adapted to these conditions and it is advisable to use the full range models.

The Φ values of the two replicates from the soils mostly show good agreement, except for some 3p and 4p_t set-ups.

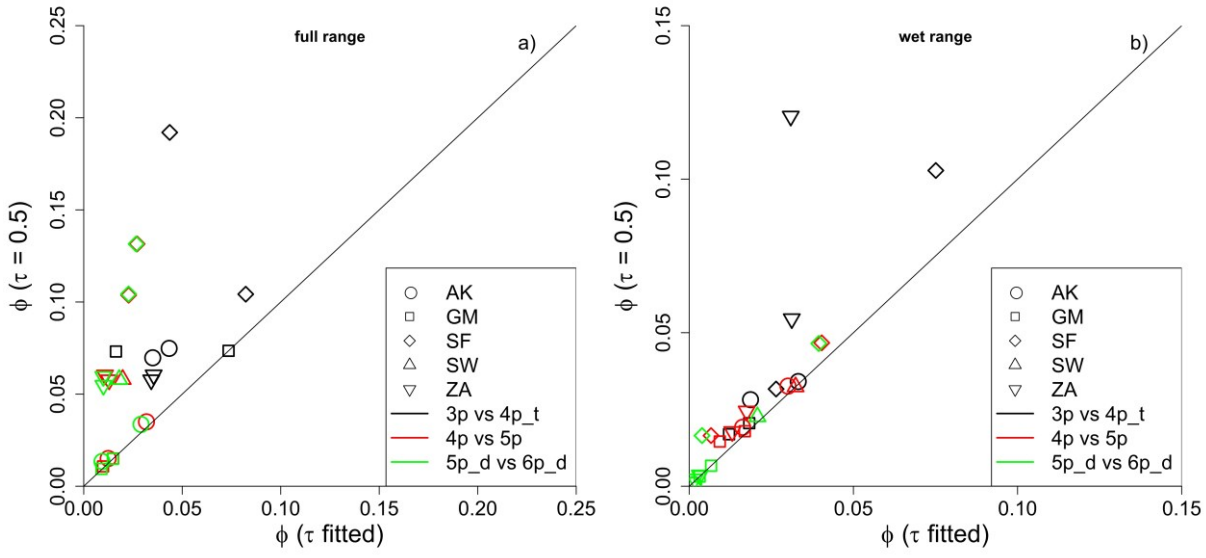

Fig. 2.2: Sensitivity of model performance on fitting parameter τ. Objective function value (Φ) of model set-ups in which τ was set to 0.5 is plotted vs. the ones in which τ was fitted, while keeping the rest of the model set-up the same.

2.3.3 Impact of fitting K_s

The optimization of K_s leads to a strong reduction of Φ. This is shown for almost all model set-ups and soil samples in this study (Fig. 2.3). For the **full range,** Fig. 2.3a indicates that in the bimodal model set-ups (green symbols) K_s is not a very sensitive parameter. Although the fitted K_s varied from the measured one (Fig. 2.4), the fitting only weakly improved the results, except for the *Sphagnum* peat. Conversely for the **wet range**, K_s shows to be a sensitive parameter for the bimodal model set-ups, too.

As described in the Sections 2.1 and 2.2.5.3, fitting of K_s leads mostly to K_s values that are lower than ones measured directly at full saturation. As seen in Fig. 2.4 this effect is not valid for all samples.

For the **full range** (Fig. 2.4a)**,** the K_s values generally increase from unimodal to bimodal models, except for the *Sphagnum* peat for which no general trend can be observed. For the unimodal models all fitted K_s values were lower than the measured except for the 4p model set-ups from the *Sphagnum* peat and the 4p model set-ups from ZA. This agrees with common results on mineral soils (Schaap and Leij, 2000; van Genuchten and Nielsen, 1985). Generally, the K_s values from the bimodal models were higher than the measured ones. For some cases, e.g., ZA (4p, 6p_d, 8p_d) and SF (4p), the fitted K_s values have a good agreement to the measured ones.

For the **wet range** (Fig. 2.4b) the fitted K_s values are higher than those of the full range. As for the full range, the *Sphagnum* peat shows a different characteristic with no general trend with higher measured K_s values than fitted. For the other soils almost all fitted K_s values were higher than the measured ones except for one set-up of GM (4p) and the two 4p set-ups of AK. In contrast to the full range, no general trend between unimodal and bimodal models could be observed for the wet range.

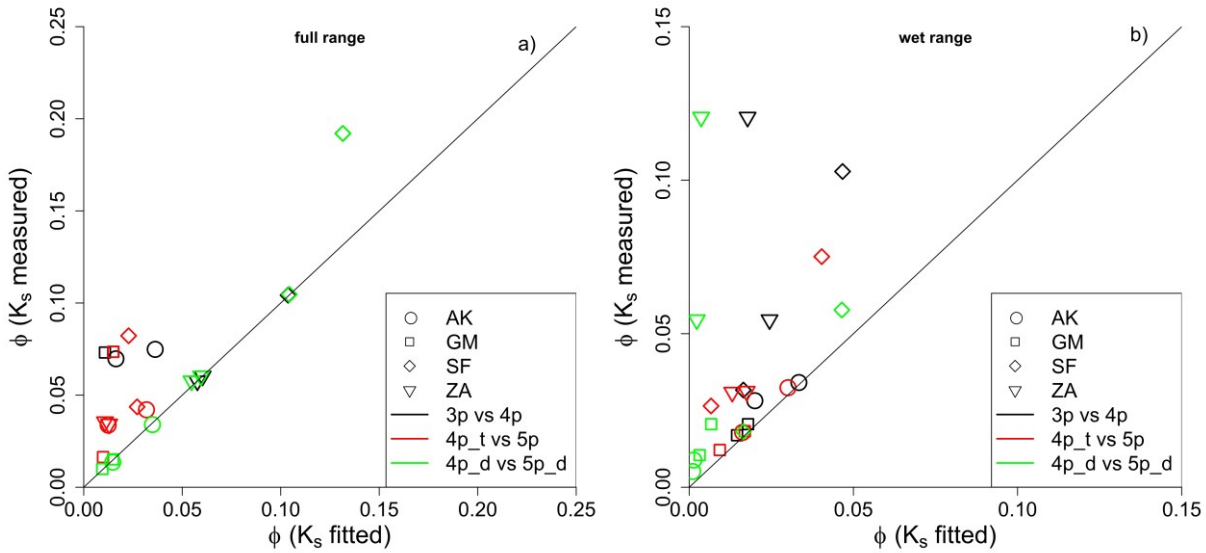

Fig. 2.3: Sensitivity of model performance on fitting parameter K_s. Objective function value (Φ) of model set-ups in which K_s was fixed to the measured value is plotted vs. the ones in which K_s was fitted, while keeping the rest of the model set-up the same.

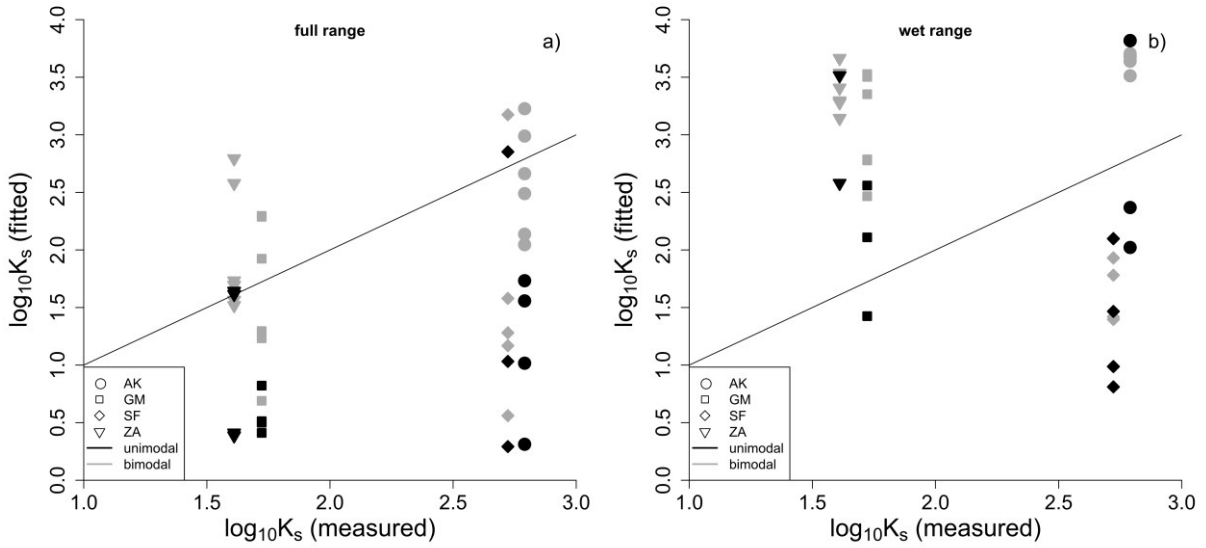

Fig. 2.4: K_s fitted vs. K_s measured, without the model set-ups were K_s was set to the measured values (3p, 4p_t, 4p_d).

2.3.4 Importance of macropores

Dimitrov et al. (2010) demonstrated the importance of macropores for the modeling of the hydrology of peatlands. In the evaporation experiments of our study, the influence of the macropores can be seen at the beginning of the experiments at pressure heads from 0 to -60 cm. The low water holding capacity of the macropores and the high amount of water

stored in the macropores lead to slowly decreasing pressure heads despite high evaporation rates, as shown as an example for one in Fig. 2.5.

As the unimodal *vGM* model cannot account for the macropores of a bimodal pore size distribution, the high evaporation rates and quickly decreasing water contents at the beginning of the experiment lead to lower simulated pressure heads than measured pressure heads (Fig. 2.5a). A solution is given by the simulated bimodal model set-ups, shown, for example, in Fig. 2.5b. Notice the good agreement between simulated and measured pressure heads between 0 to -60 cm.

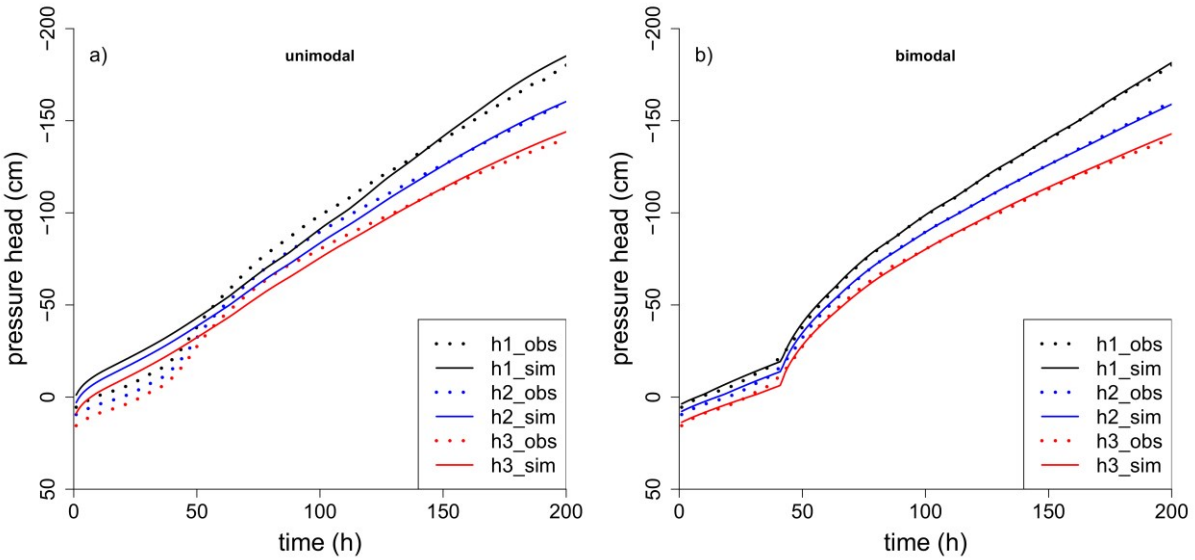

Fig. 2.5: Measured and simulated pressure heads for AK1 for wet range. a) unimodal 5p model, b) bimodal 6p_d model. Legend: Measured pressure heads '_obs', simulated pressure heads '_sim' for the upper 'h1' (-5.5 cm), middle 'h2' (-9.5 cm) and bottom 'h3' (-15.5 cm) tensiometer.

The strong improvement of the model performance seen in Fig. 2.5b is also demonstrated in Fig. 2.6 by comparing Φ of the unimodal and bimodal model set-ups. Accounting for macropores leads to lower Φ, in particular for the wet range (Fig. 2.6b).

For the **full range** (Fig. 2.6a), the bimodal model set-ups only improve the model performance for the '3p vs. 4p_d' set-ups. As the 3p set-ups are generally the worst simulations (Fig. 2.1), the flexibility increases with one additional parameter given in the 4p_d set-ups. For the other bimodal set-ups, Φ is generally dominated by the fit in the dry range with less weight on the pressure head range of the macropores. Hence, the improvement of the model performance appears to be comparatively low.

For the **wet range** (Fig. 2.6b), almost all samples show a strong reduction of Φ from a uni- to a bimodal model set-up. For samples from AK, the bimodal model leads to the strongest

relative improvement. The peat soil of this site, which is covered by willows, contains leaves and branches in the upper part of the soil. The high fraction of larger spaces between the plant residues causes the most pronounced macropore effect for the AK samples. Results for ZA also show the importance of using a bimodal model, which, however, cannot be explained by large spaces between coarse plant residues, as this site is used as extensive grassland. Instead, the sapric horizon is characterized by aggregates which characteristically develop in degraded peat soils. A bimodal pore size distribution seems to be given by the inter-aggregated pores. In the case of the *Sphagnum* peat, the bimodal models do not improve model performance for the '4p vs. 5p_d' and the '5p vs. 6p_d' comparisons. An indication for a bimodal pore size distribution of the *Sphagnum* peat can be seen in Fig. 2.7c for the directly derived water retention function at only about -400 cm. As the model set-ups for the wet range terminate at -200 cm, the unimodal *vGM* model was able to depict the hydraulic properties well without a bimodal model. Starting from already good performances, the Φ for the amorphous organic soils (SW, GM) are further improved by the bimodal models.

For all cases, no stronger differences in Φ between the '6p_d and 8p_d' model set-ups have been found (Fig. 2.1). The optimized values of α_2 and n_2 for the wet range often reached values close to the upper parameter limit of $\alpha_2 = 1$ and $n_2 = 10$. These parameter limits are already very high and a further increase would not lead to much better model performance but rather to an increased instability of the numerical solution. The results indicate that the simplified bimodal model, that uses fixed values for $\alpha_2 = 1$ and $n_2 = 10$ and thus only accounts for the fraction of the largest macropores, is a practical approach to obtain accurate model results.

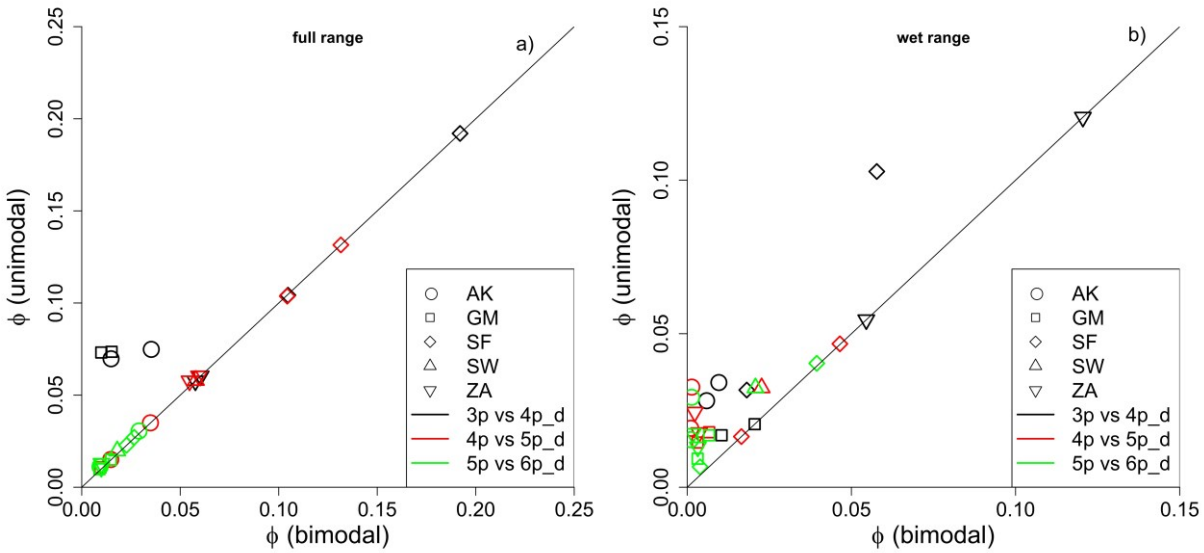

Fig. 2.6: Objective function value (Φ) of unimodal vs. bimodal model set-ups.

2.3.5 **Peat soil hydraulic properties and suggestions for practical applications**

In Fig. 2.7a a set of selected model set-ups is compared with directly derived hydraulic properties for one sample of the study sites AK referred as AK1 (Fig. 2.7a and b) and SF (referred as SF2) (Fig. 2.7c and d). It is noticeable that the difference between the two retention curves that are based on two different water contents, one of them accounting for the volume loss due to shrinkage, the other not, is rather small compared to the differences between functions that were derived from inversely fitting different model set-up to the experimental data. As the simplified method of Schindler (1980) assumes a vertical linear contribution of the water contents and pressure heads over the sample, a problematic assumption for the relatively large soil samples of our study, some systematic error must be expected for the directly derived hydraulic properties. Nevertheless, the directly derived functions can serve as a reference for the inversely-derived functions. For some fitted set-ups, there is good agreement with directly derived hydraulic properties, especially for sample AK1. The different water retention functions of AK1 (Fig. 2.7a) show similar characteristics especially for the pressure head range between -50 cm and -500 cm. For higher pressure heads there are some discrepancies, which are mainly caused by the systematic error of the directly derived functions, due to the non-linear water content profile at the initial phase of the experiment. In the directly derived water retention function, the mean tensiometer value of 0 cm corresponds to a water level that is in the center of the soil sample. The upper part is already unsaturated, leading to an underestimation of the water contents at the initial pressure

heads in the directly derived water retention functions. For the inverse estimation, θ_s was fixed to the value of the fully saturated sample.

The water retention characteristics for SF2 (Fig. 2.7c) are more variable than those of AK1. For the **full range**, the highest discrepancy to the directly derived retention function is indicated by the 4p model, which also showed high Φ values. For the 5p and 6p_d models the discrepancies get smaller with a good agreement between -70 cm to -500 cm. Looking at the **wet range**, the directly derived and inversely-fitted water retention functions match very well for the 6p_d model, even if the reduction of Φ using a bimodal model was negligible. The 4p and 5p model set-ups fit well for pressure heads from -20 cm to -200 cm.

The hydraulic conductivity curves show a high variability for both shown samples (Fig. 2.7b and d). For the range of the directly derived unsaturated hydraulic conductivity (pressure heads < ~-50), all curves for the *Sphagnum* peat (SF2), except for the 4p models, show similar characteristics. For AK1, the hydraulic conductivity curves from the models fitted to the full range have a better agreement with the directly derived curves than those fitted to the wet range only. This is consistent with the observation that stronger gradients only occurred under dry conditions in the full range and thus the shape parameter τ is only a sensitive parameter when fitting the full range.

The variability of the inversely-determined hydraulic properties raises the question which model set-up is best suited to simulate the unsaturated water flow in organic soils. Models are always characterized by some structural model error. When applying *vGM*-based models to organic soils, this error may be higher than for mineral soils given the specific characteristics of organic soils. In practice, the negative effect of this structural model error should be minimized as far as possible. Our results indicate that the model is not able to describe both the dry and wet range well with a single parameter set, thus, it is a practical solution to restrict the pressure head range during calibration to the most relevant range for specific applications and site conditions. Instead of restricting the range, individual weighting to specific ranges could also be introduced. Thus, if field measurements are available and if pressure heads do not fall below -200 cm for most times and parts of the soil, a reduction of the modeled pressure head range to 0 to -200 cm is advisable, or alternatively a method should be applied that gives higher weight on the wet range when fitting the full range. In contrast, if a good prediction of the actual evaporation rates from bare organic soil is intended (in our experiments the potential evaporation rate was pre-defined using the measured data), the calibration range should range to values much lower than -800 cm. For bare organic soils, the

uppermost centimeters are supposed to fully dry out during dry periods. A specific consideration of such conditions is beyond the scope of this paper.

Results clearly indicated that the bimodal model that accounts for macropores is essential to achieve a good representation of the water content dynamics in the wet pressure head range. To simplify the bimodal macropore model of Durner (1994), the parameters α_2 and n_2 can be set to 1 and 10, which led to accurate results for all investigated organic soils in this study. For only one soil, the *Sphagnum* peat, the bimodal model did not seem to provide a major improvement. This soil is characterized with the highest fraction of macropores (35 % of the pores are drained at pressure heads > -50 cm, see Fig. 2.7), but obviously the transition to smaller pores occurs rather continuously. A bi-modality is not apparent in the wet range, and thus, the wet range can be equally well described with an unimodal function.

If the pressure heads from field measurements fall below -200 cm, our results indicate that using the default value of $\tau = 0.5$ for mineral soils is not recommendable except for the degraded peat of GM with an organic carbon content of only 18 %. According to this, the impact of τ increases from highly degraded to more natural pristine organic soils.

The results of this study indicate that the usage of hydraulic properties derived by classical laboratory measurements only (hanging water column and pressure plate for the water retention characteristic, constant- or falling head experiments for the saturated hydraulic conductivity) can lead to high model errors. The main problems are the fixed K_s values and the determination of parameter τ, which both result in an inaccurate unsaturated hydraulic conductivity function. Therefore, we recommend the use of dynamic experiments, such as evaporation or MSO experiments in combination with inverse optimization, to determine the hydraulic properties. If this is not possible, the macropore fraction should at least be determined from the experimentally derived retention curve and treated explicitly as a rapidly filling and emptying water reservoir when modeling the water dynamics in peat soils. In future, when data from more dynamic experiments with peat soils becomes available in literature, the derivation of default τ values for different peat soils may be also useful to improve the modeling when only parameters of classical methods are available. Applying the different hydraulic properties to reproduce measured tensiometer, water content and water level data in the field under transient conditions could provide more information about the most accurate way to model the water flow in organic soils.

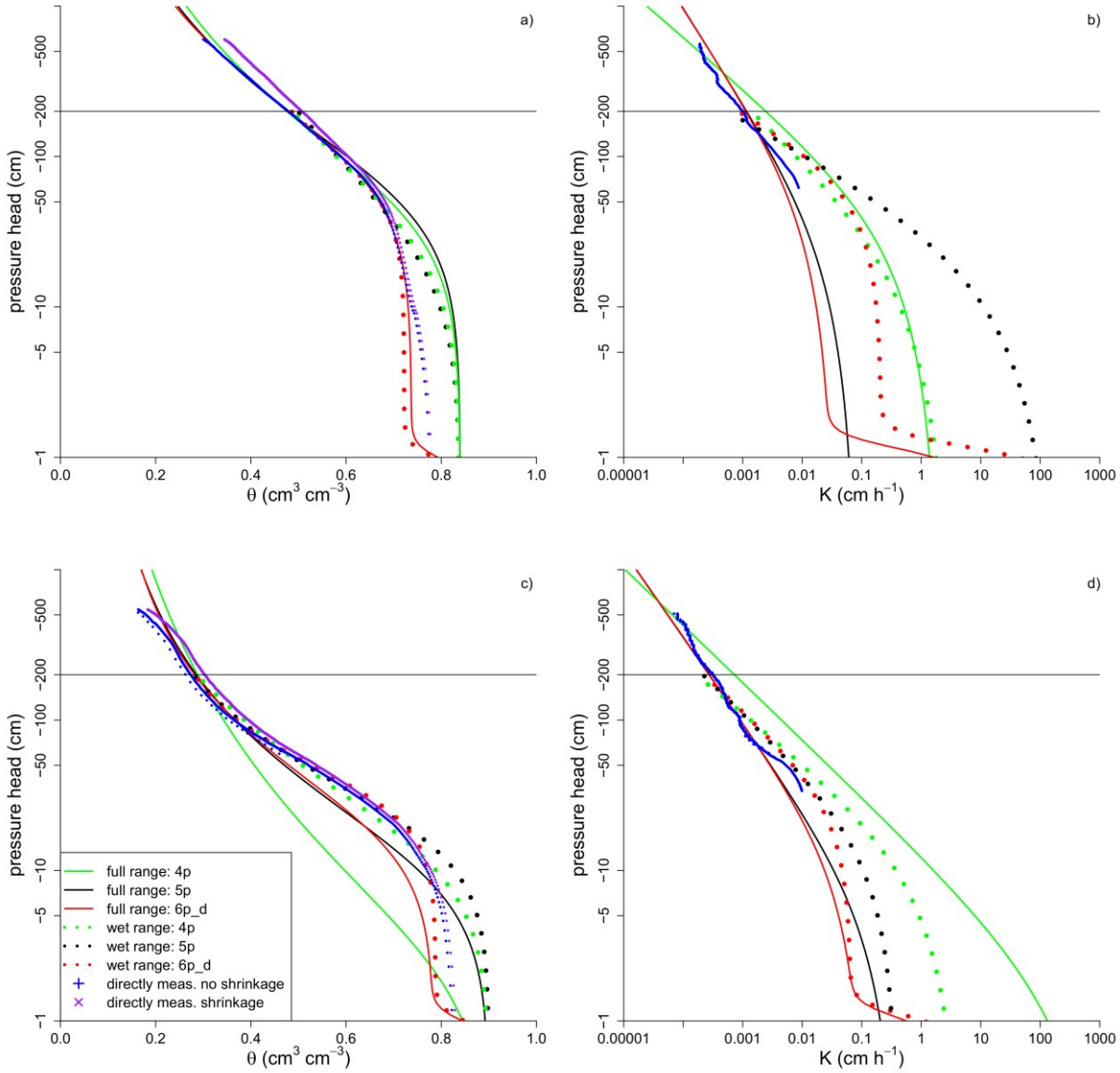

Fig. 2.7: Directly- and inversely-derived water retention curve for AK1 (a) and SF2 (c) and unsaturated hydraulic conductivity for AK1 (b) and SF2 (d).

2.4 Conclusions

The five different investigated organic soils of this study show contrasting properties and thus represent in part the broad variability of organic soils. The present study shows that the simulation of the unsaturated water flow in organic soils with the Richards' equation and *vGM*- and bimodal soil hydraulic models can lead to results of very variable quality. These single-domain models that were originally developed to model unsaturated flow in mineral soils are also frequently used to model hydrology of peatland areas. Our findings point out options to improve the performance of these simple models when they are applied to organic

soils. We expect e.g. a better description of vertical moisture distribution profiles and water level fluctuations when considering these options.

For our evaporation experiments, the model performance depended on the model set-up (unimodal or bimodal *vGM*, fixing or optimizing certain parameters), and the peat type (botanical origin and degree of peat decomposition). When an adequate model set-up (our detailed recommendations are mentioned below) is chosen, modeled data fit the measured pressure heads and evaporation rates fairly well. Although organic soils have changing porosities during experiments due to shrinkage, and thus the physical basis of the Richards' equation is not fulfilled in terms of a rigid matrix, its application to peat soils seems to be a practical approach. However, the results also indicated that there is a weak trend towards better model performance for soils with higher degree of decomposition, and thus more rigid, mineral soil-like behavior.

However, we stress that these conclusions were drawn for dewatering conditions. For wetting conditions, in particular strong rainfall events, potential preferential and non-equilibrium flow cannot be described by the single-domain approach, especially when there are large macropores and cracks in the soil. Also hysteresis and hydrophobicity effects were not analyzed. Further experimental studies that are conducted under alternating flow directions are needed to evaluate model performance of single-domain approaches under the full range of natural boundary conditions.

Two major aspects need to be considered when modeling water flow in organic soils. Accounting for macropores is crucial and becomes apparent when focusing on the model performance of the wet pressure head range (here defined from 0 to -200 cm). A simplified bimodal model, with one additional fitting parameter that accounts only for the very large macropores, provided a much better representation of the measured pressure heads and evaporation rates than the unimodal model. Therefore, a practical approach for hydrological models is given and can also be realized on large scale applications under the limitation that preferential and non-equilibrium flow cannot be described by the single-domain Richards equation model used in the study.

When field pressure heads are expected to decrease below -200 cm for large parts of the soil profile, it is necessary to get an estimate of the *vGM* parameter τ, because results of this study indicated that τ from peat soils can strongly differ from the default value of 0.5 often used for mineral soils. As mentioned in section 2.3.2 there is a necessity to describe a less steep

decreasing hydraulic conductivity function than the one predicted by $\tau = 0.5$ which is shown by mostly negative optimized τ values. The negative τ values are partly able to describe the less steep decreasing conductivity function and lead for most of our simulations to a strong improvement of Φ. Using a different model, e.g. the one of Peters (2013) accounting for film and corner flow, would also lead to a less steep decreasing unsaturated hydraulic conductivity. Whether such a model is better suited to describe the observed unsaturated conductivity is beyond the scope of this paper.

Acknowledgements:

We acknowledge the financial support by the joint research project ‘Organic soils’ funded by the Thünen Institute. We appreciate practical and theoretical support from Niko Roßkopf (Humboldt University, Berlin), Benedikt Scharnagl (Technical University, Braunschweig), Maik Hunziger, Marc Jantz, and Annette Freibauer (Thünen Institute, Braunschweig). We are grateful to Corrado Corradini as Editor, Juan V. Giraldez as Associated Editor and the three anonymous reviewers for their helpful comments and suggestions.

Appendix A. Supplementary material

Supplementary data associated with this article can be found, in the online version, at http://dx.doi.org/10.1016/j.jhydrol.2014.04.047.

3 One-dimensional expression to calculate specific yield for shallow groundwater systems with microrelief

Abstract

Although the importance to account for microrelief in the calculation of specific yields for shallow groundwater systems is well recognized, the microrelief influence is often treated very simplified, which can cause considerable errors. We provide a general one-dimensional expression that correctly represents the effect of a microrelief on the total specific yield that is composed of the soil and surface specific yield. The one-dimensional expression can be applied for different soil hydraulic parameterizations and soil surface elevation frequency distributions. Applying different van Genuchten parameters and a simple linear microrelief model, we demonstrate that the specific yield is influenced by the microrelief not only when surface storage directly contributes to specific yield by (partial) inundation but also when water levels are lower than the minimum surface elevation. Compared with a simplified representation of the soil specific yield, in which a mean soil surface is assumed for the calculation of soil specific yield, the correct representation can lead to lower as well as higher soil specific yields depending on the specific interaction of the soil water retention characteristics and the microrelief. The new equation can be used to obtain more accurate evapotranspiration estimates from water level fluctuations and to account for the effect of microtopographic subgrid variability on simulated water levels of spatially distributed hydrological models.

Keywords: specific yield, surface storage, water table fluctuation, van Genuchten, microrelief

3.1 Introduction

Water table depth is one of the crucial state variables of shallow groundwater systems such as wetlands and riparian zones. Shallow groundwater ecosystems are highly dependent on the typical site-specific water table depth dynamics and react very sensitively to its disturbance (Dorrepaal et al., 2009; Jenerette et al., 2012). The water level monitoring, interpretation and modification in course of restoration projects are of crucial importance for nature conservation. For flood control, knowledge about the free water storage capacity and water release behavior before and after heavy rainfall periods is essential for the prediction accuracy of forecasting models (De Roo et al., 2003). Furthermore, water table depth fluctuations are

increasingly used for evapotranspiration and groundwater recharge estimates following the pioneering work of White (1932) (Loheide et al., 2005; Mould et al., 2010; Fahle and Dietrich, 2014; McLaughlin and Cohen, 2014; Wang and Pozdniakov, 2014). For these scenarios and applications, a detailed physical and quantitative understanding of the fluctuations and how they are related to the ability of the system to store water is a prerequisite.

For flat soil surfaces, the water table depth dynamics within the soil profile of shallow groundwater systems as a response to boundary fluxes is primarily controlled by the water retention characteristics of the soil in and above the range of the water level fluctuations. Fig. 3.1a and Fig. 3.1b shows the integrals of two soil moisture profiles, $A_{zu,soil}$ and $A_{zl,soil}$, that are determined by the water retention characteristics of a soil at two hydrostatic equilibria of an upper (*zu*) and a lower water level (*zl*). Their difference ΔA_{soil} ($A_{zu,soil}$ - $A_{zl,soil}$) is shown in Fig. 3.1c. For the case of a decreasing water level, ΔA_{soil} is equal to the amount of water released by a soil, e.g. due to evaporation. In a normalization step, ΔA_{soil} is usually divided by the water level change (Δz), which results into a variable that is known as specific yield (S_y) (Childs, 1960). S_y is often used for the analysis and the modeling of water level fluctuations. For homogeneous zones of deeper groundwater systems, this value is constant. In contrast, for shallow groundwater systems with homogeneous soils, it changes with depth depending on the distance to the soil surface (Duke, 1972; Crosbie et al., 2005; Cheng et al., 2014; Wang and Pozdniakov, 2014), because the soil moisture profile above the water level is truncated by the soil surface before reaching residual water content. Because of the truncation, the soil volume that can release water is still increasing when water levels decrease; i.e. S_y is increasing with depth.

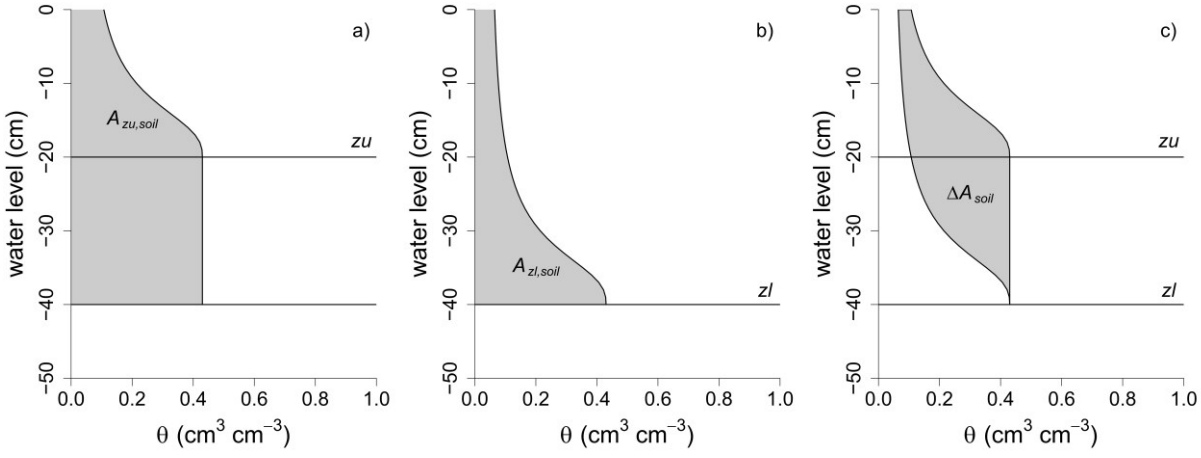

Fig. 3.1: Integrals of the soil moisture profiles ($A_{zu,soil}$, $A_{zl,soil}$) of an upper water level (*zu*) (a), lower water level (*zl*) (b) and the difference (ΔA_{soil}) between $A_{zl,soil}$ and $A_{zu,soil}$ (c).

Following Fig. 3.1 and the paragraph in the preceding text, the specific yield of the soil ($S_{y,soil}$) for a certain depth increment between *zu* and *zl* can be calculated as the difference of the integrals of two soil moisture profiles ($\Delta A_{soil} = A_{zu,soil} - A_{zl,soil}$) of two water levels divided by Δz with the following equation (e.g. Crosbie et al., 2005 and Cheng et al., 2014):

$$S_{y,soil} = \frac{1}{\Delta z} \cdot \left(A_{zu,soil} - A_{zl,soil} \right) = \frac{1}{\Delta z} \cdot \left(\underbrace{\Delta z \cdot \theta_s + \int_{zu}^{0} \theta(z) dz}_{A_{zu,soil}} - \underbrace{\int_{zl}^{0} \theta(z) dz}_{A_{zl,soil}} \right) = \theta_s - \frac{1}{\Delta z} \int_{zu}^{zl} \theta(z) dz \qquad 3.1$$

where *zl* is the lower and *zu* is the upper water level ($\Delta z = zu - zl$) with *z* being 0 at the soil surface (later in case of a microrelief $z = 0$ corresponds to the mean elevation of the soil surface) and negative below the ground. $\theta(z)$ is the volumetric water content at pressure head $h = z$. It equals the saturated water content θ_s for pressure heads $h > 0$. Several authors gave analytical expressions for calculating S_y based on the parameterization of the water retention function by Brooks and Corey (1964) (Duke, 1972; Nachabe, 2002) and by van Genuchten (1980) (Crosbie et al., 2005; Cheng et al., 2014) in the following referred as *VG*. It should be noted that analytical expressions calculating S_y with *VG* as parameterization for θ are an approximation, e.g. by means of Taylor series in Cheng et al. (2014), with increasing errors for larger water level changes.

For periods of inundation, S_y is defined by the specific yield above the soil surface ($S_{y,surface}$), which is here assumed to be 1, which corresponds to an open water surface. In some studies, a volume replacement by the plant material fraction (e.g. tree trunks) has been considered, which reduces $S_{y,surface}$ accordingly (Sumner, 2007; McLaughlin and Cohen, 2014). For water level changes approaching the soil surface, changes in soil water content are small. According to equation (3.1), this leads to S_y values near 0 for water levels close to the soil surface with an abrupt transition to 1 in case of inundation. It should be noted that the transition from surface to soil storage is, except for bare soil, not abrupt but continuous and successively influenced by plant material. The separation into soil and surface storage is a conceptual simplification that is commonly made to approximate this distinct change of S_y along this transition. Depending on the vegetation, part of the vegetation layer could also be attributed to the soil compartment when it acts like a porous system that significantly releases water in the range of the occurring matrix potential fluctuations. This is, for example the case for the peat moss layer in bog ecosystems.

Many kinds of landscapes that (can) occur at shallow groundwater levels are characterized by a distinctive microrelief leading to a mosaic of inundated and non-inundated areas such as e.g. pits and mounds in forests (Lyford and MacLean, 1966; McClellan et al., 1990), heathlands (Myerscough et al., 1996), ridge and slough environments (Sumner, 2007), hummocks and hollows in peatlands (Nungesser, 2003) and corrugated fields as relics of arable cultivation (Sittler, 2004). A schematic microrelief with an exemple water level at the mean surface height of the microrelief (μ) is shown in Fig. 3.2. A microrelief can be described as cumulative frequency distribution ($F_{(s)}$) of the soil surface elevations. Traditional approaches would lead to very different S_y values for the two dip wells 1 and 2. For the water level given in Fig. 3.2 at μ, dip well 1 would be completely flooded resulting in S_y of 1, and S_y of dip well 2 would only be influenced by the water retention characteristics of the soil (also indicated in Fig. 3.2). However, as partly inundated areas around dip wells influence water level changes, S_y should be calculated as spatial average. Following this, for both dip wells, 50% of the microrelief is inundated in Fig. 3.2 at the given water level at μ. Thus, S_y is a combination of $S_{y,soil}$ and $S_{y,surface}$ with a continuous transition from $S_{y,soil}$ to $S_{y,surface}$ for a rising water level depending on the distribution of soil surface elevations (Sumner, 2007).

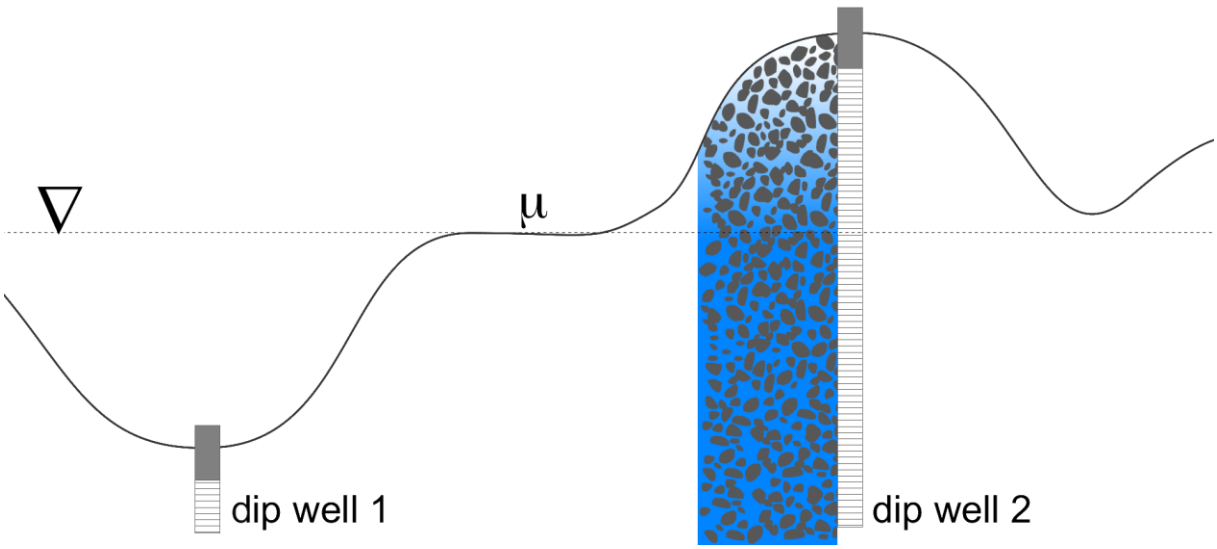

Fig. 3.2: Exemplary microrelief with a water level at the mean surface elevation (μ), which here corresponds to 50% inundation. The saturated and unsaturated zones of the soil are illustrated to demonstrate the vertical distribution of air-filled pore space that is available for further water storage. Further, two dip wells are indicated at different surface elevations.

Ignoring the transition leads to unrealistic low S_y values for shallow water level changes in areas with a microrelief. The importance to account for this transition is well recognized (McLaughlin and Cohen, 2014). However, the way it is accounted for often occurs in a

simplified manner, in which a constant $S_{y,soil}$ is assumed. In this approach, S_y equals to $S_{y,soil}$ for water levels below the lowest height and to $S_{y,surface}$ above the highest height of the microrelief. In between, *Sy* is interpolated by the fraction of inundated area (McLaughlin and Cohen, 2014).

To our knowledge, the study by Sumner (2007) is the only study in which both the nonlinear specific yield of the soil (that approaches zero close to the soil surface) and the effect of the microrelief have been considered simultaneously. In his study, this was realized by averaging S_y over multiple soil columns of different surface elevations. In this paper, we revisit the simultaneous consideration of nonlinear $S_{y,soil}$ and microrelief effects for the calculation of S_y. There are two reasons for revisiting this topic. Firstly, the 'multi-column' approach of Sumner (2007) needs a high number of soil columns to achieve convergence for the mean *Sy* value, i.e. to achieve a proper integration about the microrelief. Albeit providing correct results, this approach is computationally inefficient. The inefficiency may become a relevant problem when a high number of these calculations are required either for a spatially distributed model or during inverse parameter estimation. Secondly, although Sumner (2007) presented a correct representation of a simultaneous consideration of nonlinear $S_{y,soil}$ and microrelief effects, the study failed to illustrate and discuss the important implications on S_y when water levels are below the soil surface. We believe that this is one reason that this approach has not been adopted in all subsequent publications on this topic.

In this paper, we present a new one-dimensional (1D) expression for the calculation of S_y that accounts for both the effect of a continuously increasing contribution of surface storage and the effect of the soil volume distribution around the mean soil surface on S_y. With the correct 1D representation, we demonstrate that S_y values are also affected by the microrelief when water levels are below the lowest soil surface elevation. Differences are illustrated by comparing total S_y values assuming a flat soil surface at the mean soil surface elevation ($S_{y,flat}$) (calculated according to equation (3.1)) and soil specific yield values that are correctly calculated by accounting for microrelief effects ($S_{y,uneven}$).

3.2 Theory

In the following, we consider a 1D effective representation of a soil column with a flat or uneven soil surface. Accordingly, the total specific yield (S_y) for a certain depth increment is composed of the soil specific yield ($S_{y,soil}$) and the surface specific yield ($S_{y,surface}$).

$$S_y = S_{y,soil} + S_{y,surface} \tag{3.2}$$

Assuming $F_s(z)$ is the cumulative frequency distribution normalized between 0 and 1 of soil surface elevations, $S_{y,surface}$ can be calculated as

$$S_{y,surface} = \begin{cases} 1 & \text{zl} \geq z_{elev,\max} \\ \dfrac{1}{\Delta z}\int_{zl}^{zu} F_s(z)dz & zl < z_{elev,\max} \text{ and } zu > z_{elev,\min} \\ 0 & zu \leq z_{elev,\min} \end{cases} \tag{3.3}$$

with $S_{y,surface} = 0$ when zu is below the lowest elevation ($z_{elev,min}$) of the soil surface and $S_{y,surface} = 1$ when zl is above the highest elevation ($z_{elev,max}$) of the soil surface. For a flat surface, $S_{y,surface}$ abruptly changes from 0 to 1 at the soil surface, and for uneven surfaces, this transition is continuous.

In a 1D representation of $S_{y,soil}$ that includes any microrelief effects, the parameter $S_{y,soil}$ must be interpreted as a spatial average. For heights above the lowest surface elevation, the soil volume covers only parts of the total volume. Thus, to obtain the spatially averaged (effective) soil moisture, the soil moisture must be multiplied by the fraction that is actually covered by soil ($1\text{-}F_s(z)$). This has to be performed for the whole soil moisture profile in dependence on the cumulative distribution of the surface elevations ($F_s(z)$). Beside the horizontal reduction of the soil moisture profiles, the soil moisture profiles need to be vertically extended to the maximum height of the surface elevation. This can easily be seen looking at Fig. 3.2. The soil moisture profile of dip well 1 should be extended to the maximum height of the surrounding microrelief. The complete spatially averaged (effective) soil moisture profiles can then be used to calculate $A_{zl,soil}$ and $A_{zu,soil}$.

Including the correct representation of the microrelief in the calculation of the soil moisture profiles gives

$$A_{zl,soil} = \int_{zl}^{\infty} \left(1 - F_s(z)\right) \theta(z - zl)dz \tag{3.4}$$

$$A_{zu,soil} = \int_{zl}^{\infty} \left(1 - F_s(z)\right) \theta(z - zu)dz \tag{3.5}$$

The bounds of the integrals are set to infinity because the cumulative frequency distribution reaches 1 at the highest surface elevation. At this point the effective soil moisture is 0, which results from the term (1-$F_s(z)$).

Following section on Introduction, $S_{y,soil}$ is given by ΔA_{soil} ($A_{zu,soil}$ - $A_{zl,soil}$) divided with Δz. Substituting equations (3.4) und (3.5) into equation (3.1) leads to

$$S_{y,soil} = \frac{1}{\Delta z} \cdot \left(\int_{zl}^{\infty} (1 - F_s(z)) \theta(z - zu) dz - \int_{zl}^{\infty} (1 - F_s(z)) \theta(z - zl) dz \right)$$
$$= \frac{1}{\Delta z} \cdot \int_{zl}^{\infty} (1 - F_s(z)) [\theta(z - zu) - \theta(z - zl)] dz \qquad 3.6$$

For a flat soil surface, equation (3.6) simplifies to equation (3.1).

3.3 Discussion and Conclusions

3.3.1 Microrelief influence on effective soil moisture profile and specific yield

In the following, the influence of the microrelief on the effective 1D soil moisture profile is demonstrated (Fig. 3.3). For demonstration, we assume a linear surface elevation model (corresponding to a uniform frequency distribution) in the calculation of the effective soil moisture profiles and specific yields. The linear model requires two microrelief parameters, i.e. the lowest and highest surface elevation. The contribution of the linear surface storage starts at -20 cm and ends at 20 cm (Fig. 3.3b). The linear model can be replaced by more complex frequency distributions when adequate data is available. The influence is illustrated with van Genuchten parameters of two sands that are well documented in ROSETTA (Schaap et al., 2001) implemented in HYDRUS 1D (Šimůnek et al., 2013), which is a frequently used soil hydraulic parameter catalogue. For ‘sand 1’, we used soil hydraulic parameters (*VG*) of the default sand from HYDRUS-1D (θ_s: 0.43, θ_r: 0.045, α: 0.145, n: 2.68). For ‘sand 2’, soil hydraulic parameters (*VG*) were derived by ROSETTA (Schaap et al., 2001) for a pure (100%) sand (θ_s: 0.376, θ_r: 0.0507, α: 0.0344, n: 4.4248). The parameters indicate that both sands, 1 and 2, are unimodal sands that start to dewater substantially at matrix potentials of about -7 cm (=1/α) and -30 cm, respectively.

Fig. 3.3a shows the effective soil moisture profiles for a water level change from -30 to -10 cm for 'sand 1' for i) a flat surface and ii) an uneven surface. The effective soil moisture profile for case ii) is extended in dependence on the distribution of the surface elevations (in

our case up to 20 cm above the mean surface elevation). Below the mean surface elevation, the effective soil moisture is linearly reduced in dependence on the surface storage starting from -20 cm. The resulting integrals of the moisture profiles of the two cases ($\Delta A_{soil,flat}$ and $\Delta A_{soil,uneven}$) thus clearly differ in their vertical distribution.

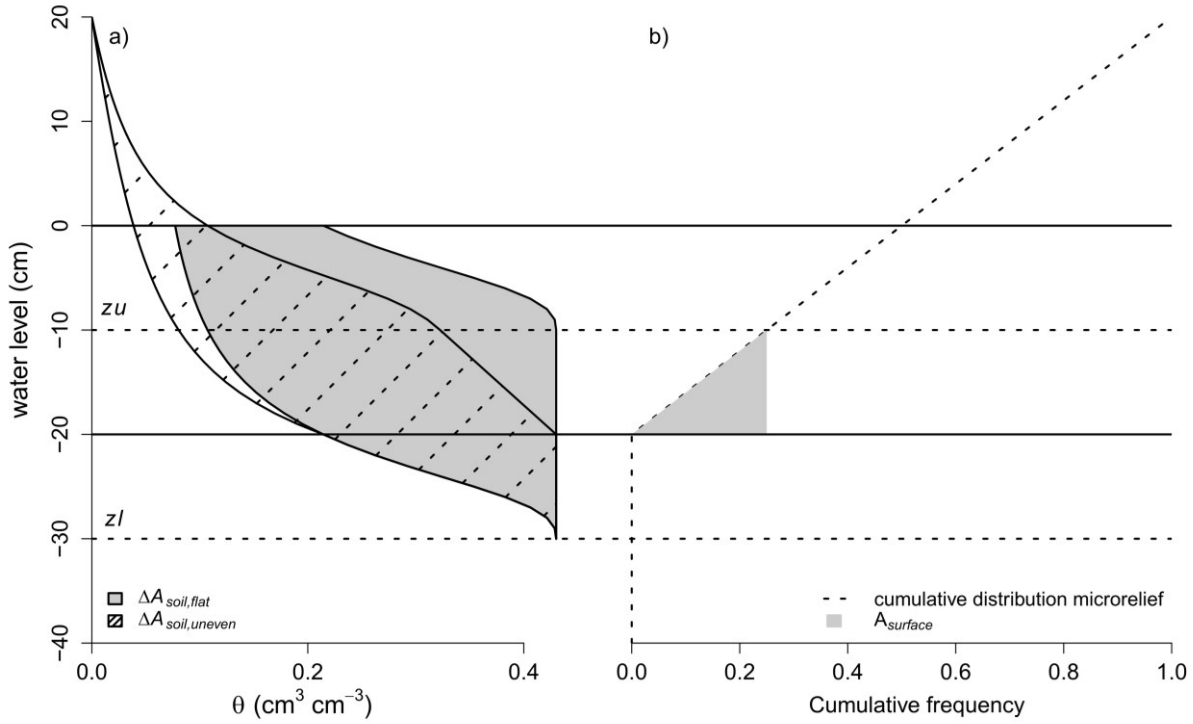

Fig. 3.3: Influence of the soil surface elevation distribution on the effective soil moisture (θ) profiles for a water level change from zl = -30 cm to zu = -10 cm. a) Effective soil moisture profiles of a flat surface ($\Delta A_{soil,flat}$) (grey area) and uneven surface ($\Delta A_{soil,uneven}$) (hatched area). Retention characteristic is described with *VG* parameters for 'sand 1'. b) Cumulative linear surface elevation distribution (F_s) (dashed line) and the integral of the surface storage ($A_{surface}$) (grey area).

To illustrate the implication for S_y, Fig. 3.4 shows S_y values of water level changes of 1 cm between -100 and 20 cm. S_y values that were calculated assuming a flat soil surface at the mean surface elevation are referred as $S_{y,flat}$, and S_y values that were calculated by taking into account the microrelief effect are referred as $S_{y,uneven}$. As expected from the soil water retention function, $S_{y,flat}$ decreases with lower water levels approaching 0 towards the flat soil surface. In contrast, $S_{y,uneven}$ between -20 to 20 cm water level height is strongly controlled by the surface storage with S_y reaching 1 at $z = 20$ cm. This effect of the increasing inundated fraction on S_y is well recognized and accounted for in previous studies (McLaughlin and Cohen, 2014). However, when the microrelief effect on S_y has been accounted for in previous studies, the specific yield contribution of the soil was only accounted for as a constant value that is simply reduced by the fraction of the inundated area. We emphasize that this differs from equation (3.6) in which $S_{y,soil}$ is not a constant value but the microrelief affects the full soil moisture integral. It can be noted from Fig. 3.4 that the microrelief has a considerable

influence on S_y even for water levels below the lowest surface elevation, i.e. before the direct storage contribution of the microrelief to S_y. Fig. 3.4a shows S_y values for 'sand 1'. Note the reduced S_y values between -40 and -20 cm. It results from the reduced soil volume in the pressure range in which the soil water capacity (i.e. the first derivative of the water retention function) of 'sand 1' is highest. The contrary effect, with higher S_y values just below -20 cm, is shown in Fig. 3.4b for 'sand 2'. This sand has the highest capacity in the soil volume above the mean elevation; i.e. S_y values are increased by this additional soil volume compared with the flat surface reference. The two examples demonstrate the interaction of soil hydraulic parameters and microrelief and its effect on vertical distribution of S_y.

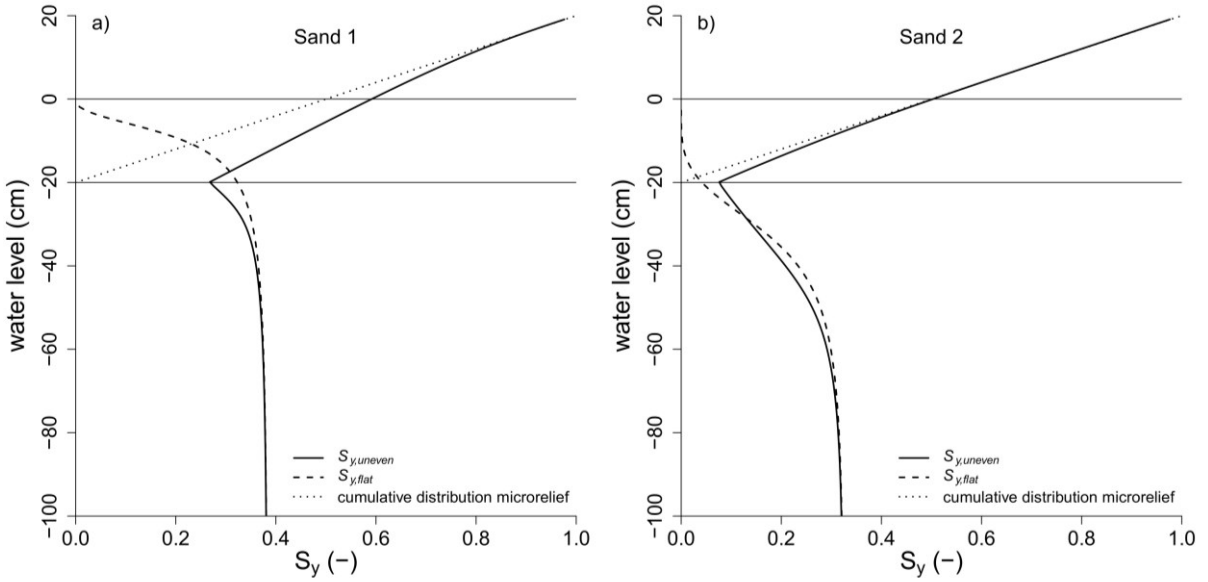

Fig. 3.4: S_y values of water level changes of 1 cm between -100 and 20 cm for a simplified flat surface representation ($S_{y,flat}$) and for an uneven surface ($S_{y,uneven}$). Illustrated for 'sand 1' (a) and 'sand 2' (b).

The difference between $S_{y,uneven}$ and $S_{y,flat}$ depends on the frequency distribution of the soil surface elevations and the retention characteristics of the soil. Above the lowest surface elevation, $S_{y,uneven}$ is mainly controlled by $S_{y,surface}$, i.e. by the range ($z_{elev,max}$ - $z_{elev,min}$) and the type of the microrelief frequency distribution (uniform, normal, etc.). Below the lowest surface elevation, we noticed that varying the type of the microrelief frequency distributions has a minor effect on $S_{y,soil}$. It is rather the range of the microtopographic height variation in combination with the retention characteristics of the soil that determines whether a strong effect can be expected or not. As a thumb rule, stronger effects occur when the soil releases relevant portions of its capillary water at matrix potentials that are within the range of heights of the microtopographic variation. In the examples in the preceding text, this corresponds to matrix potentials between 0 to -40 cm. Thus, stronger effects can be expected for coarse substrates.

We emphasize that in our examples, we assumed soil homogeneity for demonstration purpose, i.e. an effective parametric description of the soil profile, but soil moisture profiles of layered soils could equally be considered with the presented approach.

3.3.2 Possible applications of the equation

Here, we provided a simple 1D equation for calculating $S_{y,uneven}$ that is valid for small and large water level changes and can be applied with any parameterization of θ and frequency distribution of surface elevations. The proposed equation can make a significant improvement in several applications, in which the effect of microtopographic variability on S_y must be represented with a 1D model conceptualization. In general, the resulting S_y depth distributions can be used to obtain more accurate estimates of water level fluctuations for regions with shallow groundwater levels.

As an application example, we here highlight the relevance of our study for the various recent papers that focus on calculating evapotranspiration from water level fluctuations with the method of White (1932). In these studies, S_y is the most crucial parameter. It became obvious in our discussion in the preceding text that the consideration of its depth dependency will be important to derive reliable evapotranspiration estimates for different water table depths. Here, we provide the necessary equation to obtain physically correct vertical S_y profiles from site-specific soil and microrelief characteristics. To our knowledge, in all recent studies on the estimation of evapotranspiration from water level fluctuations (Cheng et al., 2014; McLaughlin and Cohen, 2014; Wang and Pozdniakov, 2014), either $S_{y,flat}$ or constant $S_{y,soil}$ was used without taking into account the full microrelief effect on $S_{y,soil}$. In case of uneven surfaces, this may lead to considerable errors.

As a second application example, we want to highlight the possible use of the equation in spatially distributed models. Because of computational limitations, spatially distributed catchment (or larger scale) models are often computed on spatial grids that are much coarser than the typical microtopographic variation. Thus, an effective parameterization is needed to account for the subgrid (i.e. within a grid cell) height variability of the soil surface. Similar to Manning's roughness coefficient (Manning et al., 1890) that accounts for the resistance of microrelief and vegetation to open channel or overland flow, our approach can be used to obtain the S_y depth distributions for each grid cell from the information about the subgrid microtopographic variability. With the increasing availability of detailed digital elevation models from laser scanning data, it is easily possible to account for subgrid variability for

each grid cell individually. Our simple equation ensures a computationally efficient application. In coupled hydrological models, in which the unsaturated zone is modeled dynamically with Richards' equation, the soil model domain needs to be reduced by the cumulative frequency distribution of the surface elevations similar as to that we proposed in our derivation of equation (3.6). A discussion of the implementation of our approach in such fully coupled hydrological models is beyond the scope of this paper.

Acknowledgements

We acknowledge the financial support by the joint research project ‘Organic Soils’ funded by the Thünen Institute. We appreciate the support from Bärbel Tiemeyer (Thünen Institute, Braunschweig) and Enrico Frahm (PTB, Braunschweig). We are grateful to Andy Baird for his review that included several helpful comments and suggestions, to a second anonymous reviewer and to Jim Buttle as editor.

4 Simple approach for the *in situ* determination of soil water retention characteristics in shallow groundwater systems

Abstract

We present a novel approach for the *in situ* determination of pedon to field scale soil water retention characteristics that is applicable to shallow groundwater systems. The simplicity of the approach is given by the very limited data requirements, which only comprise precipitation, water level, and, if relevant, microrelief data. Our approach is built on two assumptions: i) for shallow groundwater systems with medium- to high conductive soils the soil moisture profile is always close to hydrostatic equilibrium and ii) over short time periods lateral fluxes into and out of the system are negligible. Given these assumptions, the height of a water level rise due to a precipitation event mainly depends on the soil water retention characteristics, the precipitation amount, the initial water level depth and, if present, the microrelief.

We use this dependency, to determine van Genuchten parameters by Bayesian inversion. Proof-of-concept is demonstrated by synthetic data. Water retention characteristics are very well-constrained for the low suction range. Further, the method is applied to real field data from a *Sphagnum* bog with microrelief. Results indicate that observations of water level rises caused by precipitation events can contain sufficient information to constrain the water retention characteristics around dip wells to a plausible range. Application limits and potential systematic errors are discussed. We propose that our approach represents a promising tool to characterize field variability of soil water retention characteristics with widely available data.

Keywords: peat, soil water retention characteristics, van Genuchten, unsaturated zone, microrelief

4.1 Introduction

The characterization of soil hydraulic properties, including their field variability and scale dependency, is an ongoing research challenge in soil science for decades (Jury et al., 2011). Still, most commonly, soil hydraulic properties are obtained for relatively small soil samples by laboratory measurements imposing steady state (e.g. hanging water column) (Durner and

Lipsius, 2005; Reynolds et al., 2002b) or transient conditions (e.g. evaporation experiments) (Dettmann et al., 2014). However, hydraulic properties obtained in the laboratory may not be representative for field conditions and often disagree with hydraulic properties determined *in situ* (Basile et al., 2003). Soil samples are often too small to sample a representative elementary volume of the soil heterogeneity that is characteristic for the specific soil. Additionally, samples may be disturbed by the sampling procedure, e.g. due to compaction or disturbance of the soil structure. Further, soil samples may behave differently in the laboratory compared to the soil at field conditions, as it is the case for clay and peat that present different shrinkage characteristics once cut from the coherent soil body and root system (Mitchell, 1991; Mitchell and Van Genuchten, 1992). Therefore, for applications on field scale, *in situ* measurements should be preferred because they are more representative (Paquet et al., 1993) and obtain data in the natural environment, including interactions between different soil layers and scales (Wollschläger et al., 2009).

Several methods for the hydraulic characterization of a soil at field conditions exist. The saturated hydraulic conductivity can be measured with bail tests (Hvorslev, 1951) or by infiltration based methods, e.g. double ring infiltrometer (Reynolds et al., 2002a). Tension disc – or pressure ring infiltrometer can be used for obtaining the unsaturated hydraulic conductivity at specific pressure heads (Ankeny et al., 1991; Basile et al., 2003). This method is only applicable for low suctions (approximately > -25 cm) (Bodhinayake et al., 2004). The direct *in situ* determination of the water retention characteristics (*WRC*) is limited to simultaneous measurements of water content (θ) and pressure head. As these are 'point'-like measurements, this approach requires an appropriate amount of replicates per horizon. Additionally, measurements of θ often require soil specific calibrations, especially for soils with high soil organic carbon contents and distinctive shrinkage and swelling characteristics (Nagare et al., 2011; Pepin et al., 1992; Shibchurn et al., 2005). An alternative to the direct *in situ* measurements is given by the indirect determination of hydraulic parameters with inverse optimization using *in situ* measured state variables (Jadoon et al., 2012; Wollschläger et al., 2009). However, this approach requires various measurements as input (precipitation, evaporation, surface- and groundwater in- and outputs) besides the observed state variables.

In shallow groundwater systems, which are the focus of this study and comprise peatlands, riparian zones or other types of wetlands, the *WRC* are crucially influencing the water level fluctuations and specific hydrological conditions, and therefor the physical, chemical and biological processes (Dimitrov et al., 2010; Holden et al., 2004; Lafleur et al., 2005;

McLaughlin and Cohen, 2014; Waddington et al., 2015). Unfortunately, for shallow groundwater systems, knowledge about *WRC* at the field scale is scarce due to difficulties of common *in situ* methods. Infiltration methods are problematic due to the influence of the shallow groundwater level that lowers infiltration. Furthermore, accurate *in situ* measurements of θ are difficult to obtain in wetlands with high soil organic carbon contents (Mortl et al., 2011), which is of concern for both the direct and inverse determination of *WRC*. On the contrary, water level and standard meteorological data are easy to obtain and widely available for shallow groundwater systems. As mentioned above, water level depth dynamics as response to boundary fluxes contain information about the *WRC* of a soil. To our knowledge, this information has not been used yet to inversely estimate soil hydraulic properties.

Many kinds of landscapes with shallow groundwater levels are characterized by a distinctive microrelief that influences groundwater level dynamics at high water levels when partial inundation occurs and as well at low water levels due to the heterogeneously distributed soil volume (Dettmann and Bechtold, 2015). Thus, water level dynamics are dependent on both, the *WRC* and the microrelief. Dettmann and Bechtold (2015) gave a one-dimensional analytical expression combining the *WRC* and the microrelief effect on the spatially averaged specific yield (S_y). For its application, information about the microrelief as cumulative surface elevation is needed. Besides ground-based surveys, there is an increasing availability of detailed digital elevation models from laser scanning, which can be used to characterize the microrelief.

In this study, we present an approach to inversely estimate the soil *WRC* of shallow groundwater systems from frequently available data on water levels, precipitation (*P)* and microrelief. Instead of using a continuous soil hydrological model, we only focus on periods of stronger *P* events. Our approach is built on two assumptions: i) for shallow groundwater systems with medium- to high conductive soils, the soil moisture profile is close to hydrostatic equilibrium before and after rain events and ii) over short time periods lateral fluxes into and out of the system are negligible. Given these assumptions, water level rises are directly linked to the *P* amounts. The height of the water level rise depends on the soil *WRC*, the initial water level and the frequency distribution of the microrelief. We investigate the approach on two different applications. First, proof of concept is demonstrated by synthetic data with and without *P* data error. Second the method is applied to real data of an ombrotrophic *Sphagnum* bog complex with shallow groundwater levels.

4.2 Material and Methods

4.2.1 Theory

Assuming hydrostatic equilibrium in the soil before and after a precipitation (P) event and neglecting lateral fluxes, the amount of P is equal the difference of the integrals of the two soil moisture profiles, $A_{zl,soil}$ and $A_{zu,soil}$, of a lower (zl) and an upper water level (zu) (Dettmann and Bechtold, 2015). For even surfaces and water levels below ground, the difference (ΔA_{soil}) is,

$$\Delta A_{soil} = A_{zu,soil} - A_{zl,soil} = \underbrace{\Delta z \cdot \theta_s + \int_{zu}^{0} \theta(z)dz}_{A_{zu,soil}} - \underbrace{\int_{zl}^{0} \theta(z)dz}_{A_{zl,soil}} = \Delta z\ \theta_s - \int_{zu}^{zl} \theta(z)dz \quad 4.1$$

with $\Delta z = zu\text{-}zl$, and z being 0 at the mean elevation of the soil surface and negative below ground. $\theta(z)$ represents the volumetric water content at pressure head $h = z$ and θ_s is the saturated water content.

ΔA_{soil} decreases with shallower water levels. When zl and zu are above ground, i.e. for periods of total inundation, P is equal Δz, i.e. the height difference of two open water surfaces, further referred as $\Delta A_{surface}$. Following this, the amount of water received by a system for a depth increment between zl and zu can be separated into ΔA_{soil} and $\Delta A_{surface}$ with an abrupt transition from ΔA_{soil} to $\Delta A_{surface}$ for even surfaces.

For uneven surfaces, ΔA_{soil} and $\Delta A_{surface}$ should be combined as spatial average, for which Dettmann and Bechtold (2015) introduced a one-dimensional expression. The expression is briefly presented here. A microrelief can be described as cumulative frequency distribution (F_s) of the soil surface elevations. Then, $\Delta A_{surface}$ can be calculated with,

$$\Delta A_{surface} = \int_{zl}^{zu} F_s(z)dz \quad 4.2$$

with $F_s = 1$ above the highest elevation and $F_s = 0$ below the lowest elevation.

If ΔA_{soil} and $\Delta A_{surface}$ are combined to calculate the total difference, ΔA, the soil moisture profiles must be multiplied by the fraction that is actually covered by the soil ($1\text{-}F_s(z)$) over the profile to obtain the spatially averaged (effective) soil moisture profiles. For a one-

dimensional representation of ΔA_{soil} that accounts for microrelief effects, equation (4.1) turns into (Dettmann and Bechtold, 2015),

$$\Delta A_{soil} = \int_{zl}^{\infty} \left(1 - F_s(z)\right)\left[\theta(z - zu) - \theta(z - zl)\right] dz \,. \tag{4.3}$$

The soil moisture profile is vertically extended above the maximum height of the surface elevation by the upper integral bound being infinity, for which the cumulative frequency distribution of the microrelief is 1 and the effective soil moisture profile is 0. Equation (4.3) is equal to equation (3.6) of Dettmann and Bechtold (2015), in which the term was divided by Δz to obtain specific yield (S_y).

ΔA is calculated by combining equation (4.2) (ΔA_{soil}) and equation (4.3) ($\Delta A_{surface}$),

$$\Delta A = \underbrace{\int_{zl}^{zu} F_s(z) dz}_{\Delta A_{surface}} + \underbrace{\int_{zl}^{\infty} \left(1 - F_s(z)\right)\left[\theta(z - zu) - \theta(z - zl)\right] dz}_{\Delta A_{soil}} \,. \tag{4.4}$$

4.2.2 Modeling Framework

4.2.2.1 Definition of the soil surface

For many environments, it is hard to determine a clear position of the soil-vegetation interface, not only given the spatial variability but also due to the continuous vertical transition from soil to vegetation. This is for example the case for the peat moss layer in *Sphagnum* bog ecosystems (indicated in Fig. 4.1). When placing a level staff onto the ground, a position is measured at which the penetration resistance increases to a degree that the level staff is not further penetrating into the soil. In this study, for the modeling, we seek for a position of the soil-vegetation interface that optimally separates the two water storage volumes, ΔA_{soil} and $\Delta A_{surface}$. This 'optimal' position may not be consistent with the survey measurement, as for the water storage modelling it is best set where the strongest increase of large easily drainable macro pores occurs, which commonly increase from depth to surface (Moore et al., 2015, Morris et al., 2015). This nearly coincides with the strongest increase of S_y. As this position is not known beforehand, the position of the interface was a parameter in the inversion. We refer to the measured mean surface elevation with parameter μ, which is defined to be zero in all model applications. Parameter $\Delta\mu$ (indicated in Fig. 4.1) is the optimized position of the interface of ΔA_{soil} and $\Delta A_{surface}$. All water levels are related to μ.

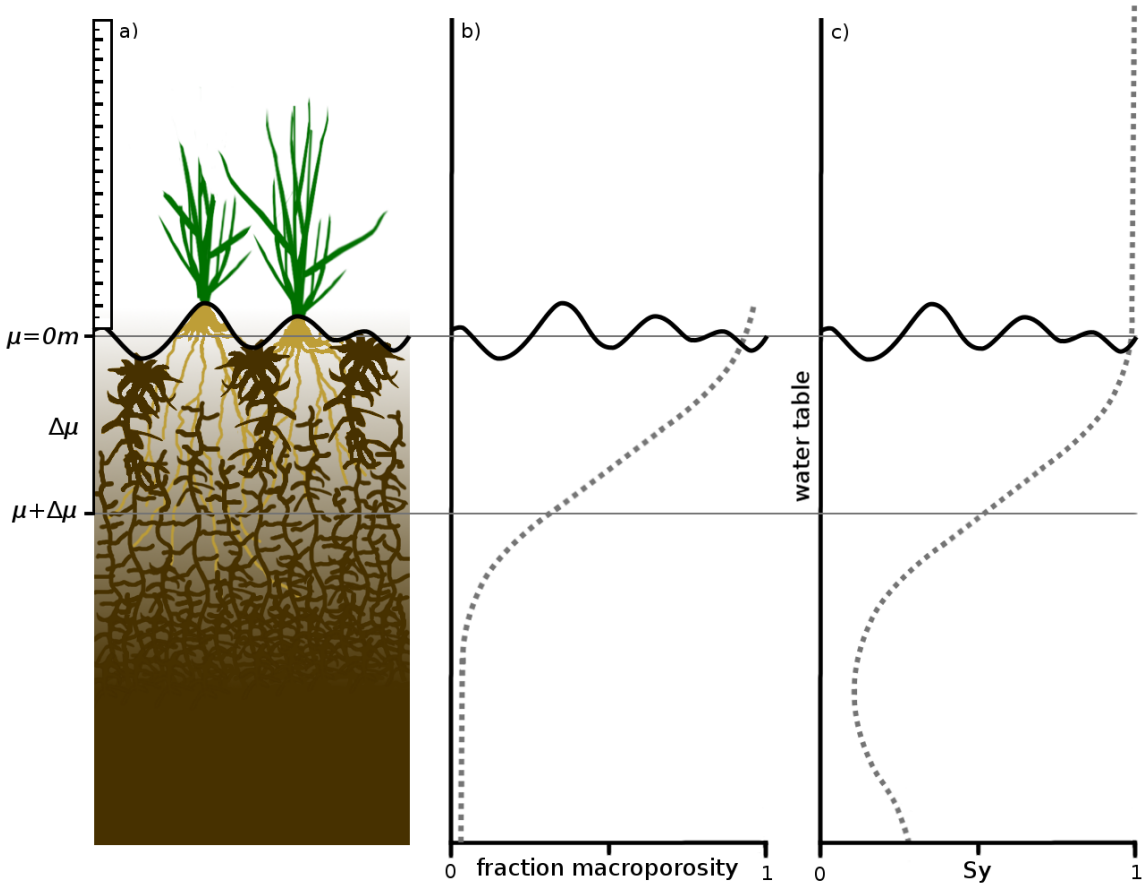

Fig. 4.1: Schematic illustration of soil-vegetation transition. It is focused on the vertical soil heterogeneity and therefore microrelief is only gently indicated: a) Exemplary *Sphagnum* soil profile and increasing pore sizes from bottom to top. Mean surface elevation (μ) and the optimized transition between surface storage and soil ($\mu + \Delta\mu$). b) Increasing macroporosity from bottom to top. c) Influence of surface storage on specific yield (S_y).

4.2.2.2 Soil water retention function

We describe the *WRC* by the frequently used parameterization of van Genuchten (*VG*) (van Genuchten, 1980),

$$\theta(z) = \begin{cases} \theta_r + \dfrac{(\theta_s - \theta_r)}{(1+(\alpha z)^n)^m} & for\ z \le 0 \\ \theta_s & for\ z > 0 \end{cases} \qquad 4.5$$

where $\theta(z)$ represents the volumetric water content at pressure head $h = z$. θ_s and θ_r ($cm^3\ cm^{-3}$) represent the saturated and residual water content. α (cm^{-1}), n (-) and m (-) are empirical parameters with m = 1-1/n. The soil is approximated as a homogeneous one-layer system.

4.2.2.3 Inversion Scheme

For both, even and uneven surface model applications, we optimized the effective *VG* parameters n, α, and θ_r of a one-layer soil system. θ_s was set a priori to the constant value 0.9, which is a separately determined value for the study site.

For the inverse optimization the optimized *VG* parameters are stored in $\mathbf{x}_1 = [n\ \alpha\ \theta_r]$ and, for the simulations accounting for microrelief (uneven surface), in $\mathbf{x}_2 = [\Delta\mu]$. Observed *zu* ($\mathbf{zu}_{obs} = [zu_{obs,1},\ldots,zu_{obs,N}]$) are compared with simulated *zu* ($\mathbf{zu}_{sim} = [zu_{sim,1},\ldots,zu_{sim,N}]$) using,

$$\varepsilon_i(\mathbf{x}_1,\mathbf{x}_2) = \mathbf{zu}_{obs,i} - \mathbf{zu}_{sim,i}(\mathbf{x}_1,\mathbf{x}_2) \quad i = 1,...,N \tag{4.6}$$

with N representing the numbers of observations. For applications with flat surfaces $\mathbf{zu}_{sim}$ only depends on $\mathbf{x}_1$.

For the calculation of $\mathbf{zu}_{sim}$, equation (4.5) was substituted into equation (4.4). According to the theory presented above, the resulting term was set equal the amount of P,

$$\underbrace{\int_{zl}^{\infty}(1-F_s(z))\left[\left(\theta_r+\frac{(\theta_s-\theta_r)}{(1+(\alpha(z-zu_{sim}))^n)^m}\right)-\left(\theta_r+\frac{(\theta_s-\theta_r)}{(1+(\alpha(z-zl))^n)^m}\right)\right]dz}_{\Delta A_{Soil}}+\underbrace{\int_{zl}^{zu_{sim}}F_s(z)}_{\Delta A_{surface}}=P \tag{4.7}$$

As equation (4.7) cannot be solved algebraically for $\mathbf{zu}_{sim,}$ the value was determined numerically. The cumulative frequency distribution of soil surface elevations $F_s(z)$ are described by a normal (Gaussian) distribution for uneven surfaces and by a step function at $z = 0$ for flat surfaces.

4.2.2.4 Optimization routine

For global optimization, we used the Markov Chain Monte Carlo algorithm entitled DifferRential Evolution Adaptive Metropolis ('DREAM') (Vrugt et al., 2008; Vrugt et al., 2009a). The algorithm evolves a posterior probability density function (*pdf*) of individual parameters which are treated as probabilistic variables considering the observed data set. Starting with an initial population within the feasible parameter space (prior distribution), the *pdf*s are evolved in multiple individual Markov chains combining the prior distribution and the data likelihood. Further information about the algorithm can be found in various publications (Vrugt et al., 2008; Vrugt et al., 2009b; Vrugt et al., 2009a; Vrugt and Ter Braak, 2011; Wöhling and Vrugt, 2011) and will not be repeated herein.

Following this, the parameters in $\mathbf{x}_1$ and $\mathbf{x}_2$ were derived as probabilistic distributions resulting in an ensemble of parameter characterizations that are each consistent with the observed data. For this case the aggregated $\varepsilon(\mathbf{x}_1,\mathbf{x}_2)$ criterion is called the likelihood. Details can be find in Box and Tiao (1992) and Scharnagl et al. (2015) and will not be repeated herein. However, we used a reduced likelihood function as suggested in Scharnagl et al. (2011) where the standard derivation of $\varepsilon(\mathbf{x}_1,\mathbf{x}_2)$ is eliminated,

$$p(\tilde{y} \mid x) \propto \left(\sum_{i+1}^{n} \varepsilon_i (x_1, x_2)^2 \right)^{-\frac{N}{2}} . \qquad 4.8$$

4.2.2.5 Model configuration

For all model applications the prior distribution were set as uniform distribution limited by lower and upper parameter boundaries that cover most soil types (Tab. 4.1). θ_s was fixed a priori to 0.9, related to θ_s values determined by Dettmann at al. [2014]) in a previous study (SF2) with laboratory experiments. For applications to uneven surfaces, the standard deviation (σ) of the normal distribution of surface elevations was set a priori according to the values listed in Tab. 4.2.

'DREAM' was run with standard configuration evolving three (in case of an even soil surface) or four (uneven surface) parallel chains. The uniform prior distribution was sampled using latin hypercube sampling. As convergence criteria Gelman and Rubin (1992) $\hat{R}$ convergence diagnostic was set to $\hat{R} < 1.1$. After the target distribution achieved convergence, 'DREAM' was run for 50000 additional function evaluations to generate the *pdf*.

Tab. 4.1: upper and lower parameter bounds of the van Genuchten parameters (θ_r, α, n) and the mean surface elevation of the microrelief (μ).

parameter	lower bound	upper bound
θ_r (cm^3 cm^{-3})	0	0.4
α (cm^{-1})	0.001	0.5
n (-)	1.01	30
$\Delta\mu$ (cm)	-20	20

Tab. 4.2: mean and lowest water levels and standard deviation (σ) of the normally distributed microrelief around the three investigated dip wells.

dip well	mean water level (m)	lowest water level (m)	σ (m)
'south'	-0.15	-0.44	0.071
'central'	-0.18	-0.44	0.089
'north'	-0.04	-0.32	0.061

4.2.3 Model application

The approach developed in this study was tested in two different applications. First, to demonstrate the applicability of the approach, a synthetic water level time series was generated based on known *VG* parameters and boundary conditions and assuming a flat surface. Afterwards, the approach was applied to water level time series from three dip wells located in an ombrotrophic bog field site (*Sphagnum* peat) that was characterized by an uneven soil surface.

4.2.3.1 Event detection criteria

In this study, we investigated water level rises from *zl* to *zu* as response to *P*, in the following referred as events, with $\Delta z > 0.02$ m, $zu < 0$ m, mean slope of the rise > 0.004 m h^{-1} and a total sum of $P > 2$ mm.

4.2.3.2 Application to synthetic data

The synthetic time series was created using the finite-element code HYDRUS-1D (Šimůnek et al., 2013) with parameters and boundary conditions from the field site. The modeled time series ranged from 2010/09/15 to 2014/11/11 and had the same length as the measured water level time series from the site.

The soil profile of 1 m height was discretized into 1001 elements with an element refinement towards the top. As soil hydraulic parameters, we used van Genuchten-Mualem (van Genuchten, 1980; Mualem, 1976) parameters derived by evaporation experiments and inverse parameter optimization for the field site (see Dettmann et al., 2014; supplemental material; 'SF2 wet range 5p': θ_s: 0.9 cm^3 cm^{-3}, θ_r: 0.12 cm^3 cm^{-3}, α: 0.0456 cm^{-1}, n: 1.72, ks: 10 cm h^{-1}, τ = -1.15). The lower boundary flux was set to zero.

The top boundary condition was set to atmospheric. P was measured with a station at the field site for the time periods 2010/09/15 – 2011/03/28, 2012/04/25 – 2012/05/16 and 2013/01/01 -

2014/10/03. For the missing time periods P data from the German weather forecast station Eberfing (47°47’45.6”N 11°12’00.0”E; distance to study site approximately 10 km) was used. With data from the same station, we calculated the FAO-crop-reference evaporation (Allen, 2000). The daily values were separated into hourly values in proportion to global radiation values calculated with Allen (2013). As the potential evaporation, calculated with the FAO-crop-reference evaporation, led to unrealistic low water levels and moisture conditions, w*e* assumed a crop coefficient of 0.5 for the *Sphagnum* peat. This is an averaged estimate for crop coefficients from several authors reporting values between approximately 0.3 to 0.8 (Campbell and Williamson, 1997; Kellner, 2001; Lafleur et al., 2005).

From the detected *P* events, *WRC* were optimized following section 4.2.2 (even surface). However, as *P* measurements usually are very uncertain, we additionally ran an application with forced *P* data error. Therefor, the *P* amounts of the detected events were multiplied with normally distributed random numbers (mean = 1, standard deviation = 0.1).

4.2.3.3 Application to field data

For the application to real data, we analyzed water level time series from three dip wells (‘south’, ‘central’, ‘north’) from a near-natural ombrotrophic bog complex (‘Schechenfilz’; 47° 48' N 11° 19’ E) in Germany. All dip wells are located at the plateau of the raised bog.

The bog has a five to six meter thick peat layer mainly under permanently water saturated conditions. The dominating peat substrate is *Sphagnum* moss, which is the dominating ground vegetation as well. Other occurring vegetation types are sedges, heather meadows and in the wooded areas of the bog slow growing bog-pines (Hommeltenberg et al., 2014).

Around the three dip wells, the composition of the vegetation differs. Around dip well ‘south’ only *Sphagnum* mosses occur. Dip well ‘central’ is surrounded by a combination of *Sphagnum* mosses, sedges, heather meadows and bog-pines. The composition around dip well ‘north’ is likely to those of dip well ‘central’, except the bog pines which are missing.

The northern part of the bog was partly affected by peat cutting until the 1950s (Hommeltenberg et al*.,* 2014). As the peat cutting occurred only in parts, the peat layer is spatially variable showing different stages of decomposition. However, in most parts the bog is still rather pristine. Dettmann et al. (2014) classified the peat near the dip well ‘central’ as weakly decomposed with H2 on the von Post scale, which classifies the degree of peat humification based on the proportion of visible plant remain and soil water color (von Post and Granlund, 1926). Around the dip well ‘north’ relict ditches occur which can be seen at

satellite pictures. Higher degrees of decomposition cannot be excluded around this dip well. The south of the bog complex was not affected by peat cutting and the *Sphagnum* peat around dip well 'south' is pristine.

Sphagnum mosses are characterized by their high porosities, low bulk densities and high soil organic carbon contents. Proceeding decomposition of organic particles result in smaller pores and higher bulk densities (Boelter, 1969; Moore et al., 2015). Dettmann et al. (2014) reported porosities from 90 – 95 % and bulk densities about 0.06 g cm^{-3} for the *Sphagnum* moss near dip well 'central'. Due to spatial variability, porosities and bulk densities can differ in relation to different decompositions and original peat substrates.

Water levels of all three dip wells are most of the year close to the surface with a mean water level for the available time series (2010/09/15 – 2014/11/11) of -0.15 m (dip well 'south'), -0.18 m (dip well 'central') and -0.04 m (dip well 'north'). The minimum water levels are -0.44 m (dip well 'south' and 'central') and -0.32 m (dip well 'north') (see also Tab. 4.2).

Microrelief of the field site

The bog complex 'Schechenfilz' has a distinctive microrelief consisting of hummocks and hollows. As water level changes are affected by the microrelief, the surface elevation was measured around the three investigated dip wells. Along six transects of 8 m, each beginning at the dip well, elevations were measured every 0.25 m in relation to the elevation of the dip well. However, as mentioned in section 4.2.2, *Sphagnum* bogs are characterised by a continuous transition from peat soil matrix to the top soil vegetation (Fig. 4.1), and it is hardly possible to define and measure a soil-vegetation interface. Thus, to obtain objective and reproducible elevation data, we placed the level staff (locating surface: 17 cm^2; weight: 1.8 kg) onto the ground without adding manually any extra pressure.

Fig. 4.2a illustrates exemplary data of a transect around dip well 'south'. The dip well is located at distance 0 m in Fig. 4.2a. Fig. 4.2b shows the surface elevation distributions of all transects around dip well 'south'. Usually water level depths are related to the surface height of the dip well location (0 m in Fig. 4.2b). However, this makes water level depths dependent on the specific position of the dip well and the comparison of water level depths with other dip wells in the study site might be rather a result of the specific microtopographic position of the dip well than of different water level depths. Therefore, in this study, all water levels are given as spatial average around the dip well, related to a mean surface elevation (μ) of zero.

Elevations around all three dip wells are approximately normally distributed. Tab. 4.2 shows the standard deviations (σ) around the dip wells 'south', 'central' and 'north'.

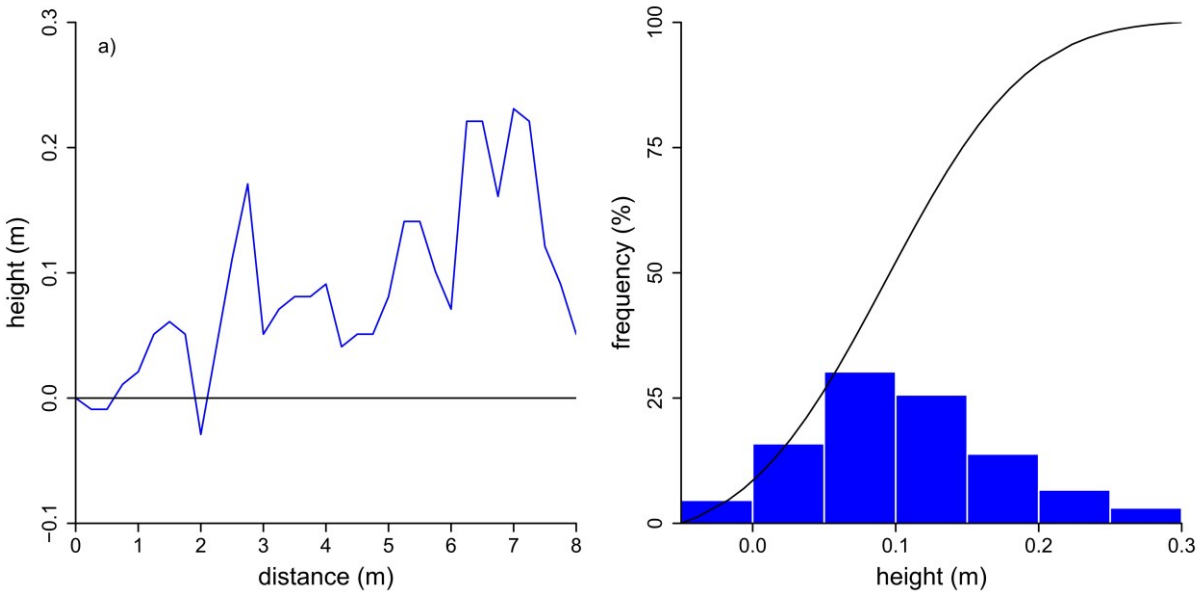

Fig. 4.2: a) Heights along one transect at dip well 'south'. Measured heights are in relation to the elevation of the dip well which is is located at distance 0 m. Measurements were made all 0.25 m. b) Cumulative surface elevation distribution (F_s) of all six measured transects.

4.3 Results and discussion

4.3.1 Evaluation of synthetic examples

For the synthetically generated time series, 36 events fulfilled the predefined criteria. For both synthetic examples (without and with forced rainfall error) the water level rises can be predicted accurately with the obtained *pdf*s of the *VG* parameters (not shown). As expected, the uncertainty increased for the simulation with forced rainfall error.

The estimated *pdf*s of the *VG* parameters α, n and θ_r are illustrated in Fig. 4.3. The horizontal axes of the figures only show a fraction of the parameter space of the uniform prior distributions for the parameters α and n due to the narrow *pdf*s that were obtained.

For the example without forced rainfall error, α and n were identified very well (Fig. 4.3 blue area). θ_r is uncertain as the lowest water level in the synthetic example was -0.31 m. Hence there is no sufficient information for lower pressure heads (higher suctions) and θ_r cannot be defined well. The widths of the *pdf*s of the forced rainfall error example are, compared to the example without forced rainfall error, increased (Fig. 4.3 red shaded area). However, the parameters α and n are still fairly well constrained. θ_r remains uncertain.

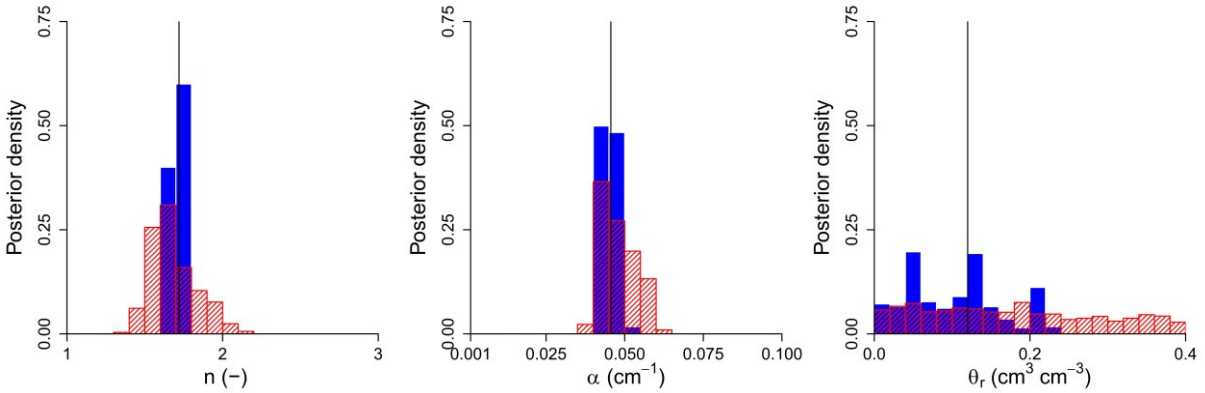

Fig. 4.3: Posterior density functions (*pdf*s) of the optimized van Genuchten (*VG*) parameters for the synthetic example without forced rainfall error (blue) and with forced rainfall error (red shaded). *VG* parameters of synthetic time series are indicated by the black vertical lines.

The *WRC* resulting from the *pdf*s are depicted in Fig. 4.4. Without forced rainfall error the *WRC* can be predicted almost perfectly. Notice the good agreement between the input *WRC* of the synthetic time series and the 95% confidence intervals (CI_{95}) of the optimization. Fig. 4.4 indicates that uncertainties are high for pressure heads below -31 cm, which corresponds to the minimum water level of the time series and thus information about higher suctions at lower water level stages is missing.

The results of the synthetic examples demonstrate that the approach developed in this study can lead to well defined *pdf*s of the parameters, even when *P* data is erroneous.

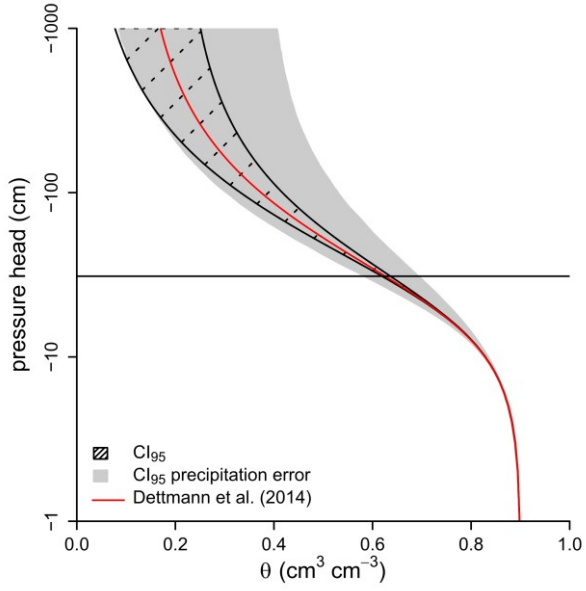

Fig. 4.4: 95% confidence intervals (CI_{95}) of the optimized van Genuchten (*VG*) parameters for the synthetic example without forced precipitation (*P*) error (shaded area) and with forced *P* error (grey area).

4.3.2 Evaluation of field data examples

4.3.2.1 Event detection and prediction of water level rises

For dip well ‘south’ 145 events, for ‘central’ 114 events and for ‘north’ 115 events fulfilled the predefined criteria. Differences in the amount of detected events among the dip wells are caused by differences in the values Δz, *zu* and mean slope of the water level rise.

Fig. 4.5a illustrates water level rises from *zl* to *zu* vs. S_y, calculated from the detected events at dip well ‘central’ ($S_y = \Delta z/P$; Logsdon et al., 2010). Most of the detected events are close to the surface. As seen in Fig. 4.5a, for water levels approaching the surface S_y values are increased. This clearly indicates the contribution of the surface storage at shallow water levels and demonstrates the necessity to account for the microrelief when predicting shallow water level changes. For lower water levels the influence of the *WRC* of the soil is increasing, but the microrelief also affects deeper water level rises (Dettmann and Bechtold, 2015).

Fig. 4.5a further indicates that a macroporous layer (with high S_y values) below the measured mean surface elevation contributes to the surface storage (see also section 4.2.2). This can be seen by the S_y values for the events with water levels between ~-0.2 and -0.1 m. Applying the normally distributed surface elevations of the microrelief ($\sigma = 0.089$ m, $\mu = 0$) at dip well ‘central’ to a water level change from -0.2 to -0.1 m, this results into a $S_{y,surface}$ value of 0.054 (after division by Δz). Thus, S_y values shown in Fig. 4.5a have an offset to the expected behavior of about 0.10 m. This offset can be explained by a top soil layer that acts like a porous system that releases water in the range of occurring matrix potential fluctuations. How deep the top surface soil acts like surface storage is shown by the optimization of $\Delta\mu$ as mentioned in section 4.2.2.

The simulated water level changes, obtained from the *pdf*s CI_{95}, match the observed ones fairly accurately for both deep and shallow water levels (Fig. 4.5b).

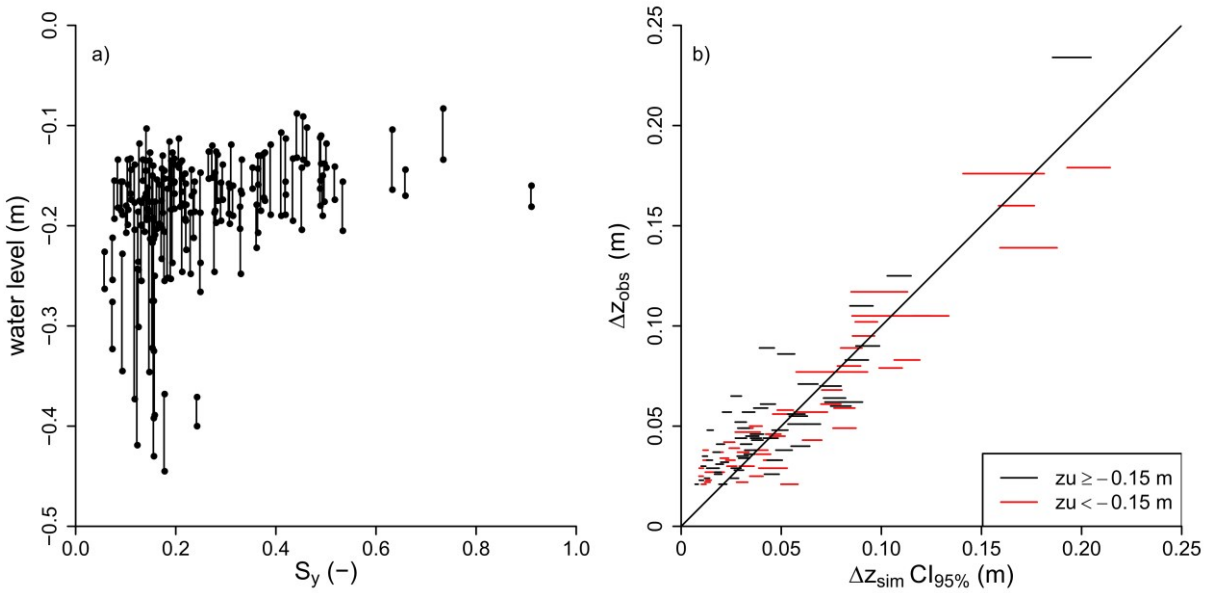

Fig. 4.5: a) Water level rise (from *zl* to *zu*) vs. specific yield (S_y) of the detected events at dip well 'central'. S_y is calculated for each event ($S_y = \Delta z/P$). b) Observed water level changes (Δz_{obs}) vs. 95% confidence intervals (CI_{95}) of simulated water level changes (Δz_{sim}) for dip well 'central'. The red lines represent Δz with $zu < -0.15$ m and the black lines Δz with $zu \geq -0.15$ m.

4.3.2.2 Prediction of posterior density functions and water retention characteristics

Posterior density functions

The *pdf*s of the estimated *VG* parameters and $\Delta\mu$ of the surface distribution for dip wells 'south' and 'central' are depicted in Fig. 4.6 (horizontal axes for parameters α, n and $\Delta\mu$ are narrowed from the uniform prior). The corresponding CI_{95} quantiles of the optimized parameters n, α and $\Delta\mu$, for all three simulated dip wells, are given in Tab. 4.3.

In proportion to the prior distribution of n (1.01 - 30), α (0.001 – 0.5 cm^{-1}) and $\Delta\mu$ (-20 to 20 cm) the *pdf*s of dip well 'south' and 'central' are well constrained. In contrast, results of dip well 'north' demonstrate the applicability limits of our approach. For dip well 'north', the inversion failed to constrain parameter n at the lower boundary of the prior distribution and the *pdf* of parameter α is wide compared to the dip wells 'south' and 'central'. This leads to unrealistic *WRC* within the CI_{95}. We interpret this as a failure of our approach for dip well 'north'. Water levels at dip well 'north' are approximately 0.1 m shallower than at the other dip wells. For dip well 'south' and 'central' S_y values are increased for events with $zl < -0.3$ m reaching S_y values of approximately 0.2 (indicated in Fig. 4.5a for dip well 'central'). The increasing S_y values at comparatively low water levels indicate that the soil substantially releases water at equivalent pressure heads in the upper soil. For constraining the *VG* parameters α and n this information is crucial because these parameters define at which pressure heads the soil dewaters substantially and how abruptly this occurs. The lowest water

level in the time series for dip well ‘north’ was -0.32 m. Below -0.3 m three events have been detected with S_y values between $0.07 – 0.08$. However, these S_y values are not increased compared to events at higher water levels. Following this, at dip well ‘north’, the lowest water levels are not sufficient to dewater the top soil substantially. Therefor the *VG* parameters n and α cannot be constrained.

For all dip wells, the inversion failed to constrain θ_r. Similar to the synthetic examples the information of the lowest levels is not sufficient to constrain θ_r. Hence θ_r will not be shown further herein.

In the following paragraphs the *WRC* of dip well ‘south’ and ‘central’ will be discussed.

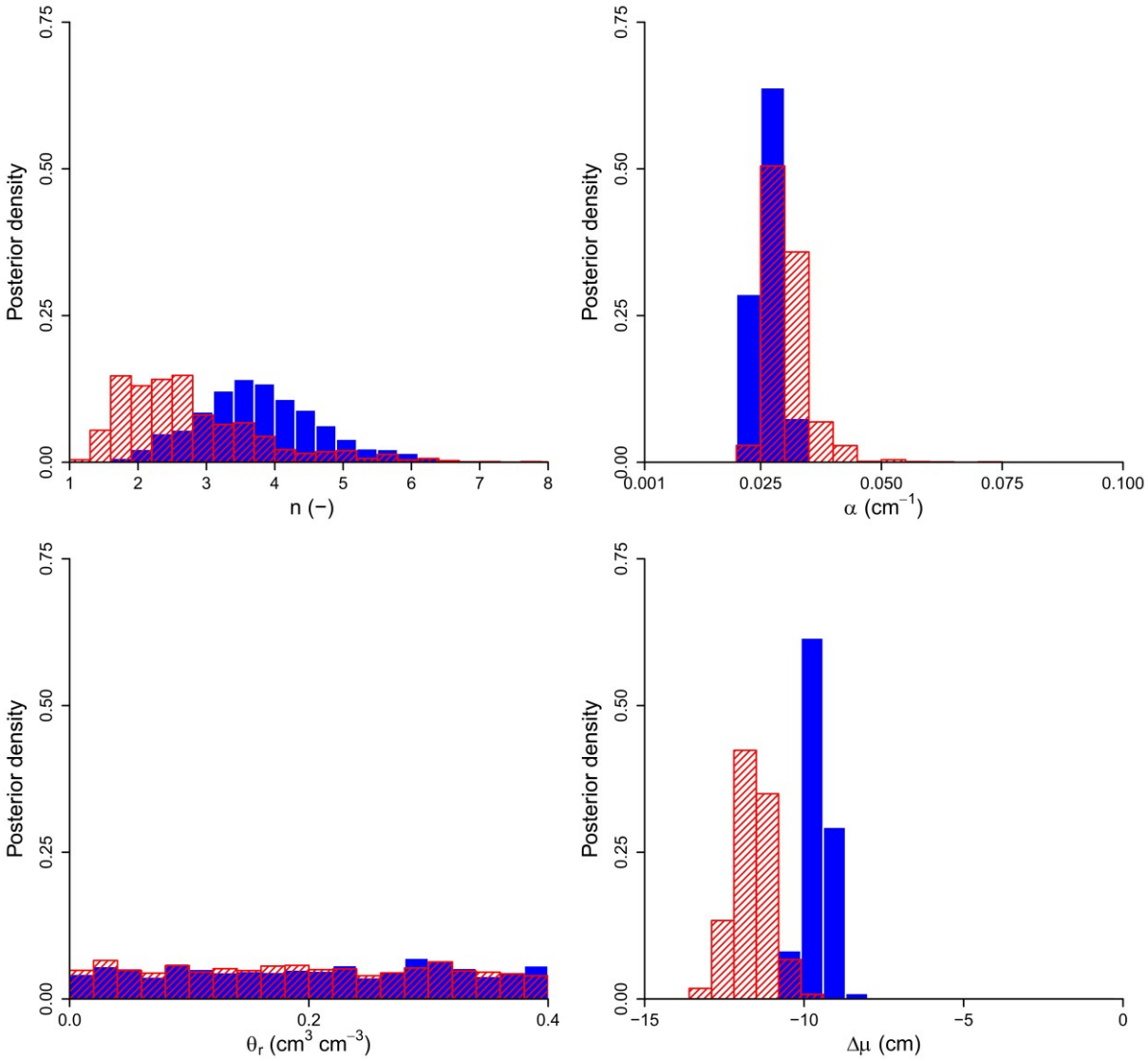

Fig. 4.6: Posterior density functions (*pdf*s) of the optimized van Genuchten (*VG*) parameters and the shift to the mean surface elevation ($\Delta\mu$) of the microrelief. Red: *pdf*s of dip well ‘central’, blue: *pdf*s of dip well ‘south’.

Tab. 4.3: lower and upper bands of the 95% confidence intervals (CI_{95}) of the posterior density functions (*pdf*) from the optimized parameters n, α and μ.

dip well	n (-)	α (cm^{-1})	$\Delta\mu$ (cm)
'south'	2.17 – 6.04	0.022 – 0.031	-10.3 – -8.9
'central'	1.46 – 5.78	0.025 – 0.042	-12.7 - -10.4
'north'	1.09 – 3.21	0.020 – 0.119	-2.2 - -0.1

Differences between dip well 'south' and 'central'

The uncertainty bounds (CI_{95}) of the optimized *WRC*s are visualized in Fig. 4.7. Also depicted is one of the *WRC* derived by Dettmann et al. (2014) near dip well 'central', which was used in the synthetic example. Comparing the CI_{95} uncertainty bounds in Fig. 4.7 shows a steeper decline of the *WRC* for decreasing pressure heads (increasing suctions) for dip well 'south' compared to dip well 'central'. This indicates that the peat at dip well 'south' is dewatering more abruptly. This may be an effect of different peat degradations and plant compositions of the peat substrates. According to Bartels and Kuntze (1968), pristine *Sphagnum* mosses are characterized by a more abrupt dewatering characteristic than less pristine *Sphagnum* mosses. In former centuries dip well 'central' was partly affected by peat cutting and drainage while the peat around dip well 'south' is expected to be pristine with H1 on the von Post scale. Following this, the steeper *WRC* at dip well 'south' (shown in Fig. 4.7) may be related to the more pristine peat compared to dip well 'central' where the peat is slightly decomposed (H2 on the von Post scale). However, this is contradictory to the pressure heads at which the soils start to dewater substantially indicated by the optimized α values. Generally, the *WRC* of pristine *Sphagnum* mosses are expected to dewater at higher pressure heads (lower suctions) than less pristine *Sphagnum* mosses (Boelter, 1969). This cannot be confirmed by the *WRC* obtained in this study. Therefore, the differences of the *WRC* may be further influenced by different plant composition of the peat substrates with pure *Sphagnum* at dip well 'south' and the combination of *Sphagnum*, sedges, heather meadows and bog-pines at dip well 'central'.

There are also methodological errors that may have contributed to the differences in α. They are discussed in section 4.3.2.4.

Comparison with literature data

The optimized *pdf*s of n are consistent with *WRC* of *Sphagnum* peat from several previous studies with n values between 2 and 2.82 (Price et al., 2008), n = 1.9 for fibric and n = 1.7 for

hemic peat (Letts et al., 2000) and $n > 3.8$ (Bartels and Kuntze, 1968; parameters were optimized using the values of Fig. 1 in Bartels and Kuntze). Dettmann et al. (2014) studied the *WRC* of the *Sphagnum* at the study site near dip well 'central' with evaporation experiments and inverse optimization. For the simulations with accurate model performances under wet conditions (referred as 'wet range' in Dettmann et al. (2015)) n values ranged from 1.50 – 2.29. This is within the range of the predicted *pdf*s of this study for dip well 'central'.

However, while several authors agreed about the abrupt dewatering capacity of pristine *Sphagnum* mosses with high n values (Bartels and Kuntze, 1968; Letts et al., 2000; Price et al., 2008), the range of published α values is comparatively large. Values of α in Dettmann et al. (2014) near dip well 'central' ranged from 0.027 to 0.045 for the simulations under wet conditions with an accurate model performance. Price et al. (2008) reported a large proportion (decreasing with depth) of easily drainable pores with α values from 10.47 – 0.1 cm^{-1} (depths from 5 – 25 cm). However, by the conceptual separation into ΔA_{soil} and $\Delta A_{surface}$ and the optimization of $\Delta\mu$ (results in section 4.3.2.3) we account for easily drainable pores (approximately down to 0.10 – 0.15 m depth) by $\Delta A_{surface}$. Following this, a direct comparison with α values obtained near the top surface from Price et al. (2008) is not meaningful. As opposed to this, the α value from Bartels and Kuntze (1968) (approximately 0.03 cm^{-1}) are an order of magnitude smaller, and start dewatering substantially at lower pressure heads (higher suctions). Letts et al. (2000) reported α values from 0.08 cm^{-1} for fibric to 0.02 cm^{-1} for hemic peat.

It should be noted that in contrast to these literature data, the *WRC* in this study were not determined for laboratory samples, but *in situ* and for a larger scale. As often observed for mineral soils, parameters can deviate considerably between these methods. A direct comparison can thus serve as an approximate plausibility check only.

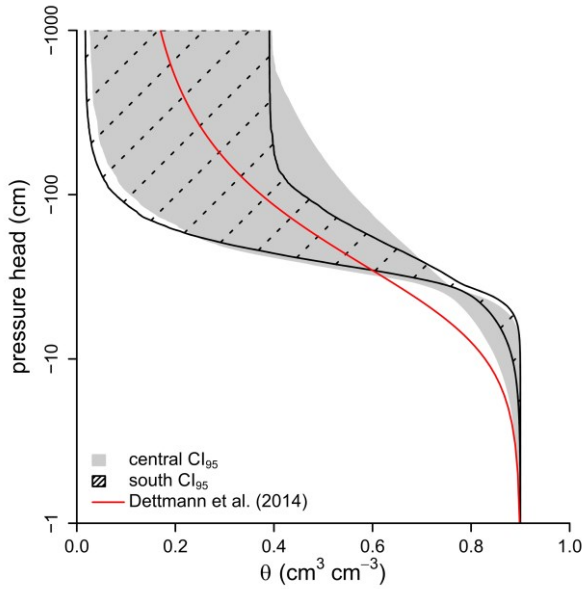

Fig. 4.7: Water retention characteristics (*WRC*) 95% confidence intervals (CI_{95}) for dip wells 'south', 'central' and *WRC* by Dettmann et al. (2014) near dip well 'central'.

4.3.2.3 Transition between soil and surface storage

The CI_{95} of the derived *pdf*s of $\Delta\mu$ (Fig. 4.6) are between -8.9 and -10.4 cm for dip well 'south', between -10.4 and -12.7 cm for dip well 'central' and between -2.2 and -0.1 cm for dip well 'north' (also listed in Tab. 4.3). Regarding dip well 'central', the *pdf* of $\Delta\mu$ is confirming the visual assumption from Fig. 4.5a, that approximately the top 0.1 m of the soil contain a high amount of macropores, i.e. presents high S_y values and thus is better described by $\Delta A_{surface}$. Analogue, this was observed for dip well 'south'. For dip well 'north' the *pdf* of $\Delta\mu$ shows values close to 0.

4.3.2.4 Discussion of uncertainties

Uncertainties of input variables

Fig. 4.5a shows a high variability of the depth dependency of S_y of the analyzed events. This can be attributed to several potential error sources, which can be separated into precipitation- and soil-related errors and can be both statistical and systematic.

About 35 percent of the *P* events were measured with a gauge within the bog, 30 to 325 m away from the three dip wells. Given the proximity, the error due to spatial variability of *P* can be considered as low for these data. However, data gaps were filled with data from the German weather forecast station Eberfing, which is 10 km away. Spatial variability of *P* can be high for such distances. Further, the distance leads to temporal offset of the rainfall. For the gap filled data, thus, we expect higher errors for the total *P* sums of the events.

Measurements with *P* gauges are adversely affected by undercatch bias, induced by wind turbulence, evaporative losses, wetting losses or mechanical plugging (Groisman and Legates, 1994). The *P* undercatch is highly variable depending on the wind characteristic (Neff, 1977). On average, measured *P* are lower than the actual *P*. In contrast, measured *P* values are higher than the amount of water that actually infiltrated due to interception in the vegetation layer.

Regarding Δz, several model assumptions for the soil processes are not entirely fulfilled in reality. Macropore flow, lateral flow, hydraulic gradients within the soil profile before and after *P,* and water repellency effects are variable in their presence and intensity among the different events and thus lead to statistical and systematic errors.

During macropore flow, water is bypassing the soil matrix through interaggregate space, shrinkage cracks and fissures, root channels or faunal tunnels (Dekker and Ritsema, 1996). As result, water levels rise abruptly, with a successive decline after the maximum when water redistributes into the soil matrix. We observed water level declines directly after the water level maximum for a variety of events for both deep and shallow water level rises, but not for all. If water levels declined, the length and steepness of the decline was very variable. This shows that macropore flow is variable and the intensity depends on several conditions, like e.g. the *P* intensity or water repellency condition of the *Sphagnum* moss before P. Water repellency is a time-dependent physical property of the soil (Dekker and Ritsema, 1996). It depends on the initial moisture of an event, and can induce macropore flow. Generally *Sphagnum* mosses are reported to be water repellent (Michel et al., 2001). However, to our knowledge studies are rare and only available for horticultural substrates. For the investigated study site with water levels mostly near surface, we expect water repellency in the top centimetres of the surface for low water levels. As the decline behaviour after water level rises was very variable and for longer time periods lateral water fluxes may become important, we decided not to correct Δ*z* for the decline. Thus, if macropore flow and water repellency are relevant for our site, measured Δ*z* are systematically higher than the prediction of a model that ignores these processes.

Further, upward hydraulic gradients within the soil profile before and after *P*, and lateral fluxes during the event may generate further uncertainty. If upward flux gradients within the soil profile occurred due to an evapotranspiration period before the event, parts of *P* would wet up the soil instead of causing Δ*z*. However, we expect the soil moisture profile close to hydrostatic equilibrium before and after *P* events as observations from Dettmann et al. (2014) showed for this peat soil. If water levels are very low, the assumption of hydrostatic

equilibrium within the soil profile may not be acceptable anymore and needs to be accounted for. The critical value depends on the soil-specific unsaturated conductivity. In particular, for shallower water levels, lateral (surface) water fluxes directed out of the bog system may occur during the time span of the event, which are neglected in our approach. Both upward hydraulic gradients and lateral fluxes lead to measured Δz that are systematically lower than the prediction of a model that neglect these influences. It can be noted that for both input variables, P and Δz, there are statistical errors and opposing systematic errors. As sufficient information about the error sources are not available for a reliable quantification, our philosophy in this paper was not to attempt to correct for any bias and to apply the data as they are.

Influence of uncertainties on obtained water retention characteristics

In section 4.3.2.2, we discussed the differences between the obtained *WRC* at dip well 'south' and 'central' and how they could be explained by field variability. From the uncertainty discussion, here, it becomes obvious that also methodological errors that deviate among the dip wells may have contributed to these differences. The observed water level rises at dip well ‘south’ and ‘central’ showed different Δz for the same P events. For most events, Δz was higher at dip well ‘south’ than at dip well ‘central’. This led to a lower α value at dip well ‘south’.

Most of the error sources above may have led to higher Δz at dip well 'south' compared to dip well 'central'. The most evident influence may have had the different compositions of the vegetation at the two dip wells. At dip well ‘central’, a combination of *Sphagnum* mosses, sedges, heather meadows and bog-pines is present, while dip well 'south' is surrounded by *Sphagnum* mosses only. We expect substantially higher interception for the higher vegetation at dip well 'central', which directly decreases Δz as less water actually infiltrated.

Further, one could argue that water repellency and macropore flow is more relevant at dip well 'south' compared to 'central'. The lower vegetation at dip well 'south' may have led to an enhanced drying of the uppermost soil-vegetation layer, which may provoke flow channeling due to water repellency, and thus, macropore flow. In contrast, higher vegetation at dip well 'central' additionally decreased rainfall intensity due to the retardation effect of the canopy, which further increased potential macropore flow at dip well 'south' compared to 'central'.

Summarizing, both, statistical and systematic uncertainties, influence the variability of the observed events (indicated in Fig. 4.5a). This leads to less constrained *pdf*s of the optimized

parameter set. Systematic uncertainties further can have different extend for different dip well sites, and, therefore, may lead to apparently different *WRC* within a study site. The magnitude of these uncertainties relative to the actual field variability cannot be quantified in this study.

4.3.3 **Benefit of the new approach**

Here, we provided a new approach for the determination of representative *WRC*, obtained *in situ* in the natural environment, as spatial average around a dip well. The proposed approach only requires water level and *P* measurements, and for field sites with uneven surfaces, additional information about the surface elevation distribution of the microrelief around the dip well. Therefore, the time consuming determination in laboratory on small soil samples and typical uncertainties of such methods (e.g. compaction or disturbance of the soil structure) can be avoided. Furthermore, the *WRC* of our approach are obtained for more representative soil volumes compared to laboratory soil samples.

Given the widely available data, field variability can be investigated within a study site at several dip wells or between different study sites. Together with other variables like land cover, ditch network, peatland characteristics or climatic boundary conditions the obtained *WRC* may improve the understanding of peat forming processes and the specific hydrological conditions within a peat- or wetland. Further, the *WRC* that can be derived by the new approach may improve large-scale processed-based hydrological models or water management strategies in terms of flood mitigation or agricultural issues. Furthermore, peatland hydrological models play an increasing role for the upscaling of greenhouse gas emissions (Bechtold et al., 2014). At catchment scale, more representative peat hydraulic properties determined at the available dip wells may improve such an upscaling.

As application example, we want to highlight the relevance of our study to improve the methodology of an evapotranspiration estimation approach. Evapotranspiration is frequently estimated by water level depth fluctuations following the method of White (1932) (Loheide et al., 2005; Mould et al., 2010; Fahle and Dietrich, 2014; McLaughlin and Cohen, 2014; Wang and Pozdniakov, 2014). The method of White (1932) uses diurnal patterns consisting of a water level decline at daytime and a recovery phase overnight. Following the theory of White (1932) and section 4.2.1, the evapotranspiration for shallow groundwater level can be calculated directly with equation (4.4)), if knowledge about the *WRC* is available. Using the *WRC* obtained by the approach of this study improves the estimation substantially. First, the *WRC* are directly estimated at the dip well and the *VG* parameters are available as *pdf*s. Thus,

uncertainties can be propagated to the evapotranspiration estimates. In our opinion this is essential, because evaporation estimates usually are highly uncertain. Second, surface storage plays a major role for the estimation at shallow groundwater systems. However, if the top vegetation at the soil surface contributes to the surface storage, as it is shown by the optimization of $\Delta\mu$, surface storage is substantially underestimated. The optimization of $\Delta\mu$ gives the possibility for a better estimation of the surface storage. This leads to more realistic evapotranspiration estimates.

The optimization of $\Delta\mu$ can substantially contribute to microrelief research of shallow groundwater systems. For these systems, a separation into vegetation and soil layer is often difficult. The particular height of this interface cannot be defined objectively, regardless if data is derived by surveying or by laser scanning data. The optimization of $\Delta\mu$ gives an objective estimation about the depth of the soil-vegetation interface from a hydrological perspective.

4.4 Summary and Conclusions

Our study indicates that observations of water level rises caused by *P* can contain sufficient information to predict *in situ* pedon to field scale *WRC* for soils of shallow-groundwater systems. For two of the three investigated dip wells, obtained *WRC* are in a plausible range and comparable to those of previous studies (Bartels and Kuntze, 1968; Dettmann et al., 2014; Letts et al., 2000; Price et al., 2008).

For low pressure heads (high suctions), indicated uncertainty was high. In general, uncertainty can be reduced with high quality and continuous *P* data observed directly at the field site. Further, there are several potential systematic errors due to simplified model assumptions. Given the lack of knowledge about detailed peat properties, it is hard to evaluate their relevance. Non-equilibrium phenomena as hydrophobicity and macropore flow may be investigated by the water level declines after the maximum of the events in combination with soil moisture probes. More knowledge about such processes could help to improve the method developed in this study. A quantitative consideration was beyond the scope of this paper and should be topic of future research.

Our approach requires water levels that are low enough that part of the upper soil dewaters substantially under hydrostatic equilibrium conditions. For one dip well, this was not sufficiently the case and the approach failed. For the other two dip wells, we consider the

estimation as a valuable information about the wet range of the *in situ WRC*. However, it should be emphasized that our approach does not account for vertical soil heterogeneity, but estimates effective parameters for a homogeneous representation of the soil. In particular for peat soils, vertical heterogeneity often occurs and can be high (Morris et al., 2015), and functions describing typical vertical trends could be considered as an advancement of our approach.

Acknowledgements:

We acknowledge the financial support by the joint research project 'Organic Soils' funded by the Thünen Institute. We appreciate support from Bärbel Tiemeyer (Thünen Institute, Braunschweig), Enrico Frahm (PTB, Braunschweig), Eike Maurer, Annette Freibauer (Thünen Institute, Braunschweig), Benedikt Scharnagl (UFZ, Halle), Marika Bernrieder and Janina Hommeltenberg (KIT, Garmisch-Partenkirchen).

5 Synthesis

5.1 Summarizing conclusions

This thesis deals with the determination of peat soil hydraulic properties at different scales. Therefore hydraulic properties have been derived in the laboratory and at a field site. Together with other variables like land cover, ditch network, peatland characteristics and climatic boundary conditions the results can improve the understanding of peat forming processes and the specific hydrological conditions in peatlands as well as several applications like the modeling of water and solute flow processes and the estimation of boundary fluxes (e.g. evapotranspiration) for water budget calculations or hydrological models. This in turn can support water management strategies for flood mitigation, agricultural issues or rewetting strategies and therefore contribute to a sustainable usage and nature conservation of peatlands.

Many previous studies focused on the determination of hydraulic properties of organic soils (Bartels and Kuntze, 1973; Boelter, 1969; Gnatowski et al., 2010; Grover and Baldock, 2013; Ilnicki, 1982; Kechavarzi et al., 2010; Letts et al., 2000; Olszta and Kowalski, 1996; Price et al., 2008; Price and Whittington, 2010; Schwärzel et al., 2006; Thompson and Waddington, 2013; Weiss et al., 1998). However, despite the significance of an accurate description of unsaturated zone processes, only very few studies focused on the applicability of the Richards' equation on organic soils, which is questionable, as the physical basis of the Richards' equation in terms of a rigid soil matrix is not fulfilled. Furthermore, no study evaluated the influence of certain *vGM* parameters on model performances and the possibility to account for macropore flow by the bi-/multimodal *vGM* based model of Durner (1994) and Priesack and Durner (2006).

Therefore, in the first study of this thesis (section 2), laboratory evaporation experiments were conducted for five different peat and organic soils and combined with inverse parameter optimization, in order (1) to analyze the applicability of the Richards' equation and *vGM* based models to simulate unsaturated flow in organic soils, (2) to evaluate the influence and sensitivity of different models with different parameter set-ups, and (3) to give recommendations how model parameter configuration should be set for an accurate modeling of the hydrological conditions of peatlands. The five investigated peat and organic soils represented a broad variability in terms of peat substrate, land use and vegetation, b_d, ε and *SOC* content.

The results pointed out that the simulation of the unsaturated water flow in peat and organic soils with the Richards' equation and *vGM* based soil hydraulic models lead to good model performances for a wide range of different peat and organic soils when adequate model set-ups are chosen. Thereby, two major aspects needed to be considered: (1) accounting for macropores is crucial for an accurate description of pressure heads near saturation. Therefore a simplified bimodal model that accounts only for the large, very easily drainable macropores provides a very accurate representation of the measured pressure heads and (2) for pressure heads below approximately -200 cm, knowledge about the *vGM* parameter τ is necessary, as it can strongly differ from the default value of 0.5 often used for mineral soil. Considering these options leads to a better description of vertical moisture distribution profiles and water level fluctuations.

The hydraulic properties derived from the first study of this thesis might be used for large scale models of the sites. Whether they can reproduce field conditions, e.g. water level dynamics, can only be determined by forward model runs for these sites. This is beyond the scope of this thesis.

For several applications *in situ* measurements of soils hydraulic properties would be an asset. Therefore a new *in situ* method of pedon to field scale soil *WRC* has been developed in this thesis. The method derives *VG* parameters (van Genuchten without the *K(h)* from Mualem) by water level rises after *P* events with Bayesian inversion. Therefore, if present, considering the microrelief is crucial because, in shallow groundwater systems, water level rises are strongly related to the microrelief, leading to a mosaic of inundated and non-inundated areas, and therefore mitigating water level rises. Moreover, the soil moisture profiles, which must be interpreted as spatial average, are affected by the microrelief as the soil volume covers only parts of the total volume. However, considering the influence of the microrelief on the soil moisture profiles and on water level dynamics with Bayesian inversion requires a conceptual 1D equation.

Therefore, in the second part of this thesis (section 3) a 1D equation for calculating S_y for shallow groundwater systems with microrelief was developed. The results clearly point out, that S_y is an interaction between soil hydraulic parameters and the microrelief, even if the water level changes are below the microrelief. The derived equation can improve several applications, like the calculating of evapotranspiration from water level fluctuations with the method of White (1932) or spatially distributed hydrological models in which the spatial grids are coarser than the typical microtopographic variation. For the calculation of the

evapotranspiration with the method of White (1932), accurate S_y values are of particular importance. If S_y is calculated with the *WRC* of a soil, it is decreasing with water level changes approaching the soil surface as changes in θ are small (Trübger, 2007). Frahm et al. (2010) mentioned that this leads to underestimated evapotranspiration calculations for shallow water levels when the method of Hays (2003) (modified White method) is used. Transposing the equation of Hays (2003) to S_y, with water level changes and the Penman-Monteith (Allen et al., 1998) evaporation, Frahm et al. (2010) showed that S_y values increase for water level changes near surface. With the conceptual 1D equation developed in this thesis, this finding can be represented by a mathematical formulation using the *WRC* of a soil and the cumulative frequency distribution of the microrelief. Furthermore, the derived equation is the basis for the third part (section 4) of this thesis, in which a new method for the *in situ* determination of *WRC* was developed as mentioned in the preceding.

The new developed *in situ* approach is applicable to shallow groundwater systems and only uses water level, *P* and, if relevant, microrelief data. Results demonstrate that the water level rises as results of *P* events contain enough information about the *WRC* of a soil to constrain the *VG* parameters α and n by Bayesian inversion, although there are various sources of uncertainties, like erroneous *P* measurements, macropore flow, water repellency or lateral fluxes during the *P* events. The approach requires water levels that are low enough that part of the upper soil dewaters substantially under hydrostatic equilibrium conditions. The *VG* parameter θ_r failed to constrain due to missing sufficient information for lower pressure heads. Nevertheless, the presented approach was able to characterize the field variability of soil *WRC* within a *Sphagnum* bog without any artificial disturbance of the soil. Furthermore, the depth of the transition from vegetation to soil layer could be estimated from a hydrological perspective. Both results have the potential to improve several applications. The derived *WRC* can be used directly for the calculation of evapotranspiration, following the method of White (1932) with declining water levels using equation (4.4). Furthermore, the *VG* parameters were determined as *pdf*s and therefore uncertainties can be propagated to the evapotranspiration estimates. The estimation of the depth of the soil-vegetation interface improves the calculations of the surface storage, which substantially influences evapotranspiration.

While the first study investigated a broad range of different peat and organic soils, the third study only investigated the *WRC* of a *Sphagnum* bog for one field site. The *Sphagnum* bog was also investigated in the first study. In both studies, the *WRC* of the *Sphagnum* bog had the expected steep dewatering capacity which is characteristic for pristine *Sphagnum* peat.

However, even if the *WRC* of the first study are within the *pdf*s of the third study for the *VG* parameters α and n, the principal dewatering behavior differed. The *WRC* determined *in situ* showed a steeper dewatering capacity than the *WRC* from the first study. Furthermore, α values of the *in situ* method tend to be lower. As often observed for mineral soils, parameters can deviate considerably between laboratory and field data and a direct comparison can thus serve as an approximate plausibility check only. Nevertheless, both methods lead to reliable results and have their specific advantages. The conclusions of the first study were drawn for dewatering conditions, while the third study investigated *WRC* for wetting conditions under *P* events. Furthermore, in the first study both *WRC* and *K(h)* have been determined simultaneously, while the third study only derived *WRC*. As this thesis proved the applicability of the closed-form equation of *vGM* on peat and other organic soils, the derived *in situ WRC* might be used to infer *K(h)*. Therefore, additional K_s measurements should be performed. This could be done with bail tests (Hvorslev, 1951) at the same dip wells at which the *WRC* are determined. Optimally, they should be combined with tension disc infiltrometer measurements for the characterization of macropore and preferential flow paths. Furthermore, parameter τ is needed. As pressure heads in the investigated field site did not fall below -200 cm, as mentioned in section 2, using the standard value of 0.5 might lead to sufficient *K(h)*. An alternative might be the usage of τ values derived from the first study. Whether this leads to realistic *K(h)* functions is beyond the scope of this thesis.

5.2 Outlook and further research needs

This thesis contributes to several open research questions regarding peatland hydrology, especially to the characterization of unsaturated hydraulic properties of peat soils. Although hydraulic properties of peat soils have been derived at different scales and for a broad range of different peat and organic soils, the hydraulic properties of peat soils are too variable and unique to cover all types of peat soils within this thesis. This thesis only determined very decomposed (H10 on the von Post scale; von Post and Granlund, 1926) and pristine (H1-H2 on the von Post scale) peat and other organic soils. Hence, for a general improvement of the understanding of hydrological processes in peatlands, soil hydraulic properties should be determined for a broader range of peat soils with different stages of decomposition. This would promote several major challenges and the development of pedotransfer functions.

Beside the variability of hydraulic properties of peat soils there are several issues regarding the physical and hydraulic properties of peat soils like hysteresis, water repellency, shrinkage,

swelling and preferential flow, which substantially influence the hydrological conditions in peatlands.

For both mineral and peat soils hysteresis is a challenging soil property. Due to air entrapment θ values at the same pressure heads differ during dewatering and wetting (Haines, 1930). However, most methods obtain hydraulic properties either for dewatering or wetting. In this thesis hydraulic properties were determined for both dewatering and wetting conditions. However, differences are rather a result of the methods, which deviate considerably, than a result of hysteresis. Hence, the results are not sufficient for investigations about hysteresis.

Hysteresis effects might be enhanced by the distinctive shrinkage and swelling characteristics of peat soils under changing moisture regimes. Beside the effects on hysteresis, shrinkage and swelling leads to changing pore space geometries and therefore to temporal variable hydraulic properties (Hendriks, 2004; Price and Schlotzhauer, 1999). Several studies investigated shrinkage of peat soils under laboratory conditions and observed distinctive horizontal and vertical shrinkage (Gebhardt et al., 2012; Oleszczuk and Brandyk, 2008; Päivänen, 1982). Under field conditions, shrinkage and swelling results primarily in an oscillating surface. Fritz et al. (2008) measured the oscillating surface and found the relationship to the water level to be linear or non-linear. It is a major challenge to identify the drivers (e.g. peat type or -thickness, water level depth, b_d) for peatland oscillation caused by shrinkage and swelling under field conditions and (1) develop models which can accurately predict the surface elevation heights in dependence to the water level and (2) parameterize those models for a broad range of peat soils. Optimally, shrinkage measurements should be combined with measurements of the soil hydraulic properties to estimate the temporal variability of the soil hydraulic properties in dependence on shrinkage, swelling and soil moisture. This would improve the understanding of the system substantially.

A further issue regarding peat properties is water repellency. Water repellency is a time-dependent physical property of the soil (Dekker and Ritsema, 1996). Dry peat soils are reported to be water repellent (Michel et al., 2001). However, to my knowledge studies are rare and only available for horticultural substrates. Water repellency influences preferential flow paths and might enhance hysteresis. Thus, water repellency of peat soils in laboratory and under field conditions should be further investigated from a chemical and a hydrological perspective, in order to understand the chemical processes of water repellency and the influences on peatland hydrology.

Both shrinkage and water repellency can either be reversible or irreversible and peat soils physical and hydraulic properties therefore might change temporally or permanently. It is a remaining challenge to quantify among which moisture contents shrinkage and water repellency are reversible or irreversible and how peatlands with irreversible disturbed peat soils react on changes of their hydrological conditions, e.g. on rewetting scenarios.

Finally, it should be mentioned that peat flow and transport processes are extremely complex and affected by a variety of physical, chemical and biological processes. Thus, it is a major challenge to characterize unsaturated flow and transport processes and choose appropriate methods for the intended interest as "*measurements of hydraulic properties for regional, continental, or global scales are virtually impossible*" (Schaap, 2005) and no method provides 'true' hydraulic properties. Nevertheless, although there many further research challenges to understand the hydrological conditions in peatlands in general, the findings of this thesis improve the determination of unsaturated hydraulic properties of peat soils as well as the understanding of the hydrological processes in peatlands.

References

Ad-hoc-AG Boden, 2005. Bodenkundliche Kartieranleitung (Soil survey manual), 5th Edn. Bundesanstalt für Geowissenschaften und Rohstoffe in Zusammenarbeit mit den Staatlichen Geologischen Diensten der Bundesrepublik Deutschland, hannover, 438 pp.

Allen, R.G., 2000. Using the FAO-56 dual crop coefficient method over an irrigated region as part of an evapotranspiration intercomparison study. Journal of Hydrology, 229(1-2): 27-41.

Allen, R.G., 2013. REF-ET: Reference evapotranspiration calculation software for FAO and ASCE Standardized Equations. University of Idaho and Dr. Richard. Allen.

Allen, R.G., Pereira, L.S., Raes, D., Smith, M., 1998. Crop evapotranspiration-Guidelines for computing crop water requirements-FAO Irrigation and drainage paper 56. FAO, Rome, 300(9): D05109.

Ankeny, M.D., Ahmed, M., Kaspar, T.C., Horton, R., 1991. Simple field method for determining unsaturated hydraulic conductivity. Soil Science Society of America Journal, 55(2): 467-470.

Baden, W., Eggelsmann, R., 1963. Zur Durchlässigkeit der Moorböden. Zeitschr. f. Kultur. u. Flurbereinigung: 226.

Baird, A.J., 1997. Field estimation of macropore functioning and surface hydraulic conductivity in a fen peat. Hydrological Processes, 11(3): 287-295.

Bartels, R., Kuntze, H., 1968. Ungesättigte hydraulische Leitfähigkeit von Moorböden. Göttinger Bodenkundliche Berichte, 1: 155-161.

Bartels, R., Kuntze, H., 1973. Peat properties and unsaturated hydraulic conductivity of peat soils. Zeitschrift fuer Pflanzenernaehrung und Bodenkunde, 134(2): 125-135.

Basile, A., Ciollaro, G., Coppola, A., 2003. Hysteresis in soil water characteristics as a key to interpreting comparisons of laboratory and field measured hydraulic properties. Water Resources Research, 39(12).

Bechtold, M. et al., 2014. Large-scale regionalization of water table depth in peatlands optimized for greenhouse gas emission upscaling. Hydrology and Earth System Sciences, 18(9): 3319-3339.

Beckwith, C.W., Baird, A.J., Heathwaite, A.L., 2003. Anisotropy and depth-related heterogeneity of hydraulic conductivity in a bog peat. I: Laboratory measurements. Hydrological Processes, 17(1): 89-101.

Blackwell, M.S., Hogan, D.V., Maltby, E., 2002. 15 Wetlands as Regulators of Pollutant Transport. Agriculture, Hydrology and Water Quality: 321.

Bodhinayake, W., Si, B.C., Noborio, K., 2004. Determination of hydraulic properties in sloping landscapes from tension and double-ring infiltrometers. Vadose Zone Journal, 3(3): 964-970.

Boelter, D.H., 1969. Physical properties of peats as related to degree of decomposition. Proceedings. Soil Science Society of America, 33: 606-609.

Bolger, B.L., Park, Y.J., Unger, A.J.A., Sudicky, E.A., 2011. Simulating the pre-development hydrologic conditions in the San Joaquin Valley, California. Journal of Hydrology, 411(3-4): 322-330.

Box, G.E.P., Tiao, G.C., 1992. Bayesian Inference in Statistical Analysis, New York City.

Bragazza, L. et al., 2006. Atmospheric nitrogen deposition promotes carbon loss from peat bogs. Proceedings of the National Academy of Sciences of the United States of America, 103(51): 19386-19389.

Brooks, R.J., Corey, A.T., 1964. Hydraulic Properties of Porous Media, Hydrology Paper No. 3, Fort Collins: Colorado State University.

Brunner, P., Simmons, C.T., 2012. HydroGeoSphere: A Fully Integrated, Physically Based Hydrological Model. Ground Water, 50(2): 170-176.

Bullock, A., Acreman, M., 2003. The role of wetlands in the hydrological cycle. Hydrology and Earth System Sciences Discussions, 7(3): 358-389.

Byrne, K.A. et al., 2004. EU peatlands: Current carbon stocks and trace gas fluxes. CarboEurope-GHG Concerted Action–Synthesis of the European Greenhouse Gas Budget, Report, 4: 2004.

Campbell, D.I., Williamson, J.L., 1997. Evaporation from a raised peat bog. Journal of Hydrology, 193(1-4): 142-160.

Campbell, G.S., 1974. A simple method for determining unsaturated conductivity from moisture retention data. Soil science, 117(6): 311-314.

Campbell, G.S., Smith, D.M., Teare, B.L., 2007. Application of a dew point method to obtain the soil water characteristic, Experimental Unsaturated Soil Mechanics. Springer, pp. 71-77.

Cheng, D.-h., Wang, Y.-h., Duan, J.-b., Chen, X., Yang, S.-k., 2014. A new analytical expression for ultimate specific yield and shallow groundwater drainage. Hydrological Processes.

Childs, E., 1960. The nonsteady state of the water table in drained land. Journal of Geophysical Research, 65(2): 780-782.

Clothier, B., Scotter, D., 2002. Unsaturated Water Transmission Parameters Obtained from infiltration. In: Dane, J.H., Topp, G.C. (Eds.), Methods of Soil Analysis; Part 4 - Physical Methods. Soil Science Society of America, Inc., Madison, pp. 879-898.

Crosbie, R.S., Binning, P., Kalma, J.D., 2005. A time series approach to inferring groundwater recharge using the water table fluctuation method. Water Resources Research, 41(1): 1-9.

Daigneault, C.V., Nichols, K., Hall, M., 2012. The Importance of Wetlands in Ecosystem Services: with Special Attention on Flood Attenuation, Carbon Sequestration, Hydrogeology, Water Quality, Biodiversity, and Social and Local Values. ERSC 3160H - Wetlands final report.

Dane, J., Hopmans, J.W., 2002. Laboratory. In: Dane, J.H., Topp, G.C. (Eds.), Methods of Soil Analysis: Part 4 - Physical Methods. Soil Science Society of America, Madison, pp. 675-719.

Darcy, H.P.G., 1856. Dètermination des lois d'ècoulement de l'eau à travers le sable.

De Roo, P.J.A. et al., 2003. Development of a European flood forecasting system. Intl. J. River Basin Management, 1(1): 12.

Decagon Devices, 2014. WP4C Dewpoint PotentiaMeter Operator's Manual. Decagon Devices, Inc., Pullmann, WA.

Dekker, L.W., Ritsema, C.J., 1996. Variation in water content and wetting patterns in Dutch water repellent peaty clay and clayey peat soils. CATENA, 28(1): 89-105.

Dettmann, U., Bechtold, M., 2015. One-dimensional expression to calculate specific yield for shallow groundwater systems with microrelief. Hydrological Processes.

Dettmann, U., Bechtold, M., Frahm, E., Tiemeyer, B., 2014. On the applicability of unimodal and bimodal van Genuchten–Mualem based models to peat and other organic soils under evaporation conditions. Journal of Hydrology, 515(0): 103-115.

Dimitrov, D.D., Grant, R.F., Lafleur, P.M., Humphreys, E.R., 2010. Modeling the Subsurface Hydrology of Mer Bleue Bog. Soil Science Society of America Journal, 74(2): 680-694.

Dorrepaal, E. et al., 2009. Carbon respiration from subsurface peat accelerated by climate warming in the subarctic. Nature, 460(7255): 616-619.

Du Rietz, G.E., 1949. Huvudenheter och huvudgränser i svensk myrvegetation. Svensk Botanisk Tidskrift, 43: 274-309.

Du Rietz, G.E., 1954. Die Mineralbodenwasserzeigergrenze als Grundlage einer natürlichen Zweigliederung der nord-und mitteleuropäischen Moore. Vegetatio, 5(1): 571-585.

Duan, Q.Y., Sorooshian, S., Gupta, V., 1992. Effective and Efficient Global Optimization for Conceptual Rainfall-Runoff Models. Water Resources Research, 28(4): 1015-1031.

Duke, H., 1972. Capillary properties of soils - influence upon specific yield. Transactions of the ASAE, 15(4): 688-699.

Durner, W., 1994. Hydraulic conductivity estimation for soils with heterogeneous pore structure. Water Resources Research, 30(2): 211-223.

Durner, W., Flühler, H., 2005. Chapter 74: Soil Hydraulic Properties. In: M.G., A., McDonnell, J.J. (Eds.), Encyclopedia of Hydrological Sciences. John Wiley & Sons, Ltd., pp. 1103-1119.

Durner, W., Lipsius, K., 2005. Chapter 75: Determining Soil Hydraulic Properties. In: M.G., A., McDonnell, J.J. (Eds.), Encyclopedia of Hydrological Sciences. John Wiley & Sons, Ltd., pp. 1121-1144.

Fahle, M., Dietrich, O., 2014. Estimation of evapotranspiration using diurnal groundwater level fluctuations: Comparison of different approaches with groundwater lysimeter data. Water Resources Research, 50(1): 273-286.

Ferguson, I.M., Maxwell, R.M., 2010. Role of groundwater in watershed response and land surface feedbacks under climate change. Water Resources Research, 46(10).

Frahm, E., Salzmann, T., Miegel, K., 2010. Untersuchungen zum Wasserhaushalt eines natürlichen Weidenbestandes (Salix spp.) in einem nordostdeutschen Flusstalmoor. Korrespondenz Wasserwirtschaft, 1: 24 - 29.

Fraser, C., Roulet, N., Lafleur, M., 2001. Groundwater flow patterns in a large peatland. Journal of Hydrology, 246(1): 142-154.

Fritz, C., Campbell, D.I., Schipper, L.A., 2008. Oscillating peat surface levels in a restiad peatland, New Zealand—magnitude and spatiotemporal variability. Hydrological Processes, 22(17): 3264-3274.

Frolking, S., Roulet, N.T., 2007. Holocene radiative forcing impact of northern peatland carbon accumulation and methane emissions. Global Change Biology, 13(5): 1079-1088.

Gardner, W.R., Miklich, F.J., 1962. Unsaturated conductivity and diffusivity measurements by a constant flux method. Soil Sci, 93(4): 271-274.

Gebhardt, S., Fleige, H., Horn, R., 2012. Anisotropic shrinkage of mineral and organic soils and its impact on soil hydraulic properties. Soil and Tillage Research, 125: 96-104.

Gelman, A., Rubin, D.B., 1992. Inference from iterative simulation using multiple sequences. Statistical science: 457-472.

Gilvear, D., Sadler, P., Tellam, J., Lloyd, J., 1997. Surface water process and groundwater flow within a hydrologically complex floodplain wetland, Norfolk Broads, UK. Hydrology and Earth System Sciences Discussions, 1(1): 115-135.

Gnatowski, T., Szatylowicz, J., Brandyk, T., Kechavarzi, C., 2010. Hydraulic properties of fen peat soils in Poland. Geoderma, 154(3-4): 188-195.

Gorham, E., 1991. Northern peatlands - role in the carbon-cycle and probable responses to climatic warming. Ecological Applications, 1(2): 182-195.

Groisman, P.Y., Legates, D.R., 1994. The Accuracy of United States Precipitation Data. Bulletin of the American Meteorological Society, 75(2): 215-227.

Grover, S.P.P., Baldock, J.A., 2013. The link between peat hydrology and decomposition: Beyond von Post. Journal of Hydrology, 479(0): 130-138.

Haines, W.B., 1930. Studies in the physical properties of soil. V. The hysteresis effect in capillary properties, and the modes of moisture distribution associated therewith. The Journal of Agricultural Science, 20(01): 97-116.

Hays, K.B., 2003. Water use by saltcedar (Tamarix sp.) and associated vegetation on the Canadian, Colorado and Pecos Rivers in Texas. Diss., Texas A&M University.

Hendriks, R.F.A., 2004. An analytical equation for describing the shrinkage characteristics of peat soils, Wise use of Peatlands. Proceedings of the 12th International Peat Congress. Päivänen (Ed.), J., Tampere, Finland.

Hendriks, R.F.A., Oostindie, K., Hamminga, P., 1999. Simulation of bromide tracer and nitrogen transport in a cracked clay soil with the FLOCR/ANIMO model combination. Journal of Hydrology, 215(1-4): 94-115.

Hoag, R.S., Price, J.S., 1997. The effects of matrix diffusion on solute transport and retardation in undisturbed peat in laboratory columns. Journal of Contaminant Hydrology, 28(3): 193-205.

Holden, J., 2005. Peatland hydrology and carbon release: why small-scale process matters. Philosophical Transactions of the Royal Society of London A: Mathematical, Physical and Engineering Sciences, 363(1837): 2891-2913.

Holden, J., 2009. Flow through macropores of different size classes in blanket peat. Journal of Hydrology, 364(3-4): 342-348.

Holden, J., Burt, T., 2003a. Hydrological studies on blanket peat: the significance of the acrotelm-catotelm model. Journal of Ecology, 91(1): 86-102.

Holden, J., Burt, T.P., 2003b. Hydraulic conductivity in upland blanket peat: Measurement and variability. Hydrological Processes, 17(6): 1227-1237.

Holden, J., Chapman, P.J., Labadz, J.C., 2004. Artificial drainage of peatlands: hydrological and hydrochemical process and wetland restoration. Progress in Physical Geography, 28(1): 95-123.

Hommeltenberg, J., Schmid, H.P., Drösler, M., Werle, P., 2014. Can a bog drained for forestry be a stronger carbon sink than a natural bog forest? Biogeosciences, 11(13): 3477-3493.

Hopmans, J.W., Simunek, J., Romano, N., Durner, W., 2002. Inverse Methods. In: Dane, J.H., Topp, G.C. (Eds.), Methods of Soil Analysis; Part 4 - Physical Methods. Soil Science Society of America, Inc., Madison, pp. 963-1008.

Hvorslev, M.J., 1951. Time lag and soil permeability in ground-water observations.

Ilnicki, P., 1982. Hysterese der Wasserspannungskurve in organogenen Böden. Zeitschrift für Pflanzenernährung und Bodenkunde, 145(4): 363-374.

Ingram, H., 1978. Soil layers in mires: function and terminology. Journal of Soil Science, 29(2): 224-227.

Ingram, H., 1983. Mires: Swamp, bog, fen and moor. Hydrology. Ecosystems of the World, 4: 67-158.

IPCC, 2006. IPCC guidelines for national greenhouse gas inventories. In: Eggleston, H.S., Buendia, L., Miwa, K., Ngara, T., K., T. (Eds.). IGES, Japan.

Ippisch, O., Vogel, H.-J., Bastian, P., 2006. Validity limits for the van Genuchten–Mualem model and implications for parameter estimation and numerical simulation. Advances in Water Resources, 29(12): 1780-1789.

Ivanov, K.E.e., 1981. Water movement in mirelands. Academic Press Inc.(London) Ltd.

Jadoon, K.Z. et al., 2012. Estimation of soil hydraulic parameters in the field by integrated hydrogeophysical inversion of time-lapse ground-penetrating radar data. Vadose Zone Journal, 11(4).

Jarvis, N.J., 2007. A review of non-equilibrium water flow and solute transport in soil macropores: principles, controlling factors and consequences for water quality. European Journal of Soil Science, 58(3): 523-546.

Jenerette, G.D., Barron-Gafford, G.A., Guswa, A.J., McDonnell, J.J., Villegas, J.C., 2012. Organization of complexity in water limited ecohydrology. Ecohydrology, 5(2): 184-199.

Joosten, H. et al., 2013. MoorFutures®. Integration von weiteren Ökosystemdienstleistungen einschließlich Biodiversitöt in Kohlenstoffzertifikate - Standard, Methologie und Übertragbarkeit in andere Regionen. BfN-Skripten, 350: 1-131.

Joosten, H., Couwenberg, J., 2012. Bilanzen zum Moorverlust. In: Succow, M., Joosten, H. (Eds.), Moorkunde. E. Schweizerbart'sche Verlagsbuchhandlung, Stuttgart, pp. 622.

Joosten, H., Tapio-Biström, M.-L., Tol, S., 2012. Peatlands-guidance for climate change mitigation through conservation, rehabilitation and sustainable use. FAO.

Jury, W. et al., 2011. Kirkham's legacy and contemporary challenges in soil physics research. Soil Science Society of America Journal, 75(5): 1589-1601.

Kadlec, R.H., Hammer, D.E., 1988. Modeling nutrient behavior in wetlands. Ecological Modelling, 40(1): 37-66.

Karamouz, M., Nazif, S., Falahi, M., 2012. Hydrology and hydroclimatology: principles and applications. CRC Press.

Kechavarzi, C., Dawson, Q., Leeds-Harrison, P.B., 2010. Physical properties of low-lying agricultural peat soils in England. Geoderma, 154(3-4): 196-202.

Kellner, E., 2001. Surface energy fluxes and control of evapotranspiration from a Swedish Sphagnum mire. Agricultural and Forest Meteorology, 110(2): 101-123.

Kellogg, L.E., Bridgham, S.D., 2003. Phosphorus retention and movement across an ombrotrophic-minerotrophic peatland gradient. Biogeochemistry, 63(3): 299-315.

Köhne, J.M., Köhne, S., Simunek, J., 2009. A review of model applications for structured soils: a) Water flow and tracer transport. Journal of Contaminant Hydrology, 104(1-4): 4-35.

Kool, J.B., Parker, J.C., van Genuchten, M.T., 1987. Parameter-estimation for unsaturated flow and transport models - A review. Journal of Hydrology, 91(3-4): 255-293.

Kosugi, K., 1996. Lognormal distribution model for unsaturated soil hydraulic properties. Water Resources Research, 32(9): 2697-2703.

Kroes, J.G., van Dam, J.C., Groenendijk, P., Hendriks, R.F.A., Jacobs, C.M.J., 2008. SWAP version 3.2. Theory description and user manual, Alterra Report1649(02), Alterra, Wageningen, 2008.

Lafleur, P.M., Hember, R.A., Admiral, S.W., Roulet, N.T., 2005. Annual and seasonal variability in evapotranspiration and water table at a shrub-covered bog in southern Ontario, Canada. Hydrological Processes, 19(18): 3533-3550.

Leiber-Sauheitl, K., Fuß, R., Voigt, C., Freibauer, A., 2013. High greenhouse gas fluxes from grassland on histic gleysol along soil carbon and drainage gradients. Biogeosciences Discuss., 10(7): 11283-11317.

Letts, M.G., Roulet, N.T., Comer, N.T., Skarupa, M.R., Verseghy, D.L., 2000. Parametrization of peatland hydraulic properties for the Canadian Land Surface Scheme. Atmosphere - Ocean, 38(1): 141-160.

Li, Q. et al., 2008. Simulating the multi-seasonal response of a large-scale watershed with a 3D physically-based hydrologic model. Journal of Hydrology, 357(3-4): 317-336.

Limpens, J. et al., 2008. Peatlands and the carbon cycle: From local processes to global implications - A synthesis. Biogeosciences, 5(5): 1475-1491.

Logsdon, S.D. et al., 2010. Field estimation of specific yield in a central Iowa crop field. Hydrological Processes, 24(10): 1369-1377.

Loheide II, S.P., Butler Jr, J.J., Gorelick, S.M., 2005. Estimation of groundwater consumption by phreatophytes using diurnal water table fluctuations: A saturated-unsaturated flow assessment. Water Resources Research, 41(7): 1-14.

Luckner, L., van Genuchten, M.T., Nielsen, D.R., 1989. A Consistent Set of Parametric Models for the Two-Phase Flow of Immiscible Fluids in the Subsurface. Water Resources Research, 25(10): 2187-2193.

Lyford, W.H., MacLean, D.W., 1966. Mound and pit microrelief in relation to soil disturbance and tree distribution in New Brunswick, Canada. Harvard forest paper, 15: 20.

Maljanen, M. et al., 2010. Greenhouse gas balances of managed peatlands in the Nordic countries - present knowledge and gaps. Biogeosciences, 7(9): 2711-2738.

Maltby, E., 1991. Wetlands and their values. Wetlands: 8-26.

Maltby, E., Proctor, M.C.F., 1996. Peatlands: Their nature and role in the biosphere. In: Lappalainen, E. (Ed.), Global peat resources. International Peat Society, Jyskä, pp. 359.

Manning, R., Griffith, J.P., Pigot, T., Vernon-Harcourt, L.F., 1890. On the flow of water in open channels and pipes.

McClellan, M.H., Bormann, B.T., Cromack Jr, K., 1990. Cellulose decomposition in southeast Alaskan forests: effects of pit and mound microrelief and burial depth. Canadian Journal of Forest Research, 20(8): 1242-1246.

McLaughlin, D.L., Cohen, M.J., 2014. Ecosystem specific yield for estimating evapotranspiration and groundwater exchange from diel surface water variation. Hydrological Processes, 28(3): 1495-1506.

Melesse, A.M., Abtew, W., 2015. Landscape Dynamics, Soils and Hydrological Processes in Varied Climates. Springer.

Michel, J.C., Rivière, L.M., Bellon-Fontaine, M.N., 2001. Measurement of the wettability of organic materials in relation to water content by the capillary rise method. European Journal of Soil Science, 52(3): 459-467.

Minkkinen, K., 1999. Effect of forestry drainage on the carbon balance and radiative forcing of peatlands in Finland, University of Helsinki, Helsinki, 42 pp.

Mitchell, A.R., 1991. Soil surface shrinkage to estimate profile soil water. Irrigation Science, 12(1): 1-6.

Mitchell, A.R., Van Genuchten, M.T., 1992. Shrinkage of bare and cultivated soil. Soil Science Society of America Journal, 56(4): 1036-1042.

Moore, P., Morris, P., Waddington, J., 2015. Multi-decadal water table manipulation alters peatland hydraulic structure and moisture retention. Hydrological Processes.

Morris, P.J., Baird, A.J., Belyea, L.R., 2015. Bridging the gap between models and measurements of peat hydraulic conductivity. Water Resources Research, 51(7): 5353-5364.

Morris, P.J., Waddington, J.M., Benscoter, B.W., Turetsky, M.R., 2011. Conceptual frameworks in peatland ecohydrology: looking beyond the two-layered (acrotelm–catotelm) model. Ecohydrology, 4(1): 1-11.

Mortl, A., Muñoz-Carpena, R., Kaplan, D., Li, Y., 2011. Calibration of a combined dielectric probe for soil moisture and porewater salinity measurement in organic and mineral coastal wetland soils. Geoderma, 161(1): 50-62.

Mould, D.J., Frahm, E., Salzmann, T., Miegel, K., Acreman, M.C., 2010. Evaluating the use of diurnal groundwater fluctuations for estimating evapotranspiration in wetland environments: case studies in southeast England and northeast Germany. Ecohydrology, 3(3): 294-305.

Mualem, Y., 1976. A New Model for Predicting the Hydraulic Conductivity of Unsaturated Porous Media. Water Resources Research, 12(3): 513-522.

Myerscough, P.J., Clarke, P.J., Skelton, N.J., 1996. Plant coexistence in coastal heaths: Habitat segregation in the post-fire environment. Australian Journal of Ecology, 21(1): 47-54.

Nachabe, M.H., 2002. Analytical expressions for transient specific yield and shallow water table drainage. Water Resources Research, 38(10): 111-117.

Nagare, R., Schincariol, R., Quinton, W., Hayashi, M., 2011. Laboratory calibration of time domain reflectometry to determine moisture content in undisturbed peat samples. European Journal of Soil Science, 62(4): 505-515.

Neff, E.L., 1977. How much rain does a rain gage gage? Journal of Hydrology, 35(3): 213-220.

Nungesser, M.K., 2003. Modelling microtopography in boreal peatlands: hummocks and hollows. Ecological Modelling, 165(2–3): 175-207.

Ogawa, H., Male, J.W., 1986. Simulating the flood mitigation role of wetlands. Journal of Water Resources Planning and Management, 112(1): 114-128.

Oleszczuk, R., Brandyk, T., 2008. The analysis of shrinkage-swelling behavior of peat-moorsh soil aggregates during drying-wetting cycles. Agron. Res, 6(1): 131-140.

Olszta, W., Kowalski, D., 1996. Verification of the Van Genuchten method of determination of the hydraulic conductivity of peat soils. International agrophysics.

Paavilainen, E., Päivänen, J., 1995. Peatland forestry: ecology and principles, 111. Springer Science & Business Media.

Päivänen, J., 1982. Physical properties of peat samples in relation to shrinkage upon drying.

Paquet, J., Caron, J., Banton, O., 1993. In situ determination of the water desorption characteristics of peat substrates. Canadian Journal of Soil Science, 73(3): 329-339.

Parkin, G.W., Kachanoski, R.G., Elrick, D.E., Gibson, R.G., 1995. Unsaturated hydraulic conductivity measured by time domain reflectometry under a rainfall simulator. Water Resources Research, 31(3): 447-454.

Pepin, S., Plamondon, A.P., Stein, J., 1992. Peat water content measurement using time domain reflectometry. Canadian Journal of Forest Research, 22(4): 534-540.

Peters, A., 2013. Simple consistent models for water retention and hydraulic conductivity in the complete moisture range. Water Resources Research, 49(10): 6765-6780.

Peters, A., Durner, W., 2008. Simplified evaporation method for determining soil hydraulic properties. Journal of Hydrology, 356(1-2): 147-162.

Plagge, R., Renger, M., Roth, C.H., 1990. A new laboratory method to quickly determine the unsaturated hydraulic conductivity of undisturbed soil cores within a wide range of textures. Zeitschrift für Pflanzenernährung und Bodenkunde, 153(1): 39-45.

Price, J., Heathwaite, A., Baird, A., 2003. Hydrological processes in abandoned and restored peatlands: an overview of management approaches. Wetlands Ecology and Management, 11(1-2): 65-83.

Price, J.S., Schlotzhauer, S.M., 1999. Importance of shrinkage and compression in determining water storage changes in peat: the case of a mined peatland. Hydrological Processes, 13(16): 2591-2601.

Price, J.S., Whittington, P.N., 2010. Water flow in Sphagnum hummocks: Mesocosm measurements and modelling. Journal of Hydrology, 381(3-4): 333-340.

Price, J.S. et al., 2008. A method to determine unsaturated hydraulic conductivity in living and undecomposed moss. Soil Science Society of America Journal, 72(2): 487-491.

Priesack, E., Durner, W., 2006. Closed-form expression for the multi-modal unsaturated conductivity function. Vadose Zone Journal, 5(1): 121-124.

Querner, E.P., Mioduszewski, W., Povilaitis, A., Slesicka, A., 2010. Modelling peatland hydrology: three cases from northern Europe. Polish Journal of Environmental Studies, 19(1): 149-160.

Reynolds, W.D., Elrick, D.E., Youngs, E.G., Amoozegar, A., 2002a. The Soil Solution Phase - Field Methods. In: Dane, J.H., Topp, G.C. (Eds.), Methods of Soil Analysis; Part 4 - Physical Methods. Soil Science Society of America, Inc., Madison, pp. 817-878.

Reynolds, W.D., Elrick, D.E., Youngs, E.G., Booltink, H.W.G., Bouma, J., 2002b. The Soil Solution Phase - Laboratory Methods. In: Dane, J.H., Topp, G.C. (Eds.), Methods of Soil Analysis; Part 4 - Physical Methods. Soil Science Society of America, Inc., Madison, pp. 802-816.

Rezanezhad, F. et al., 2009. Examining the effect of pore size distribution and shape on flow through unsaturated peat using computed tomography. Hydrology and Earth System Sciences, 13(10): 1993-2002.

Richards, L.A., 1931. Capillary conduction of liquids through porous mediums. Physics, 1: 318-333.

Robinson, L.N., 2008. Water resources research progress. Nova Publishers.

Rodriguez-Iturbe, I., Porporato, A., Laio, F., Ridolfi, L., 2001. Plants in water-controlled ecosystems: active role in hydrologic processes and response to water stress: I. Scope and general outline. Advances in Water Resources, 24(7): 695-705.

Romano, N., Santini, A., 1999. Determining soil hydraulic functions from evaporation experiments by a parameter estimation Approach: Experimental verifications and numerical studies. Water Resources Research, 35(11): 3343-3359.

Rydin, H., Jeglum, J.K., 2013. The biology of peatlands, 2e. Oxford university press.

Schaap, M.G., 2005. Chapter 76: Models for Indirect Estimation of Soil Hydraulic Properties. In: M.G., A., McDonnell, J.J. (Eds.), Encyclopedia of Hydrological Sciences. John Wiley & Sons, Ltd., pp. 1121-1144.

Schaap, M.G., Leij, F.J., 2000. Improved prediction of unsaturated hydraulic conductivity with the Mualem-van Genuchten model. Soil Science Society of America Journal, 64(3): 843-851.

Schaap, M.G., Leij, F.J., Van Genuchten, M.T., 2001. Rosetta: A computer program for estimating soil hydraulic parameters with hierarchical pedotransfer functions. Journal of Hydrology, 251(3-4): 163-176.

Scharnagl, B., Iden, S., Durner, W., Vereecken, H., Herbst, M., 2015. Inverse modelling of in situ soil water dynamics: accounting for heteroscedastic, autocorrelated, and non-Gaussian distributed residuals. Hydrology and Earth System Sciences Discussions, 12(2): 2155-2199.

Scharnagl, B., Vrugt, J.A., Vereecken, H., Herbst, M., 2011. Inverse modelling of in situ soil water dynamics: Investigating the effect of different prior distributions of the soil hydraulic parameters. Hydrology and Earth System Sciences, 15(10): 3043-3059.

Schelle, H., Heise, L., Jänicke, K., Durner, W., 2013. Water retention characteristics of soils over the whole moisture range: A comparison of laboratory methods. European Journal of Soil Science, 64(6): 814-821.

Schelle, H., Iden, S., Peters, A., Durner, W., 2010. Analysis of the agreement of soil hydraulic properties obtained from multistep-outflow and evaporation methods. UNKNOWN, 9(4): 1080-1091.

Schindler, U., 1980. Ein Schnellverfahren zur Messung der Wasserleitfähigkeit im teilgesättigten Boden an Stechzylinderproben. Archiv für Acker- und Pflanzenbau und Bodenkunde - Archives of Agronomy and Soil Science, 24(1): 1-7.

Schindler, U., Müller, L., 2010. Data of hydraulic properties of North East and North Central German soils. Earth System Science Data, 2: 189-194.

Schuh, W., Cline, R., 1990. Effect of soil properties on unsaturated hydraulic conductivity pore-interaction factors. Soil Science Society of America Journal, 54(6): 1509-1519.

Schwärzel, K., Simunek, J., Stoffregen, H., Wessolek, G., van Genuchten, M.T., 2006. Estimation of the unsaturated hydraulic conductivity of peat soils: Laboratory versus field data. Vadose Zone Journal, 5(2): 628-640.

Shibchurn, A., Van Geel, P.J., Kennedy, P.L., 2005. Impact of density on the hydraulic properties of peat and the time domain reflectometry (TDR) moisture calibration curve. Canadian geotechnical journal, 42(1): 279-286.

Silvan, N., Sallantaus, T., Vasander, H., Laine, J., 2005. Hydraulic nutrient transport in a restored peatland buffer. Boreal Environment Research, 10(3): 203-210.

Šimůnek, J., Jarvis, N.J., van Genuchten, M.T., Gardenas, A., 2003. Review and comparison of models for describing non-equilibrium and preferential flow and transport in the vadose zone. Journal of Hydrology, 272(1-4): 14-35.

Šimůnek, J., Šejna, M., Saito, H., Sakai, M., van Genuchten, M.T., 2013. The HYDRUS-1D Software Package for Simulating the One-Dimensional Movement of Water, Heat, and Multiple Solutes in Variably-Saturated Media. Department of Environmental Sciences, University of California Riverside, California.

Šimůnek, J., Wendroth, O., van Genuchten, M.T., 1998. Parameter estimation analysis of the evaporation method for determining soil hydraulic properties. Soil Science Society of America Journal, 62(4): 894-905.

Sittler, B., 2004. Revealing historical landscapes by using airborne laser scanning. Laser-Scanners for Forest and Landscape Assessment: 258-261.

Succow, M., 2012. Genese und Aufbau der Moore an Beispielen Ostdeutschlands. In: Succow, M., Joosten, H. (Eds.), Moorkunde. E. Schweizerbart'sche Verlagsbuchhandlung, Stuttgart, pp. 622.

Sumner, D.M., 2007. Effects of capillarity and microtopography on wetland specific yield. Wetlands, 27(3): 693-701.

Taniguchi, M., Burnett, W.C., Fukushima, Y., Haigh, M., Umezawa, Y., 2008. From Headwaters to the Ocean: Hydrological Change and Water Management-Hydrochange 2008, 1-3 October 2008, Kyoto, Japan. CRC Press.

Thompson, D.K., Waddington, J.M., 2013. Peat properties and water retention in boreal forested peatlands subject to wildfire. Water Resources Research, 49(6): 3651-3658.

Trübger, E.-R., 2007. Entwicklung eines Ansatzes zur Berücksichtigung der ungesättigten Zone bei der Grundwassersimulation von Feuchtgebieten. Diss. Universität Rostock.

Van Beek, C. et al., 2007. Leaching of solutes from an intensively managed peat soil to surface water. Water, air, and soil pollution, 182(1-4): 291-301.

van Dam, J.C., Stricker, J.N.M., Droogers, P., 1994. Inverse method to determine soil hydraulic functions from multistep outflow experiments. Soil Science Society of America Journal, 58(3): 647-652.

van Genuchten, M.T., 1980. A Closed-form Equation for Predicting the Hydraulic Conductivity of Unsaturated Soils. Soil Science Society of America Journal, 44(5): 892-898.

van Genuchten, M.T., Leij, F.J., Yates, S.R., 1991. The RETC code for Quantifying the Hydraulic Functions of Unsaturated Soils. Kerr, Robert S. Environmental Research Laboratory, Office of Research and Development, US Environmental Protection Agency Ada, Okla., USA.

van Genuchten, M.T., Nielsen, D.R., 1985. On describing and predicting the hydraulic properties of unsaturated soils. Annales Geophysicae, 3:615-628.

von Post, L., Granlund, E., 1926. ödra Sveriges Torvtillgångar I (Peat resources in southern Sweden I). Sveriges Geologiska Undersökning, C 335, 19, 1–128 (in Swedish).

Vrugt, J.A., Dane, J.H., 2005. Chapter 77: Inverse Modeling of Soil Hydraulic Properties. In: M.G., A., McDonnell, J.J. (Eds.), Encyclopedia of Hydrological Sciences. John Wiley & Sons, Ltd., pp. 1151-1179.

Vrugt, J.A., Ter Braak, C.J., Clark, M.P., Hyman, J.M., Robinson, B.A., 2008. Treatment of input uncertainty in hydrologic modeling: Doing hydrology backward with Markov chain Monte Carlo simulation. Water Resources Research, 44(12).

Vrugt, J.A., Ter Braak, C.J.F., 2011. DREAM(D): An adaptive Markov Chain Monte Carlo simulation algorithm to solve discrete, noncontinuous, and combinatorial posterior parameter estimation problems. Hydrology and Earth System Sciences, 15(12): 3701-3713.

Vrugt, J.A. et al., 2009a. Accelerating Markov chain Monte Carlo simulation by differential evolution with self-adaptive randomized subspace sampling. International Journal of Nonlinear Sciences and Numerical Simulation, 10(3): 273-290.

Vrugt, J.A., ter Braak, C.J.F., Gupta, H.V., Robinson, B.A., 2009b. Equifinality of formal (DREAM) and informal (GLUE) Bayesian approaches in hydrologic modeling? Stochastic Environmental Research and Risk Assessment, 23(7): 1011-1026.

Waddington, J. et al., 2015. Hydrological feedbacks in northern peatlands. Ecohydrology, 8(1): 113-127.

Wang, P., Pozdniakov, S.P., 2014. A statistical approach to estimating evapotranspiration from diurnal groundwater level fluctuations. Water Resources Research, 50(3): 2276-2292.

Weiss, R., Alm, J., Laiho, R., Laine, J., 1998. Modeling moisture retention in peat soils. Soil Science Society of America Journal, 62(2): 305-313.

Wendroth, O. et al., 1993. Reevaluation of the Evaporation Method for Determining Hydraulic Functions in Unsaturated Soils. Soil Science Society of America Journal, 57(6): 1436-1443.

Wheeler, B., Proctor, M., 2000. Ecological gradients, subdivisions and terminology of north-west European mires. Journal of Ecology, 88(2): 187-203.

White, W.N., 1932. A method of estimating ground-water supplies based on discharge by plants and evaporation from soil. Results of investigations in Escalante Valley, Utah. U S Geol Sun Water Supply Paper, 659-A.: 1-105.

Wind, G.P., 1968. Capillary conductivity data estimated by a simple method. Publ. International Association of Scientific Hydrology /UNESCO Symposium Wageningen, 83: 181-191.

Winde, F., 2011. Peatlands as Filters for Polluted Mine Water?—A Case Study from an Uranium-Contaminated Karst System in South Africa—Part II: Examples from Literature and a Conceptual Filter Model. Water, 3(1): 323-355.

Wöhling, T., Vrugt, J.A., 2011. Multiresponse multilayer vadose zone model calibration using Markov chain Monte Carlo simulation and field water retention data. Water Resources Research, 47(4).

Wollschläger, U., Pfaff, T., Roth, K., 2009. Field-scale apparent hydraulic parameterisation obtained from TDR time series and inverse modelling. Hydrology and Earth System Sciences, 13(10): 1953-1966.

Worrall, F. et al., 2010. Peatlands and climate change. Report to IUCN UK Peatland Programme, Edinburgh.

Wösten, J., Finke, P., Jansen, M., 1995. Comparison of class and continuous pedotransfer functions to generate soil hydraulic characteristics. Geoderma, 66(3): 227-237.

WRB, 2008. World Reference Base for Soil Resources 2006. Ein Rahmen für internationale Klassifikation, Korrelation und Kommunikation, Deutsche Ausgabe, Bundesanstalt für Geowissenschaften und Rohstoffe, Hannover.

Yates, S., Van Genuchten, M.T., Leij, F., Warrick, A., 1992. Analysis of measured, predicted, and estimated hydraulic conductivity using the RETC computer program. Soil Science Society of America Journal, 56(2): 347-354.

Supplementary data associated with section 2

Site	Pressure head range	Model set-up	Φ (-)	RMSE tensiometer (cm)	Error evaporation (%)	θ_s ($cm^3\ cm^{-3}$)	θ_r ($cm^3\ cm^{-3}$)	α (cm^{-1})	n (-)	K_s ($cm\ h^{-1}$)	τ (-)	ω (-)	$\alpha 2$ (cm^{-1})	$n2$ (-)
AK1	full range	3p	0.07523	46.0	8.3	0.84	0.00	0.0658	1.24	609	0.50	-	-	-
AK1	full range	4p	0.03537	33.2	2.7	0.84	0.00	0.0199	1.38	55	0.50	-	-	-
AK1	full range	4p_d	0.03441	32.7	2.5	0.84	0.00	0.0159	1.40	609	0.50	0.05	1.00	10.00
AK1	full range	4p_t	0.04245	35.9	4.2	0.84	0.00	0.0251	1.35	609	2.44	-	-	-
AK1	full range	5p	0.03094	31.2	0.0	0.84	0.00	0.0161	1.44	2	-2.92	-	-	-
AK1	full range	5p_d	0.03398	32.6	2.3	0.84	0.00	0.0127	1.42	1706	0.50	0.10	1.00	10.00
AK1	full range	6p_d	0.02818	29.8	0.0	0.84	0.00	0.0098	1.48	139	-2.77	0.12	1.00	10.00
AK1	full range	8p_d	0.02814	29.8	0.0	0.84	0.00	0.0094	1.49	112	-2.78	0.13	0.82	1.91
AK1	wet range	3p	0.02842	9.8	0.0	0.84	0.00	0.0342	1.27	609	0.50	-	-	-
AK1	wet range	4p	0.01945	8.1	0.0	0.84	0.00	0.0307	1.29	106	0.50	-	-	-
AK1	wet range	4p_d	0.00536	4.2	0.0	0.84	0.00	0.0122	1.44	609	0.50	0.09	1.00	10.00
AK1	wet range	4p_t	0.01812	7.8	0.0	0.84	0.00	0.0315	1.28	609	4.66	-	-	-
AK1	wet range	5p	0.01573	7.1	2.8	0.84	0.00	0.0378	1.25	6641	9.16	-	-	-
AK1	wet range	5p_d	0.00052	1.3	0.0	0.84	0.34	0.0113	2.08	4403	0.50	0.24	1.00	10.00
AK1	wet range	6p_d	0.00051	1.3	0.0	0.84	0.34	0.0113	2.05	4801	0.64	0.23	1.00	10.00
AK1	wet range	8p_d	0.00051	1.3	0.0	0.84	0.34	0.0114	2.06	4810	0.63	0.23	1.00	9.80
AK2	full range	3p	0.07014	42.3	12.1	0.86	0.00	0.0540	1.19	609	0.50	-	-	-
AK2	full range	4p	0.01546	21.6	4.2	0.86	0.00	0.0142	1.34	37	0.50	-	-	-
AK2	full range	4p_d	0.01399	20.6	3.8	0.86	0.00	0.0107	1.37	609	0.50	0.05	1.00	10.00
AK2	full range	4p_t	0.03413	32.0	5.9	0.86	0.00	0.0187	1.30	609	3.23	-	-	-
AK2	full range	5p	0.01152	19.2	2.5	0.86	0.00	0.0126	1.37	11	-0.67	-	-	-
AK2	full range	5p_d	0.01384	20.6	3.6	0.86	0.00	0.0097	1.38	986	0.50	0.07	1.00	10.00
AK2	full range	6p_d	0.00842	16.6	1.4	0.86	0.06	0.0073	1.49	465	-0.97	0.10	1.00	10.00
AK2	full range	8p_d	0.00842	16.6	1.6	0.86	0.06	0.0073	1.50	312	-0.97	0.10	0.81	4.77
AK2	wet range	3p	0.03434	11.6	0.0	0.86	0.00	0.0267	1.22	609	0.50	-	-	-
AK2	wet range	4p	0.03286	11.3	0.0	0.86	0.00	0.0255	1.22	236	0.50	-	-	-
AK2	wet range	4p_d	0.00910	6.0	0.0	0.86	0.00	0.0058	1.62	609	0.50	0.10	1.00	10.00
AK2	wet range	4p_t	0.03266	11.3	0.0	0.86	0.00	0.0256	1.22	609	3.61	-	-	-
AK2	wet range	5p	0.02953	10.5	4.1	0.86	0.14	0.0315	1.24	6668	10.00	-	-	-
AK2	wet range	5p_d	0.00085	1.8	0.0	0.86	0.27	0.0072	1.82	3295	0.50	0.16	1.00	10.00
AK2	wet range	6p_d	0.00081	1.8	0.0	0.86	0.19	0.0068	1.71	5128	2.13	0.14	1.00	10.00
AK2	wet range	8p_d	0.00081	1.8	0.0	0.86	0.19	0.0068	1.71	5047	2.10	0.14	1.00	9.88
GM1	full range	3p	0.07314	47.8	6.0	0.62	0.00	0.0407	1.20	53	0.50	-	-	-
GM1	full range	4p	0.01076	17.6	2.8	0.62	0.06	0.0119	1.38	3	0.50	-	-	-
GM1	full range	4p_d	0.00992	17.0	2.6	0.62	0.05	0.0099	1.39	53	0.50	0.04	1.00	10.00
GM1	full range	4p_t	0.01635	19.0	4.8	0.62	0.00	0.0187	1.26	53	3.06	-	-	-
GM1	full range	5p	0.00978	16.5	3.0	0.62	0.00	0.0131	1.31	7	1.22	-	-	-
GM1	full range	5p_d	0.00943	16.6	2.5	0.62	0.06	0.0078	1.41	198	0.50	0.09	1.00	10.00
GM1	full range	6p_d	0.00897	16.1	2.6	0.62	0.00	0.0088	1.34	194	1.11	0.07	1.00	10.00
GM1	full range	8p_d	0.00897	16.1	2.6	0.62	0.00	0.0088	1.34	84	1.10	0.07	0.62	6.53
GM1	wet range	3p	0.02054	8.6	0.0	0.62	0.06	0.0230	1.25	53	0.50	-	-	-

GM1	wet range	4p	0.01791	8.0	0.0	0.62	0.00	0.0267	1.20	129	0.50	-	-	-
GM1	wet range	4p_d	0.02054	8.6	0.0	0.62	0.06	0.0230	1.25	53	0.50	0.00	1.00	10.00
GM1	wet range	4p_t	0.01827	8.1	0.0	0.62	0.00	0.0261	1.20	53	-2.35	-	-	-
GM1	wet range	5p	0.01692	7.8	1.0	0.62	0.00	0.0304	1.18	116469	22.75	-	-	-
GM1	wet range	5p_d	0.00667	4.9	0.0	0.62	0.31	0.0118	1.80	2252	0.50	0.16	1.00	10.00
GM1	wet range	6p_d	0.00665	4.9	0.0	0.62	0.30	0.0117	1.75	3371	1.22	0.15	1.00	10.00
GM1	wet range	8p_d	0.00665	4.9	0.0	0.62	0.30	0.0117	1.76	3185	1.12	0.15	1.00	9.90
GM2	full range	3p	0.07351	40.3	4.9	0.64	0.00	0.0429	1.18	53	0.50	-	-	-
GM2	full range	4p	0.01502	17.7	2.1	0.64	0.00	0.0131	1.29	3	0.50	-	-	-
GM2	full range	4p_d	0.01513	17.8	2.0	0.64	0.00	0.0095	1.31	53	0.50	0.05	1.00	10.00
GM2	full range	4p_t	0.07351	40.3	5.0	0.64	0.00	0.0429	1.18	53	0.50	-	-	-
GM2	full range	5p	0.01491	17.7	1.8	0.64	0.00	0.0127	1.29	3	0.26	-	-	-
GM2	full range	5p_d	0.01488	17.6	2.1	0.64	0.00	0.0113	1.30	20	0.50	0.02	1.00	10.00
GM2	full range	6p_d	0.01475	17.7	1.7	0.64	0.00	0.0109	1.30	17	0.25	0.02	1.00	10.00
GM2	full range	8p_d	0.01477	17.7	1.8	0.64	0.00	0.0109	1.30	5	0.25	0.02	0.32	7.36
GM2	wet range	3p	0.01692	6.9	0.0	0.64	0.00	0.0252	1.18	53	0.50	-	-	-
GM2	wet range	4p	0.01457	6.4	0.0	0.64	0.00	0.0209	1.20	27	0.50	-	-	-
GM2	wet range	4p_d	0.01045	5.4	0.0	0.64	0.05	0.0140	1.28	53	0.50	0.02	1.00	10.00
GM2	wet range	4p_t	0.01212	5.9	0.0	0.64	0.05	0.0207	1.22	53	4.16	-	-	-
GM2	wet range	5p	0.00930	5.1	1.2	0.64	0.00	0.0248	1.18	363	10.00	-	-	-
GM2	wet range	5p_d	0.00316	3.0	0.5	0.64	0.37	0.0119	1.91	600	0.50	0.15	1.00	10.00
GM2	wet range	6p_d	0.00316	3.0	0.5	0.64	0.36	0.0119	1.84	612	0.75	0.14	1.00	10.00
GM2	wet range	8p_d	0.00263	2.7	0.8	0.64	0.42	0.0107	2.50	293	-0.46	0.31	0.49	1.50
SF1	full range	3p	0.10425	52.9	7.8	0.95	0.00	0.0531	1.44	528	0.50	-	-	-
SF1	full range	4p	0.10371	52.6	7.8	0.95	0.00	0.0616	1.41	712	0.50	-	-	-
SF1	full range	4p_d	0.10466	53.2	7.2	0.95	0.00	0.0500	1.45	528	0.50	0.00	1.00	10.00
SF1	full range	4p_t	0.08223	43.5	10.5	0.95	0.00	0.1782	1.30	528	-1.09	-	-	-
SF1	full range	5p	0.02278	23.7	5.6	0.95	0.02	0.0310	1.58	2	-2.13	-	-	-
SF1	full range	5p_d	0.10433	52.9	7.5	0.95	0.00	0.0500	1.43	1495	0.50	0.04	1.00	10.00
SF1	full range	6p_d	0.02275	23.5	5.5	0.95	0.05	0.0242	1.66	15	-2.09	0.07	1.00	10.00
SF1	full range	8p_d	0.02275	23.5	5.6	0.95	0.04	0.0256	1.65	4	-2.10	0.05	0.40	9.91
SF1	wet range	3p	0.10283	15.1	6.7	0.95	0.00	0.1432	1.25	528	0.50	-	-	-
SF1	wet range	4p	0.04670	10.4	2.5	0.95	0.00	0.0402	1.44	29	0.50	-	-	-
SF1	wet range	4p_d	0.05773	11.6	2.3	0.95	0.01	0.0199	1.55	528	0.50	0.17	1.00	10.00
SF1	wet range	4p_t	0.07510	12.9	5.3	0.95	0.00	0.0750	1.32	528	2.36	-	-	-
SF1	wet range	5p	0.04035	9.6	1.2	0.95	0.00	0.0344	1.50	6	-0.95	-	-	-
SF1	wet range	5p_d	0.04649	10.3	2.4	0.95	0.00	0.0362	1.45	60	0.50	0.02	1.00	10.00
SF1	wet range	6p_d	0.03945	9.5	1.0	0.95	0.00	0.0279	1.53	25	-0.98	0.04	1.00	10.00
SF1	wet range	8p_d	0.03946	9.5	1.1	0.95	0.00	0.0276	1.54	26	-0.97	0.05	0.99	9.29
SF2	full range	3p	0.19204	78.4	4.7	0.90	0.00	0.0476	1.46	528	0.50	-	-	-
SF2	full range	4p	0.13153	63.9	7.0	0.90	0.00	0.4537	1.25	60983	0.50	-	-	-
SF2	full range	4p_d	0.19204	78.4	4.5	0.90	0.00	0.0476	1.46	528	0.50	0.00	1.00	10.00
SF2	full range	4p_t	0.04363	35.3	6.7	0.90	0.00	0.4999	1.25	528	-2.83	-	-	-
SF2	full range	5p	0.02709	28.5	4.6	0.90	0.06	0.0900	1.45	11	-2.54	-	-	-
SF2	full range	5p_d	0.13153	63.9	6.9	0.90	0.00	0.4498	1.25	59981	0.50	0.00	1.00	10.00
SF2	full range	6p_d	0.02661	28.3	4.3	0.90	0.10	0.0480	1.57	38	-2.41	0.14	1.00	10.00

SF2	full range	8p_d	0.02667	28.3	4.4	0.90	0.10	0.0439	1.59	19	-2.40	0.17	0.56	7.18
SF2	wet range	3p	0.03166	7.8	4.6	0.90	0.00	0.1254	1.33	528	0.50	-	-	-
SF2	wet range	4p	0.01649	5.7	2.8	0.90	0.00	0.0647	1.44	125	0.50	-	-	-
SF2	wet range	4p_d	0.01813	6.0	2.3	0.90	0.00	0.0464	1.47	528	0.50	0.09	1.00	10.00
SF2	wet range	4p_t	0.02645	7.1	3.8	0.90	0.00	0.0916	1.38	528	1.17	-	-	-
SF2	wet range	5p	0.00664	3.7	0.7	0.90	0.12	0.0456	1.72	10	-1.15	-	-	-
SF2	wet range	5p_d	0.01649	5.7	2.7	0.90	0.00	0.0646	1.44	126	0.50	0.00	1.00	10.00
SF2	wet range	6p_d	0.00390	2.8	0.9	0.90	0.22	0.0270	2.28	85	-1.47	0.16	1.00	10.00
SF2	wet range	8p_d	0.00390	2.8	1.0	0.90	0.22	0.0270	2.29	85	-1.47	0.17	1.00	7.54
SW2	full range	4p	0.05801	51.7	9.6	0.80	0.00	0.0240	1.21	138	0.50	-	-	-
SW2	full range	5p	0.01976	31.4	4.9	0.80	0.00	0.0132	1.28	5	-2.16	-	-	-
SW2	full range	5p_d	0.05796	51.8	9.3	0.80	0.00	0.0197	1.22	484	0.50	0.03	1.00	10.00
SW2	full range	6p_d	0.01801	30.7	3.7	0.80	0.00	0.0072	1.34	190	-2.09	0.08	1.00	10.00
SW2	full range	8p_d	0.01801	30.7	3.8	0.80	0.00	0.0071	1.34	45	-2.09	0.08	0.44	8.38
SW2	wet range	4p	0.03240	9.6	2.6	0.80	0.00	0.0330	1.15	131	0.50	-	-	-
SW2	wet range	5p	0.03239	9.6	2.3	0.80	0.00	0.0328	1.16	125	0.37	-	-	-
SW2	wet range	5p_d	0.02265	8.1	0.1	0.80	0.00	0.0102	1.28	263	0.50	0.05	1.00	10.00
SW2	wet range	6p_d	0.02076	7.8	0.0	0.80	0.41	0.0122	1.77	105	-2.76	0.12	1.00	10.00
SW2	wet range	8p_d	0.02053	7.7	0.0	0.80	0.48	0.0125	2.11	119	-2.63	0.17	1.00	2.38
ZA1	full range	3p	0.05769	44.7	8.2	0.75	0.00	0.0244	1.17	42	0.50	-	-	-
ZA1	full range	4p	0.05768	44.6	6.5	0.75	0.00	0.0250	1.17	44	0.50	-	-	-
ZA1	full range	4p_d	0.05769	44.7	6.4	0.75	0.00	0.0242	1.17	42	0.50	0.00	1.00	10.00
ZA1	full range	4p_t	0.03427	32.7	6.4	0.75	0.00	0.0389	1.15	42	-1.73	-	-	-
ZA1	full range	5p	0.01289	22.1	1.9	0.75	0.00	0.0146	1.22	3	-2.36	-	-	-
ZA1	full range	5p_d	0.05473	43.7	6.0	0.75	0.00	0.0089	1.21	621	0.50	0.10	1.00	10.00
ZA1	full range	6p_d	0.00998	19.5	1.6	0.75	0.00	0.0082	1.26	50	-2.19	0.06	1.00	10.00
ZA1	full range	8p_d	0.00990	19.4	1.7	0.75	0.00	0.0079	1.26	54	-2.18	0.06	1.00	2.64
ZA1	wet range	3p	0.12050	18.6	0.8	0.75	0.32	0.0324	1.30	42	0.50	-	-	-
ZA1	wet range	4p	0.01777	6.7	4.3	0.75	0.39	0.1929	1.17	3272	0.50	-	-	-
ZA1	wet range	4p_d	0.12051	18.6	0.3	0.75	0.32	0.0324	1.30	42	0.50	0.00	1.00	10.00
ZA1	wet range	4p_t	0.03092	9.4	0.0	0.75	0.42	0.0998	1.24	42	-4.59	-	-	-
ZA1	wet range	5p	0.01310	5.6	3.9	0.75	0.00	0.3089	1.06	119870	7.38	-	-	-
ZA1	wet range	5p_d	0.00363	3.2	0.8	0.75	0.39	0.0128	1.36	2555	0.50	0.23	1.00	10.00
ZA1	wet range	6p_d	0.00322	3.0	0.6	0.75	0.00	0.0123	1.13	4619	5.58	0.10	1.00	10.00
ZA1	wet range	8p_d	0.00331	3.1	0.6	0.75	0.24	0.0113	1.23	3444	2.40	0.16	1.00	2.53
ZA2	full range	3p	0.06036	48.2	8.3	0.76	0.00	0.0197	1.18	42	0.50	-	-	-
ZA2	full range	4p	0.06036	48.2	6.8	0.76	0.00	0.0196	1.18	41	0.50	-	-	-
ZA2	full range	4p_d	0.06035	48.2	6.7	0.76	0.00	0.0192	1.18	42	0.50	0.00	1.00	10.00
ZA2	full range	4p_t	0.03548	34.1	7.2	0.76	0.00	0.0320	1.15	42	-1.84	-	-	-
ZA2	full range	5p	0.01078	21.3	2.0	0.76	0.00	0.0118	1.23	2	-2.43	-	-	-
ZA2	full range	5p_d	0.05955	48.1	6.4	0.76	0.00	0.0118	1.19	379	0.50	0.05	1.00	10.00
ZA2	full range	6p_d	0.00992	20.5	1.7	0.76	0.15	0.0077	1.36	33	-2.22	0.05	1.00	10.00
ZA2	full range	8p_d	0.00989	20.4	1.8	0.76	0.18	0.0073	1.40	37	-2.19	0.06	0.99	2.80
ZA2	wet range	3p	0.05453	13.4	3.2	0.76	0.35	0.0279	1.28	42	0.50	-	-	-
ZA2	wet range	4p	0.02446	8.4	6.1	0.76	0.42	0.0695	1.22	380	0.50	-	-	-
ZA2	wet range	4p_d	0.05453	13.4	2.4	0.76	0.35	0.0279	1.28	42	0.50	0.00	1.00	10.00

ZA2	wet range	4p_t	0.03122	10.2	0.0	0.76	0.22	0.0470	1.16	42	-6.63	-	-	-
ZA2	wet range	5p	0.01750	6.8	6.1	0.76	0.00	0.0979	1.07	11733	8.30	-	-	-
ZA2	wet range	5p_d	0.00230	2.7	1.8	0.76	0.41	0.0089	1.50	1393	0.50	0.18	1.00	10.00
ZA2	wet range	6p_d	0.00166	2.3	1.7	0.76	0.00	0.0072	1.20	1977	6.10	0.08	1.00	10.00
ZA2	wet range	8p_d	0.00165	2.3	1.5	0.76	0.00	0.0069	1.20	1907	5.98	0.08	1.00	3.45

Selbständigkeitserklärung

Ich erkläre, dass ich die hier vorgelegte Arbeit selbständig und ohne fremde Hilfe verfasst, andere als die von mir angegebenen Quellen und Hilfsmittel nicht benutzt und die den benutzten Werken wörtlich oder inhaltlich entnommenen Stellen als solche kenntlich gemacht habe.

Rostock, den 15.12.2015 Ullrich Dettmann

Theses for the dissertation entitled:

Improving the determination of soil hydraulic properties of peat soils at different scales

submitted by Ullrich Dettmann

- Peat soil moisture dynamics in the unsaturated zone can be modeled with the Richards' equation although fundamental assumptions of the Richards' equation, e.g. a rigid soil matrix, are not fulfilled.

- Macropore flow is an important process in peatland hydrology and must be taken into account for most peat soils when modeling flow processes in the unsaturated zone.

- Under evaporation conditions macropore flow can be taken into account by the bimodal van Genuchten-Mualem based model of Durner (1994) and Priesack and Durner (2006).

- For many peatlands, defining a 'wet range' (pressure heads between 0 - -200 cm) is an appropriate method to improve the modeling of soil moisture dynamics, as minimum pressure heads usually don't fall below -200 cm.

- For the modeling of dry conditions (pressure heads < -200 cm) the van Genuchten-Mualem Parameter τ is an important parameter and can differ from the default value of 0.5 often used for mineral soils.

- Shrinkage is an important process for drying peat soils. Nevertheless, neglecting shrinkage leads to acceptable model results if adequate parameter configurations are chosen.

- The specific yield of shallow groundwater systems is substantially influenced by the microrelief of the landscape. Thereby, the specific yield is not only influenced by the microrelief when surface storage directly contributes to specific yield by (partial) inundation but also when water levels are lower than the minimum surface elevation.

- The integrals of two soil moisture profiles of an upper and a lower water level are horizontally reduced by the microrelief when they are interpreted as spatial average, because the soil volume covers only parts of the total volume. Consequentially, water level rises caused by precipitation events are affected by the microrelief because of partial inundation and the changed soil moisture profiles.

- The microrelief of a field site can be described with a cumulative frequency distribution of the surface height elevations. For *Sphagnum* bogs normally distributed frequency distributions usually lead to a sufficient description of the surface height elevations.

- Water level rises caused by precipitation events contain sufficient information to determine *in situ* water retention characteristics integrated around a dip well (approximately several meters) over different soil layers.

- The water retention characteristics of pristine *Sphagnum* mosses are characterized by an abrupt dewatering capacity.

- Water level rises caused by precipitation events and knowledge about the frequency distribution of the microrelief can be used to determine the depth of the vertical transition from the plant to the soil layer at a *Sphagnum* bog under a hydrological perspective.